The characterization of uncertainty for steady state multiphase flow models in pipelines

Master Thesis

Solid & Fluid Mechanics, Faculty of Mechanical Engineering

J. M. Klinkert



TU Delft Delft University of Technology

Challenge the future

The characterization of uncertainty for steady state multiphase flow models in pipelines

Master Thesis

Solid & Fluid Mechanics, Faculty of Mechanical Engineering

by

J. M. Klinkert

to obtain the degree of Master of Science
at the Delft University of Technology,
to be defended publicly on Friday January 19, 2018 at 2:00 PM.

Student number:	4118219	
Project duration:	March 20, 2017 – January 19, 2018	
Thesis committee:	Prof. dr. ir. R.A.W.M. Henkes	TU Delft
	Dr. ir. B. Sanderse	Shell and CWI (supervisor)
	Dr. ir. W.P. Breugem	TU Delft
	Dr. R. P. Dwight	TU Delft

An electronic version of this thesis is available at `http://repository.tudelft.nl/`.

TU Delft Delft University of Technology

Challenge the future

Preface

This project is the result of months of hard work and personal involvement. Before starting this MSc project, I had never heard of uncertainty quantification and it took me some time to familiarize myself with phenomena like orthogonal polynomials and sparse grids. During the course of the project, these phenomena were better and better understood. It has been a great experience to apply the knowledge I gained during both my Master's program and from this project, and to see this coming together throughout the project.
This could all only be achieved with the help of others. First, and most of all, I have to thank Benjamin Sanderse. He guided me throughout the whole project and was very patient with me. I could always contact him and visit him at the CWI. I am very grateful for the time he dedicated to providing feedback and corrections to my report, as much as for the input that helped me constantly to improve my work. Next to Benjamin, I have to thank my supervisor Ruud Henkes, for the valuable suggestions and discussions every month. Thanks to Ruud, I had the opportunity to carry out my research at Shell, which was a great opportunity to collaborate in such a large scale company. I would also like to thank the Flow Assurance team of Shell, for the guidance and support I received from them in developing this thesis. A special thanks goes out to Giuseppe Pagliuca, who helped me a lot with the implementation of PIPESIM. Finally, thanks are due to my family and friends, for the mental support throughout both my Master program and this project.

J. M. Klinkert
Delft, January 2018

Abstract

Steady state multiphase flow models are used for the design and operation of pipelines that are used in the oil and gas industry. The predictions obtained with these models contain uncertainties, which arise from model assumptions and simplifications, and from uncertainties in the input parameters. In this thesis we investigate the effect of uncertainties in the input parameters (such as the wall roughness or the superficial velocities) on two main quantities of interest in steady state multiphase flow in pipelines: the liquid holdup and the pressure drop.

The approach that we take is to describe the uncertain input parameters by probability density functions (PDFs), propagate these through the steady state models, and obtain a PDF for the quantities of interest. We use two methodologies from the field of Uncertainty Quantification (UQ) to perform the propagation step: Monte Carlo sampling, the current standard in the literature, and Polynomial Chaos Expansion (PCE), our proposed approach. Furthermore, we use Sobol indices to perform a sensitivity analysis that ranks the input parameters depending on their contribution to the output.

Our proposed UQ methodology is applied on two commonly used multiphase flow models in the oil and gas industry: a 0-D model, the Shell Flow Correlations (SFC), and a 1-D model, PIPESIM.
First, application to the SFC reveals that PCE is much more efficient than Monte Carlo sampling, and an improvement of several orders of magnitude is achieved in terms of the number of samples required for a given accuracy, while the evaluation of a single sample requires the same computation time for the two methods.
Furthermore, with UQ the flow pattern maps commonly used in industry can now be displayed in a probabilistic way. This allows the quantification of the probability that a flow regime (e.g. slug, stratified) occurs under given conditions. These are significant improvements compared to existing work that handles uncertainties in multiphase flow models.
Second, application of PCE to a multiphase pipeline, known as Goldeneye, modelled in PIPESIM revealed that several uncertain variables, namely the wall roughness, the ambient temperature and the outlet pressure, play a role in determining the liquid holdup and the pressure drop. This is in contrast to what was assumed in an earlier benchmarking study. Furthermore, our probabilistic approach allows us to make predictions under uncertainty. For instance, we can now predict that the liquid holdup of the Goldeneye pipeline will have a 65% probability to be lower than the value of 1496 m^3, the value obtained when using a deterministic setting.

Contents

Preface iii

Abstract v

List of Figures ix

List of Tables xi

Nomenclature xiii

1 Introduction 1
- 1.1 Motivation . . . 1
- 1.2 Literature review . . . 2
- 1.3 Research objectives . . . 4
- 1.4 Research outline . . . 5

2 Multiphase pipe flow and its uncertainties 7
- 2.1 Characteristics of a multiphase flow . . . 7
  - 2.1.1 The different flow regimes . . . 7
  - 2.1.2 Mechanistic modeling . . . 9
  - 2.1.3 The pressure drop . . . 10
  - 2.1.4 The liquid holdup . . . 11
  - 2.1.5 Multiphase flow prediction models . . . 12
- 2.2 Uncertainty Quantification . . . 12
  - 2.2.1 Simulation-based approaches . . . 13
  - 2.2.2 Functional expansion-based approaches . . . 15
  - 2.2.3 Sensitivity analysis . . . 16
  - 2.2.4 UQLab . . . 17
- 2.3 Methodology . . . 17

3 UQ methods for the propagation 19
- 3.1 Uncertainty Quantification . . . 19
  - 3.1.1 Simulation-based approaches . . . 20
  - 3.1.2 Functional expansion-based approaches . . . 20
  - 3.1.3 Functional expansion-based approaches on sparse grids . . . 22
- 3.2 Comparison of methods . . . 24
- 3.3 Sensitivity analysis . . . 28

4 Uncertainty propagation on 0-D steady state models 31
- 4.1 Uncertainties in a stratified flow regime: SFC compared to literature . . . 31
  - 4.1.1 Uncertainty Quantification . . . 31
  - 4.1.2 Sensitivity analysis . . . 34
- 4.2 Efficiency improvements with polynomial chaos expansion . . . 36
  - 4.2.1 Horizontal stratified flow. . . . 36
  - 4.2.2 Downward inclined stratified flow . . . 38
- 4.3 Flow Pattern Map uncertainty of the SFC . . . 40
  - 4.3.1 Determination of a flow pattern . . . 40
  - 4.3.2 The Kelvin Helmholtz instability . . . 41
  - 4.3.3 Results of UQ on IKH . . . 42
  - 4.3.4 Results of UQ on VKH . . . 46

5 Uncertainty propagation on 1-D steady state models **51**
5.1 The use of PIPESIM in the industry . . . 51
5.1.1 The design of a multiphase flow pipeline . . . 51
5.1.2 The operation of a multiphase flow pipeline . . . 52
5.2 Case study for the Goldeneye field . . . 52
5.2.1 Case description and PIPESIM model . . . 52
5.2.2 Uncertainties in the Goldeneye field . . . 55
5.2.3 Sensitivity analysis . . . 60

6 Conclusions and recommendations **63**
6.1 Conclusions. . . . 63
6.1.1 0-D model . . . 63
6.1.2 1-D model . . . 64
6.2 Recommendations . . . 64

A The application of the UQLab toolbox **67**
A.1 Quantification of sources of uncertainty . . . 67
A.2 The model blackbox . . . 67
A.3 Uncertainty propagation . . . 67
A.4 Sensitivity analysis . . . 68

B The interface of the steady-state models **69**
B.1 SFC . . . 69
B.2 PIPESIM . . . 70

Bibliography **71**

List of Figures

1.1 An example of output uncertainty using different steady state models. 2

2.1 Different flow regimes for a horizontal flow, taken from Abdulmouti [21]. 7
2.2 Different flow regimes for a vertical pipe flow, taken from Abdulmouti [21]. 8
2.3 An example of a flow pattern map for (a) a vertically inclined pipe flow and (b) a horizontal pipe flow, with atmospheric conditions and a pipe diameter of D = 0.05m. Taken from van 't Westende [22]. 8
2.4 A flow pattern map where the uncertainty region for the boundary (grey shaded) is marked, taken from Cremaschi [2]. 9
2.5 A schematic overview of the cross section of a pipe line for a stratified flow. 11
2.6 A schematic example of a pressure curve and liquid holdup curve in a pipe flow. 12
2.7 An example of some commonly used distributions, taken from the UQLab manual [12]. 14
2.8 For two uniform distributed input variables: Monte Carlo sampling (left) and LHS (right). . . . 15
2.9 An example of PCE for a simple test function with $X \sim$ U(-1,1). For only 3 nodes, the PCE function (red) already approximates the actual model (blue) quite accurately. Taken from CFD4 Lecture Notes [10]. 15
2.10 A graphical explanation of the model description. 17

3.1 The response histogram of the Fanning friction factor, calculated using Monte Carlo sampling with 2000 samples in UQLab. 20
3.2 The approximation of $f = \frac{16}{Re}$ using polynomial chaos expansion. 22
3.3 An example of a sparse grid. 23
3.4 The error estimation of the mean of the friction factor for different samples using different methods, obtained with UQLab. 24
3.5 The error estimation of the standard deviation of the friction factor for different samples using different methods, obtained with UQLab. 25
3.6 The evaluation of the PCE models at 411 nodes for the Churchill relation. 26
3.7 The error between the PCE model and the true model at 411 nodes for the Churchill relation. . . 27
3.8 A comparison of the total Sobol indices for PCE and Monte Carlo sampling. 29

4.1 The output quantities of interest for a downward inclined stratified flow, taken from Picchi [5]. . 33
4.2 The output quantities of interest for a downward inclined stratified flow, obtained from SFC. . . 33
4.3 The Sobol indices for a horizontal stratified flow, taken from Picchi [5] and SFC. 34
4.4 The different angles. 35
4.5 The Sobol indices for a downward inclined stratified flow, taken from Picchi [5] and SFC. 35
4.6 Liquid hold-up probability distribution (a) and Sobol sensitivity indices (b) for a downward inclined stratified flow. The uncertainty associated to the superficial liquid velocity is reduced by a factor of two. 36
4.7 The error estimation of the mean of the quantities of interest for a horizontal stratified flow. . . 37
4.8 The error estimation of the standard deviation of the quantities of interest for a horizontal stratified flow. 37
4.9 The Sobol indices computed using the minimum amount of PCE samples, as follows by the error estimation, for a horizontal stratified flow. 38
4.10 The error estimation of the mean of the pressure drop for a downward inclined stratified flow. . 39
4.11 The error estimation of the standard deviation of the pressure drop for a downward inclined stratified flow. 39
4.12 Comparison of theory (///) and experimental data (-) of a flow pattern map for air-water, 25° horizontal pipeline with D = 2.5 cm. Taken from Taitel & Dukler [28]. The theory is obtained from Mandhane [30]. 40

4.13 The flow pattern decision tree, taken from the Technical Guide for Shell Flow Correlations [25]. 41
4.14 The effect of viscosity on the VKH and IKH neutral stability criteria. Air-liquid, atmospheric pressure, horizontal pipe, D = 5 cm. Taken from Barnea & Taitel [29]. 42
4.15 The distribution of the liquid holdup and IKH stability criterion for the transition regime from stratified to slug flow. 44
4.16 The PDF of the IKH stability criterion, where the probability for a stratified flow is highlighted blue. 44
4.17 The cumulative density function of the IKH, with the red line highlighting the neutral stability point. 45
4.18 The point on the flow map close to the transition from stratified to slug flow, calculated with SFC, using the mean of the input parameters of interest. 46
4.19 The output quantities of interest for a transition regime. 47
4.20 The CDF for the quantities of interest, obtained for a transition from stratified to slug flow. . . . 47
4.21 A schematic confidence interval around the VKH stability criterion. 48
4.22 A schematic confidence interval around the VKH stability criterion, with an increased uncertainty of factor 2. 48
4.23 A schematic confidence interval around the VKH stability criterion, with an increased uncertainty of factor 2 and a set value for the inclination angle. 49

5.1 The location of the Goldeneye field. 53
5.2 The two PIPESIM models. 54
5.3 The comparison of the two models. 54
5.4 Metocean data for the seasonal effects on the seabed temperature at 90 m water depth in the Central North Sea, taken from the Guidelines for the Hydraulic Design and Operation of Multiphase Flow Pipeline Systems [4]. 55
5.5 CDF reconstruction, based on fig. 5.5. A 99% percentile is obtained for 5.65 $^{\circ}C$, a 90% percentile at 6.6 $^{\circ}C$. 56
5.6 The PDF of Gumbel distribution for the wall roughness. 57
5.7 The measured pressure and temperature at the outlet of the pipeline, obtained from Lommerse [32]. 57
5.8 A schematic overview of the processing of the PCE samples. 58
5.9 The hydraulic curve of the Goldeneye field. The black line presents the mean of the system inlet pressure. The grey shaded area presents the standard deviation of the inlet pressure. The red (P50), blue (P90) and green (P10) lines presents the percentile intervals. 59
5.10 The pdf of the quantities of interest at a mass rate of 49.6 kg/s. 60
5.11 The PDF of the inlet pressure of the Goldeneye field. 60
5.12 The Sobol indices of the Goldeneye field for the output quantities of interest. 61

List of Tables

2.1 The possible mechanistic models in use to calculate the pressure drop [4]. 10

3.1 Common distributions and their orthogonal polynomials basis functions. 20
3.2 The modified Legendre nodes and weights for a different interval. 21
3.3 The first Legendre polynomials for interval [-1, 1] and [1000, 2000]. 21
3.4 Sobol's indices using both PCE and Monte Carlo sampling. 30

4.1 Input parameters of the SFC. 32
4.2 Input uncertainty representation, as presented by Picchi [5]. 32
4.3 The obtained output, for both horizontal stratified flow and downward inclined stratified flow for Picchi and the SFC. 32
4.4 Input uncertainty representation of sensitive input parameters for a horizontal stratified flow. . 36
4.5 Input uncertainty representation for sensitive input parameters for a downward inclined stratified flow. 38
4.6 Input parameters of the SFC that are taken into account for the IKH. 43
4.7 input uncertainty representation for a transition flow regime. 43

5.1 Selection of the field data, used for the selected steady state interval. 53
5.2 Input parameters of interest for PIPESIM. 55
5.3 Input representation for parameters of interest for PIPESIM. 57

Nomenclature

Abbreviations

CDF	Cumulative distribution function
GCR	Gas-Condensate-Ratio
GOR	Gas-Oil-Ratio
GSA	Global sensitivity analysis
IKH	Inviscid Kelvin Helmholtz
LARS	Least Angle Regression
LHS	Latin Hypercube Sampling
MC	Monte Carlo
OLS	Ordinary Least Squares
PCE	Polynomial chaos expansion
PDF	Probability density function
PFAS	Pipeline Flow Assurance and Subsea Systems
SA	Sensitivity Analysis
SFC	Shell Flow Correlations
UQ	Uncertainty Quantification
VKH	Viscous Kelvin Helmholtz

Symbols

α	Hold-up [-]
δ_{jk}	Kronecker delta
ϵ	Residual
ϵ	Wall roughness [m]
$\hat{y}_a$	Polynomial coefficients
λ	Volume fraction [-]
$\mathbb{R}^M$	The parameter space
μ	Mean
μ	Viscosity [Pa $\cdot$ s]
ϕ, β	Inclination angle [°]
ϕ_k	Orthogonal polynomial basis function
ρ	Density [kg/m^3]

ρ	Distribution
σ	Standard deviation
σ	Surface tension [N/m]
τ	Viscous stress tensor [N/m^2]
$\mathbf{u}$	Velocity vector [m/s]
$\mathbf{X}$	Joint vector of random variables
A	Cross sectional area [m^2]
A_G	Cross sectional area occupied by gas [m^2]
A_L	Cross sectional area occupied by liquid [m^2]
D	Pipe diameter [m]
E	The expectation, i.e., the mean
E	Total specific energy
F	Body forces [N/m^2]
f	Fanning friction factor
f	Function response
g	Gravitational acceleration [m/s^2]
h_L	Liquid film height [m]
L	Characteristic length [m]
M	Number of input variables
N	Number of samples
p	Pressure [N/m^2]
Q	Volumetric flow rate [m^3/s]
q	Heat conduction
Re	Reynolds number [-]
S	Sobol index
S	Wetted wall perimeter [m^2]
t	Time [s]
T_{amb}	Ambient temperature [$^\circ C$]
u_G	Actual gas velocity [m/s]
u_L	Actual liquid velocity [m/s]
u_m	Mixture velocity [m/s]
U_{SG}	Superficial gas velocity [m/s]
U_{SL}	Superficial liquid velocity [m/s]
$V(X)$	Variance

w_k	Polynomial weights for quadrature rules
X	Random variable
x	Streamwise coordinate [m]
x_k	Polynomial nodes for quadrature rules

1 Introduction

This research focusses on improved understanding of the uncertainty associated with steady state computational models used to predict multiphase flow behavior in pipelines. First, an overview of existing literature will be given in order to obtain the research objectives. From here, the research outline is determined.

1.1. Motivation

Multiphase flows are important for the production of oil and gas. An accurate prediction of multiphase flow characteristics is a key aspect in the design process of pipeline and flow assurance systems. In order to predict the behavior of such a complex flow, several models exist. There are three ways in which such models are explored: experimentally, theoretically and computationally. Experimental studies are expensive and difficult. Consequently, multiphase predictions rely predominantly on theoretical and computational models [1]. This is also the focus of the current work.

Numerous multiphase flow models have been developed for the prediction of the flow characteristics. These models are typically based on a mechanistic approach, which uses the conservation equations of mass, momentum and energy along with empirical or semi-mechanistic closure relationships [2]. However, the complexity of these models provide a lot of sources of uncertainty [1]. Some examples of sources of uncertainty in multiphase predictions include imperfect knowledge of the input parameters and modeling assumptions. The input parameters are an important source of uncertainty, since even a small variation in the input parameters can cause significant variations in the output. Uncertainties associated with input parameters can for instance be present due to inaccuracies in measurement equipment. The challenge is to design and operate systems with a quantifiable degree of confidence [2].

The investigation of the influence of input parameter uncertainty on output parameter uncertainty is referred to as Uncertainty Quantification (UQ). UQ has not been thoroughly investigated yet in the literature for multiphase flow models used in flow assurance. As stated by Keinath [3], Royal Dutch Shell was one of the first to introduce uncertainty assessment in their approaches in the late 60's. First, uncertainty assessment was focused on comparing field data with model data, but this only recently shifted to assessing the model response to uncertainty associated with the input range. At Royal Dutch Shell, the Multiphase Flow group, part of the Pipeline Flow Assurance and Subsea Systems (PFAS) department, focusses on flow prediction and assessment of multiphase flows, using both experimental data, field data and model predictions. Assessment of uncertainties present in input parameters has not been done yet on multiphase pipeline design and operations.

Fig. 1.1 shows the pressure drop against the throughput of a pipeline network. The pressure drop is calculated using different multiphase flow models. Even though each input parameter has the same value for each case, every outcome is different. This figure shows how the system is affected by different model assumptions. Furthermore, the pressure drop computed by every model is different from the value obtained from field data. This illustrates how the system is affected by imperfect knowledge of the input parameters and their variability.

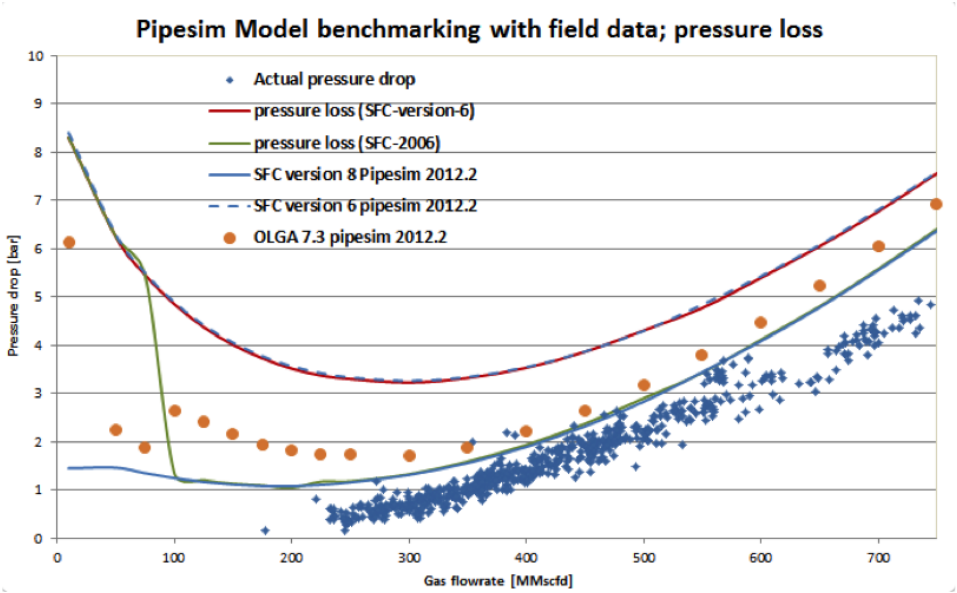

Figure 1.1: An example of output uncertainty using different steady state models.

This case study is an example of what quantifying uncertainty can contribute. By assessing uncertainty to the input, more insight can be obtained on its relation with the output quantity of interest, the pressure drop.

In this report, an investigation of the influence of uncertainty in input parameters is done for steady-state multiphase flow prediction models. By representing the input model parameters with a probability density function, associated with some type of uncertainty, the output uncertainty can be demonstrated. Furthermore, we want to investigate the influence of the different input parameter uncertainties and rank the input parameters in order of importance to the output uncertainty. This results in a better understanding of which parameter uncertainty has the largest impact on the system design and flow characteristics, and with that, which input parameter uncertainty should tried to be reduced during the design and operation of pipelines.

1.2. Literature review

Historically, flow assurance has focused on comparing field data and experimental data with model predictions [3]. Pereyra [19] compares field data and model predictions, and is one of the firsts to address uncertainties in the flow pattern map construction. The study presents a methodology for quantifying the confidence level of methods for gas-liquid two-phase flow pattern predictions in pipelines. An experimental database is compared with predictions of the Barnea unified model. 75% to 82% of the experimental data correspond to the model predictions, depending on the flow pattern. This study highlights the uncertainty in computing a flow pattern map and recommends a transition band instead of a sharp transition line, to show the uncertainty in the flow pattern transition.

A more recent example is the work of Dhoorjaty et al. [20], who seek an assessment of current multiphase simulation capabilities under flow conditions typical of the field. Three multiphase flow model tools are considered, but they do not exactly mention which tools they used. Additionally, these models are compared with their own model, the Virtuoso tool. This tool works with the same flow patterns and momentum equations as the other three tools, but they differ in the details of the closure relationships and tuning. For both two-phase and three-phase flows a comparison is made on the output quantities of interest, which are the pressure drop and liquid holdup. The different model predictions of the liquid holdup correspond reasonably well, both mutually as well as against experimental data. But when applying a small inclination on a small diameter pipe, field predictions will vary by 50%. The scatter is largest for intermediate hold-ups, in the transition region from stratified wavy flow to slug flow. The uncertainty in the pressure prediction can be reduced by 50% if the modeling parameters are adjusted properly.

One of the first case studies that considered uncertainty quantification (UQ) in multiphase flow models was performed by Holm et al. [6]. They analyzed uncertainties for oil and gas development fields, taking the Shtokman field as a case study. They aimed at finding a systematic approach in determining uncertainty. They developed a six-steps approach, 1) The identification of key flow assurance requirements. 2) The identification of key uncertain variables by one-at-a-time analysis. 3) Defining probability distributions for the input. 5) Applying Monte Carlo simlulations. 6) Obtaining probability distributions of the key flow assurance requirements. They limit themselves to one specific UQ method, namely Monte Carlo. They use the software OLGA, which contains a 1D-model. The results are presented in p10/50/90 intervals. The main outcome of their study was that the hydrocarbon liquid holdup fraction was sensitive to the liquid volume fraction at low flow rate. The inlet pressure at high flow rate was mainly sensitive to the hydraulic wall roughness.

Klavetter et al. [16] compared three propagation approaches, (namely the perturbation method, a Taylor series expansion based approach and Monte Carlo sampling) on a multiphase flow model, the TUFFP Unified Model. The case study was a horizontal multiphase flow in the slug regime. The analysis shows that the Taylor series expansion consistently overestimates the output uncertainty for all cases. The results of the perturbation method are similar to Monte Carlo simulation results, although the perturbation method does not give any information on the confidence level of the output uncertainty, in contrast to Monte Carlo sampling. Posluszny et al. [17] also performed uncertainty quantification on a vertical flow regime. Monte Carlo sampling is applied on the TUFFP Unified Model in order to determine the impact of the slug length uncertainty on the output quantify of interest, here the pressure drop and the liquid hold up.

Hoyer [18] reviewed a database of laboratory measurements, where the data is grouped per flow conditions. The most significant model parameters are identified for each group. OLGA is used for the comparison of the database. The combination of both the database and model predictions resulted in more insight in both the model uncertainties and the input uncertainties. He followed similar steps as [6]; (1) identify sources of uncertainty (2) quantify them through adequate probability distribution functions and (3) apply an appropriate propagation method, here Monte Carlo sampling type approach. The sensitivity analysis is performed using tornado plots. For his research, the wall roughness turned out to be the most sensitive input parameters with respect to uncertainty in the pressure drop.

Picchi and Poesio [5] performed both an uncertainty quantification and a sensitivity analysis on 1D-models with predictions and flow pattern transition boundaries for a two-phase pipe flow. They proposed a general approach for performing UQ and SA. They performed uncertainty quantification using Monte Carlo sampling. For the sensitivity analysis they used both quantitative methods like scatter plots, regression analysis and Sobol's method. They do not present the software they used for performing UQ and SA. For sake of brevity, Picchi and Poesio only presented the results for two flow regimes. For air/water stratified flow, the liquid flow rate and gas viscosity are the most critical parameters for the uncertainty, but also the inclination angle plays a crucial role. For an oil-in water dispersed flow, effective viscosity is important, in addition to the flow rates.

Keinath [3] focussed on the effect of uncertainties in the input values on the output quantity of interest, stating that defining uncertainty around a single parameter is as important as the identification of the input parameter itself. That study followed a similar approach as [6], where a large database of field and lab data was compared with model predictions. While the database contains a significant amount of data sets, there are still gaps and field data assessment is continuously ongoing. Understanding the variability in the input parameter for any model is extremely valuable for knowing how those variabilities propagate into a prediction uncertainty. One approach is to define a probability density function (PDF), associated with a specific parameter. Within in the PDF methodology, 5 methods are compared, which were introduced by Lee and Chen [11]. The 5 methods are (1) Simulation-based approaches, (2) Local expansion-based approaches, (3) Most probable point-based methods, (4) Functional expansion-based approaches and (5) Numerical integration-based approaches.

Keinath concludes that the definition of uncertainties on both fluid and system inputs are typically defined using experienced based knowledge and can be further refined through additional measurements. There are still several opportunities for refinement and improvement, for example continued improvement of the gathering of field data, additional focus on analytical methods, better definition of PDF of inputs, and development of flexibility to allow for additional approaches.

Cremaschi et al. [2] show the importance of determining uncertainty for flow predictions. They investigate an exhaustive list of possible techniques for performing uncertainty quantification, together with the advantages and disadvantages of these techniques. They do not perform uncertainty quantification themselves. They highlight 8 different reasons for uncertainty, of which the two most important for this research are (1) measurement errors of fluid properties and (2) inaccuracies in the model correlations. To better cope with uncertainty in the future, both short-, intermediate- and long term recommendations are given.

1.3. Research objectives

This research focusses on characterizing uncertainty in multiphase flow prediction models. The literature review shows that uncertainty quantification is a relatively new field and since only recently it is being adopted on flow assurance models. By presenting input variables with a PDF, which represents the associated uncertainty of those input variables, the output uncertainty can be demonstrated. This demonstration will result in more insight in how the model responds to uncertainty and more confidence in predictions can be obtained. In addition, a sensitivity analysis can be performed, that provides insight in the contribution of the input uncertainty to the output uncertainty. Understanding the variability in the input parameters as used in any model is extremely valuable for knowing how those variabilities propagate into a prediction uncertainty. So far, the literature review showed that only conventional models like Monte Carlo sampling are used. This research provides an extension to Monte Carlo sampling, by also applying more efficient techniques, such as the Polynomial Chaos Expansion.

The main objective of this research is:

Investigation of the effect of uncertainties in the input parameters on the output quantities of interest for steady state multiphase flow models for pipelines

In order to reach the main objective, a framework is built, which enables to systematically apply uncertainty quantification on steady state models. This framework comprises the following tasks:

1. Apply the UQ methodology on the Shell multiphase flow software in order to characterize and propagate uncertainty
2. Determine the best suitable approach for the uncertainty propagation
3. Perform a sensitivity analysis to find the most important parameters
4. Make a comparison with data from literature and with field data

In this research, uncertainty quantification is applied on two steady state multiphase flow models commonly used in the oil and gas industry. Both models will be validated using either literature or field data. A general framework will be provided, which can be used for future design and operations of a multiphase pipeline. This is relevant for Shell, since the Shell computational multiphase flow models only work with single point-values and do not take into account variability in the input parameters.

1.4. Research outline

To meet the research objective, it was first necessary to give an introduction into the subject and provide an overview of what has already been done; this was covered in the current chapter. In chapter 2, multiphase pipe flow and uncertainty quantification are introduced. Chapter 3 provides a more in depth explanation, substantiated with analytical approaches to provide more insight into UQ. Chapter 4 will focus on applying UQ to the first, 0-D, steady-state model, which applies the Shell Flow Correlations (SFC), using literature data as validation. An example of the application of UQ on the SFC will be provided with uncertainties in flow pattern predictions. Chapter 5 will provide an extension to the second, 1-D, steady-state model PIPESIM, where field data will be used as validation. For demonstration, a benchmarking study is performed on an actual gas-condensate field. Chapter 6 will give conclusions and recommendations for further research.

2

Multiphase pipe flow and its uncertainties

In order to investigate steady-state multiphase flow model predictions, uncertainty quantification techniques, such as uncertainty propagation and sensitivity analysis are applied. As this is a relatively new topic, an introduction of uncertainty quantification, the physical properties of the multiphase flow models and the software will be given in this chapter.

2.1. Characteristics of a multiphase flow

A multiphase flow is a fluid flow consisting of multiple fluid phases (i.e. gas, liquid or solid), or multiple components (i.e. liquid-liquid systems such as oil droplets in water). When working with multiphase flow models in flow assurance applications, the pressure drop and liquid holdup are commonly used output parameters in multiphase flow predictions. For a multiphase flow, there are several flow regimes, all with their own characteristics.

2.1.1. The different flow regimes

There are various typical flow patterns for both horizontal and vertical pipelines. First, the different flow regimes for a horizontal pipe will be discussed, after which we will discuss these for a vertical pipe.

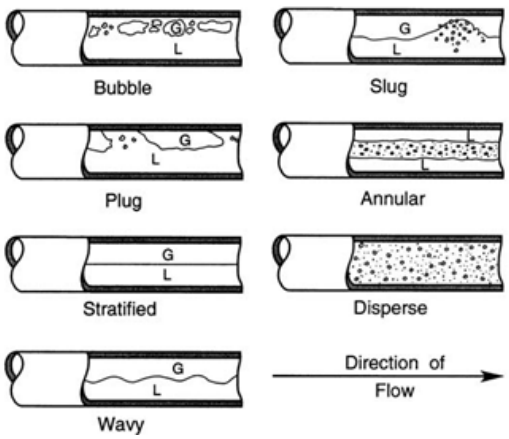

Figure 2.1: Different flow regimes for a horizontal flow, taken from Abdulmouti [21].

In fig. 2.1 one can distinguish the different flow regimes. A stratified smooth flow is characterized by two separate layers on top of each other, with the heavier fluid below the lighter one. This is a typical flow regime for a low production of both phases, here liquid and gas. When increasing the gas production a bit, small perturbations will occur, resulting in a stratified wavy flow regime. When the gas production keeps increasing, the gas will form the continuous phase and liquid is transported as droplets with the gas in the core of the flow. Close to the wall, a liquid layer forms. This is called annular flow. When the gas flow is moderate and

the liquid flow rate is increased, the interface will become unstable and a hydrodynamic slug flow will occur, also referred to as intermittent flow. Depending on the size of the gas bubbles, this is either called a plug flow (lower gas flow rate) or slug flow (increased gas flow rate). If the liquid flow rate is further increased, the liquid will form the continuous phase with a dispersion of small gas bubbles. This flow regime is called bubble flow [4].

For a vertical flow, the flow regimes are slightly different. The bubble flow regime, hydrodynamic slug and annular dispersed flow have the same behavior and flow rate properties, but for a low liquid flow rate and increasing gas flow rate, a stratified (wavy) flow does not exist but a churn flow regime appears. A churn flow is characterized by unstable gas bubbles, giving a chaotic transport of these gas bubbles of various shapes and sizes.

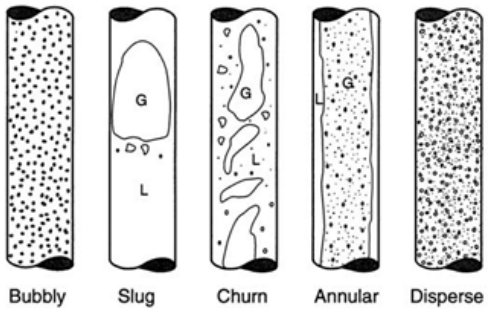

Figure 2.2: Different flow regimes for a vertical pipe flow, taken from Abdulmouti [21].

The flow pattern is determined mainly by the pipe diameter, pipe inclination, gas and liquid superficial velocities, gas and liquid densities, gas and liquid viscosities, and surface tension. A superficial velocity is the velocity of a fluid calculated as if the given fluid where the only fluid present in the pipe.
The dependence of the flow regime on these parameters can be shown in a flow pattern map. For each choice of parameters a new flow pattern map needs to be determined. A typical flow pattern map for a vertical flow and horizontal flow can be seen in fig. 2.3.

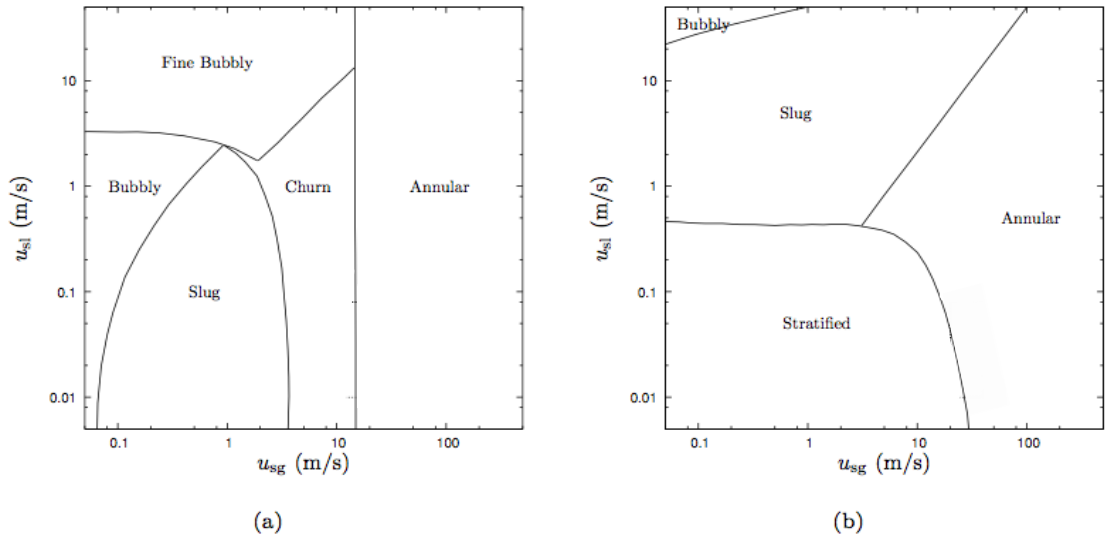

Figure 2.3: An example of a flow pattern map for (a) a vertically inclined pipe flow and (b) a horizontal pipe flow, with atmospheric conditions and a pipe diameter of D = 0.05m. Taken from van 't Westende [22].

Flow pattern boundaries are strongly dependent on fluid property characteristics of the phases, each with their own uncertainty, and are based on simplified models. The determination of the flow pattern is therefore an important source of uncertainty in multiphase flow system designs.

In fig. 2.4 an example of uncertainty in the flow pattern map is shown. The gray shading along the black lines represent the uncertainty region around the boundary of a flow regime [2].

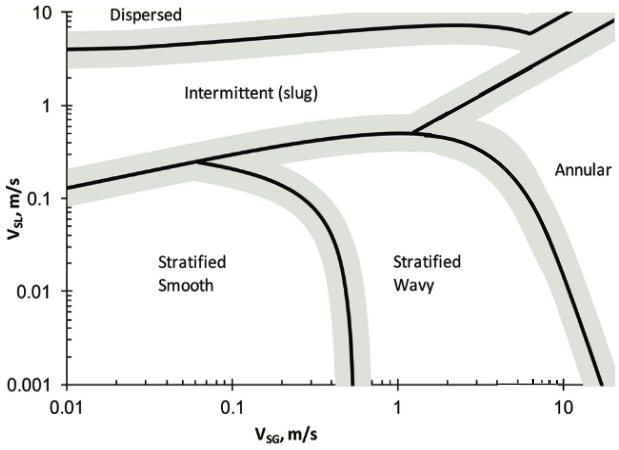

Figure 2.4: A flow pattern map where the uncertainty region for the boundary (grey shaded) is marked, taken from Cremaschi [2].

The confidence in multiphase flow predictions can be increased by quantifying the uncertainty in model predictions: this is known as uncertainty quantification. Uncertainty quantification will further be discussed in section 2.2.

2.1.2. Mechanistic modeling

In order to obtain output quantities of interest for a multiphase flow regime, mechanistic modeling is used. Mechanistic modeling uses the conservation equations of mass, momentum and energy as a starting point. These equations, the so-called Navier-Stokes equations, are given by [8]:

$$\frac{\partial \rho}{\partial t} + \nabla \cdot (\rho \mathbf{u}) = 0, \tag{2.1}$$

$$\frac{\partial \rho \mathbf{u}}{\partial t} + \nabla \cdot (\rho \mathbf{u} \otimes \mathbf{u}) = -\nabla p + \nabla \cdot \boldsymbol{\tau} + \rho \mathbf{g}, \tag{2.2}$$

$$\frac{\partial \rho E}{\partial t} + \nabla \cdot (\rho E \mathbf{u}) = -\nabla \cdot (p\mathbf{u}) + \nabla \cdot (\boldsymbol{\tau} \cdot \mathbf{u}) - \nabla \cdot \mathbf{q} + \rho \mathbf{g} \cdot \mathbf{u}, \tag{2.3}$$

where ρ is the density, t is the time and $\mathbf{u}$ is the velocity vector. p is the pressure, $\boldsymbol{\tau}$ is the viscous stress tensor and $\boldsymbol{g}$ is the gravitational acceleration. E is the total specific energy and q is the heat conduction.
For pipe flow applications, these equations are usually simplified by averaging over the pipe cross section. This leads to a one-dimension formulation, depending on the main pipe coordinate. The averaging requires the formulation of closure relations, such as for the wall friction and for the interfacial stress between phases.

To obtain relevant output parameters, like pressure drop, these conservation equations can be solved, along with empirical or semi-mechanistic closure relationships. Depending on the type of flow regime, there are different closure relationships, or sub-models. A quick overview of the mechanistic models and sub-models for the calculation of the pressure drop for different flow regimes is given in table 2.1.

These mechanistic models were first introduced by Wallis [7] and Taitel & Dukler [28]. The specific explanation of these models will not be discussed here. More information on the closure models can be found in several textbooks, like for instance Brennen [1].

Table 2.1: The possible mechanistic models in use to calculate the pressure drop [4].

Flow Pattern	**Model**	**Sub-model**
Dispersed bubble flow	Drift-flux model	Wall friction Distribution parameter Bubble rise velocity
Separated flow (stratified/annular)	Two-fluid model	Wall friction Interfacial friction Interfacial velocity Interfacial shape Liquid entrainment
Intermittent flow	Drift-flux + two-fluid model	Wall friction Distribution parameter Bubble rise velocity Void fraction in liquid slug body Slug frequency Length of liquid slug with gas bubble Bubble shape

2.1.3. The pressure drop

The pressure drop follows from the governing, one-dimensional conservation equations for mass, momentum and energy. Eq.(2.2) represents the conservation of momentum, and is also referred to as Newton's second law. Newton's law dictates a force balance in terms of acceleration of the flow, gravity forces, wall forces and pressure drop.

When applying Newton's second law, eq. (2.2), to a two-phase flow, two momentum balances follow:

$$\frac{\partial}{\partial t}\rho_G A_G U_G + \frac{\partial}{\partial x}\rho_G A_G U_G^2 = -A_G\frac{\partial P}{\partial x} - \rho_G \mathrm{g}\cos\phi A_G\frac{\partial h_L}{\partial x} - \rho_G A_G \mathrm{g}\sin\phi - \tau_{wG}S_{wG} - \tau_i S_i \tag{2.4}$$

$$\frac{\partial}{\partial t}\rho_O A_O U_O + \frac{\partial}{\partial x}\rho_O A_O U_O^2 = -A_O\frac{\partial P}{\partial x} - \rho_O \mathrm{g}\cos\phi A_O\frac{\partial h_L}{\partial x} - \rho_O A_O \mathrm{g}\sin\phi - \tau_{wO}S_{wO} + \tau_i S_i, \tag{2.5}$$

where the subscripts O and G define the phase of the fluid, here oil(O) and gas(G) respectively. These equations hold for a stratified flow [8]. Furthermore, in these equations x denotes the stream wise coordinate and A the cross sectional area covered by a certain phase. Furthermore, U is the phase velocity, ϕ is the pipe inclination with respect to the horizontal, h_L denotes the height of the liquid layer, and S_w is the wall perimeter wetted by a certain phase, S_i is the width of the interface, and τ_i is the interfacial stress.

Fig. 2.5 gives a graphical explanation of the stratified flow and the associated parameters.

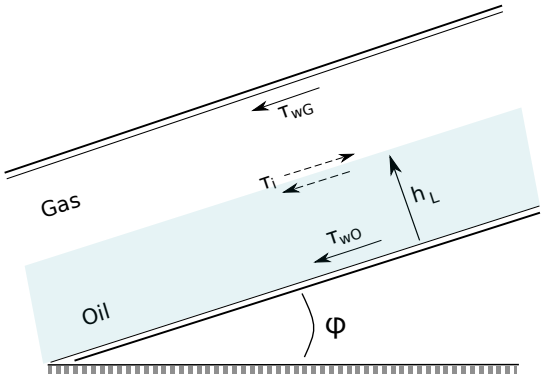

Figure 2.5: A schematic overview of the cross section of a pipe line for a stratified flow.

Based on the flow specifications and the geometry of the pipe flow, the momentum equations can be simplified. In order to solve the relevant equations for the pressure drop, several mechanistic models are used. The pressure drop in a multiphase pipeline in steady state conditions follows from a balance of pressure with the wall friction and the gravity force. The pressure drop is friction dominated at high production, whereas it is gravity-dominated at low production [4]. The pressure drop along the pipeline is commonly presented in a pressure curve, as presented in fig. 2.6.

2.1.4. The liquid holdup

The liquid holdup describes the liquid accumulation in the pipeline. This quantity is very important, for instance for the design of operations like start-up, ramp-up, pigging and blowdown [4]. An important physical property of a multiphase flow is the split into liquid and gas flow rates, Q_L and Q_G . When the volumetric gas flow rate Q_G and volumetric liquid flow rate Q_L are scaled by the pipe cross section A, one obtains the so called superficial velocities:

$$U_{SG} = \frac{Q_G}{A}, \quad U_{SL} = \frac{Q_L}{A}. \tag{2.6}$$

These superficial velocities are commonly used in multiphase flow predictions.

The liquid holdup represents the ratio of the pipe cross section occupied by the liquid A_L and the pipe cross section A. For the gas holdup a similar ratio exists for the pipe cross section occupied by the gas A_G and the pipe cross section A. The liquid holdup and gas holdup are given by:

$$\alpha_L = \frac{A_L}{A}, \quad \alpha_G = \frac{A_G}{A}. \tag{2.7}$$

Note that: $\alpha_G + \alpha_L = 1$.

A typical liquid holdup graph along the pipeline is presented in fig. 2.6.

Fig. 2.6 is also referred to as the hydraulic curve. The gravity-dominated domain will result in unstable production, which is not desirable. Obtaining a hydraulic curve during the design of a multiphase flow pipeline will give more insight in the flow behavior, and what choice of flow rate needs to be taken in order to avoid unstable production.

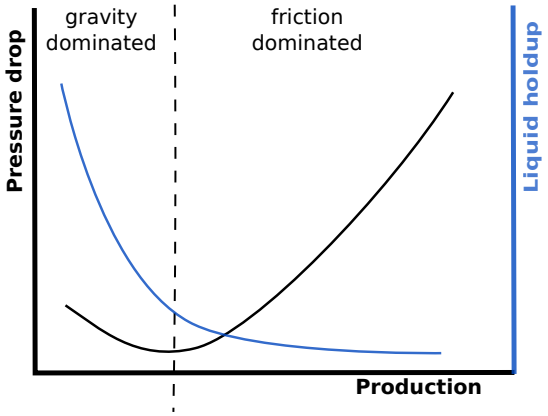

Figure 2.6: A schematic example of a pressure curve and liquid holdup curve in a pipe flow.

2.1.5. Multiphase flow prediction models

In order to predict the behavior of a multiphase flow, several computational models exist. We consider steady state models, which assume that there will be no change over time. There are multiphase flow models that take into account a single pipe segment of a pipeline, from now on referred to as 0-D models. A 0-D model calculates one specific point in the pipe without taking into account the flow development and thermal effects. From these models, a flow pattern map can be obtained, providing more insight in the flow characteristics. 1-D models are an extension of the basic 0-D model and do take into account the flow development throughout the pipeline profile. 1-D flow models are used for the assessment of a suitable design and operation settings. In this research, both models will be used. The physics and calculations behind the models are defined as "blackbox", which means that we will not interfere with the calculations and model assumptions. Only the output delivered by the model is relevant for this research.

Shell Flow Correlations

Shell Flow Correlations (SFC) is a 0-D, proprietary Shell software program which calculates for instance the holdup and pressure drop for the given phases (oil, water, gas), and constructs a flow pattern map. The input parameters are the superficial velocity, density, surface tension, viscosity (both gas and liquid for all the mentioned parameters), watercut, inclination angle, wall roughness and pipe diameter.

PIPESIM

PIPESIM is a 1-D steady-state tool developed by Schlumberger. PIPESIM simulates multiphase flow in pipelines using mechanistic modeling. For the model correlations it makes use of, among others, the Shell Flow Correlations. Either a singe branch or a complete pipeline network can be evaluated. Besides multiphase flow properties like pressure drop, liquid holdup and flow pattern, it also makes use of the thermal properties along the pipeline. The assessment of pipeline performance can be done, for instance, by obtaining a hydraulic curve.

2.2. Uncertainty Quantification

This report will focus on the application of uncertainty quantification techniques and sensitivity analysis to multiphase flow problems in pipelines. Uncertainty quantification and sensitivity analysis are defined according to Iaccarino as [9]:

Uncertainty quantification (UQ) aims at identifying the overall output uncertainty in a given system. UQ investigates the influence of an uncertainty of an input parameter on an output quantity of interest.

Sensitivity analysis (SA) investigates the connection between inputs and outputs of a model. More specifically, it allows to identify how the variability in an output quantity of interest is connected to variability in an input in the model and which input sources will dominate the response of the system. In other words, it ranks the input parameters by importance in determining the variation in the output.

These analyses are often connected and done in parallel, but a main difference is that in UQ the output is not ranked according to its input contribution.
In many uncertainty quantification applications, uncertainty propagation is a commonly used approach for performing UQ. Uncertainty propagation is a forward approach. Cremaschi [2] presented 3 steps that have to be carried out to perform uncertainty propagation:

- **Identify the type of uncertainty**
  Uncertainty can be generally divided into two types: (1) epistemic, the systematic uncertainty, which depends on the observer and can be reduced by learning, and (2) aleatoric, the statistical uncertainty, which will always occur and is representative of unknowns that differ each time one runs an experiment, and therefore is irreducible [10].

- **Select the appropriate mathematical representations for the uncertainties**
  Various mathematical representations for uncertainty exist, but the most commonly used one is probability theory, which is the analysis of random phenomena. Probability theory can be used to describe inherent, irreducible, physical randomness in a system or a lack-of-knowledge of a deterministic value. When applying probability theory, each parameter can be presented by a random variable and a corresponding probability density function (PDF). A probability density function describes the relative likelihood that a variable takes on a certain value.
  Several input parameters, including their distributions, can be grouped together in a random vector with a joint PDF. The notation used for describing the random vector $\boldsymbol{X}$ is $\boldsymbol{X} \in \mathbb{R}^M$, where M describes the number of input variables $(X_1, ..., X_M)$[12].
  The output quantity of interest is given by a model that is a function of random variables with an associated PDF. The notation, used in this research, for describing the output quantity of interest is:

$$y = f(\mathbf{X}). \tag{2.8}$$

  All propagation methods used in this research describe a probabilistic input by a distribution rather than a point value. There are many different distributions employed in many fields of applied sciences, some commonly used distributions are [12]:

  - **Uniform distribution**. Commonly used to represent variables with unknown moments and known supports on the interval [a,b] and it is represented by the notation $X \sim \mathcal{U}$(a,b).
  - **Normal or Gaussian distribution**. Commonly used to represent a measurement error and it is presented by the mean μ and standard deviation σ, using the notation $X \sim \mathcal{N}(\mu, \sigma)$.

  Examples of these distributions are also displayed in fig. 2.7.

- **Choose an appropriate propagation method to quantify the resulting uncertainty**
  Lee and Chen [11] distinguished 5 categories of uncertainty propagation methods, of which the two most important ones for our purpose are:
  (1) Simulation-based approaches, such as Monte Carlo sampling and Latin Hypercube sampling, and (2) Functional expansion-based approaches, such as Polynomial Chaos Expansion. The other techniques are less suitable for a large number of samples or dimensions or they are limited in their ability to construct a PDF, and therefore will not be treated in this report.

2.2.1. Simulation-based approaches

Simulation based approaches are a straight-forward and universally applicable sampling approach, and therefore a popular method in UQ. Two commonly used sampling methods are Monte Carlo sampling and Latin Hypercube Sampling.

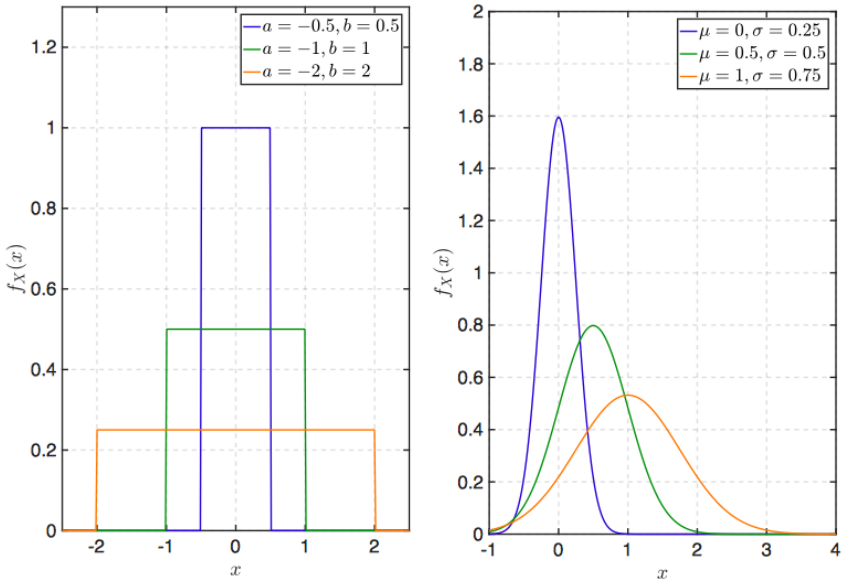

(a) Uniform distribution (b) Normal distribution

Figure 2.7: An example of some commonly used distributions, taken from the UQLab manual [12].

The Monte Carlo method

The Monte Carlo method is the most popular sampling technique and is used for forward uncertainty propagation. The Monte Carlo method is based on repeated random sampling and follows the following steps:

- Assume/determine a distribution function to represent each input variable
- Sample each input variable
- Calculate the output quantity of interest using the random samples from the input distributions
- Repeat this many times to obtain an output distribution

The output distribution is typically organized as a histogram.
The method has the advantage that it is simple, universally applicable and does not require any modification to the available computational tools. One disadvantage of using Monte Carlo is that the convergence rate is rather slow; the convergence rate of the error is approximated by:

$$C \approx \frac{1}{\sqrt{N}}, \tag{2.9}$$

where N is the number of samples. For example, when adding one extra digit to get a more accurate approximation, this will require 100 times more simulations. This increase in the number of samples makes Monte Carlo computationally expensive.

Latin Hypercube Sampling

Given the fact that Monte Carlo can get expensive, Latin Hypercube Sampling (LHS) has been developed to accelerate Monte Carlo. In order to speed up the process, the range of each input random variable is divided in intervals with equal probability. The occurrence of low probability samples is reduced, and thus the convergence is faster [9]. Fig. 2.8 shows the difference between sampling with Monte Carlo and LHS for the 2-dimensional case of 80 samples. The random variables are presented by a uniform distribution: $\mathbf{X} \sim \mathcal{U}(0,1)$. As can be seen in the figure, the samples using LHS are more equally distributed, due to the intervals with equal probability.

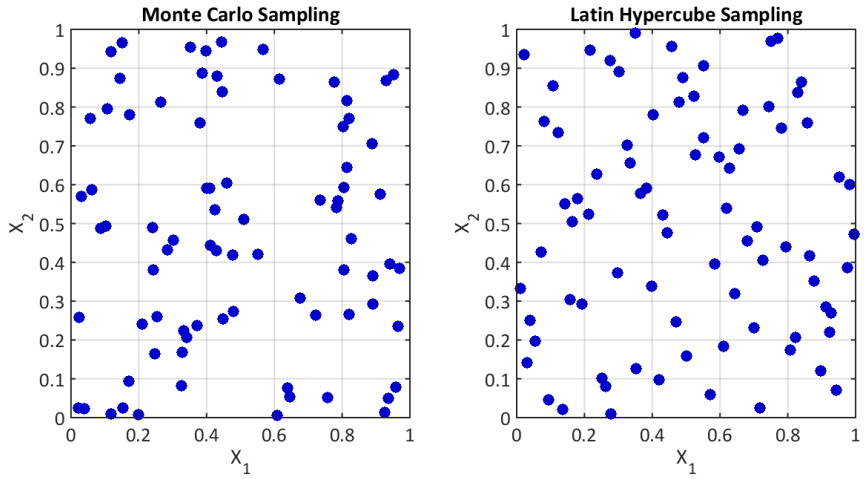

Figure 2.8: For two uniform distributed input variables: Monte Carlo sampling (left) and LHS (right).

Even though LHS is an improvement compared to Monte Carlo, it is still rather expensive when the number of input parameters increases.

2.2.2. Functional expansion-based approaches

In order to reduce computational costs, functional expansion-based approaches try to substitute the expensive-to-evaluate computational models with inexpensive-to-evaluate surrogates.

Polynomial chaos expansions

Polynomial chaos expansion (PCE) is a sampling-based method, where the model is approximated using a sum of orthogonal polynomials. The polynomial basis evaluates the model on a number of nodes. These nodes correspond to the root of the basis polynomials. By approximating the desired output by a polynomial, one can simplify and speed up the computation.

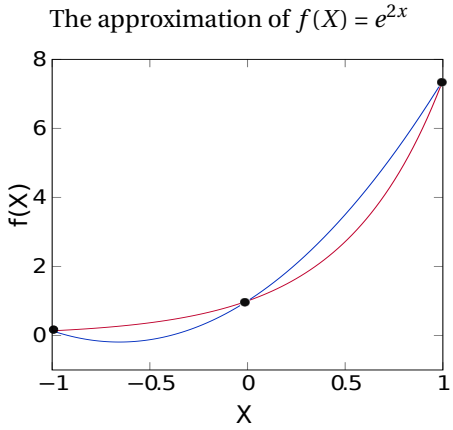

Figure 2.9: An example of PCE for a simple test function with $X \sim$ U(-1,1). For only 3 nodes, the PCE function (red) already approximates the actual model (blue) quite accurately. Taken from CFD4 Lecture Notes [10].

In fig. 2.9, a simple test function is approximated using PCE at 3 nodes. For this case, the input parameter X is assumed to have a uniform distribution between -1 and 1. The approximation is already quite accurate, and a few more nodes will make the approximation even more accurate. One can imagine that for more complex, higher dimensional problems, PCE will speed up the computations, given that less samples than simulation-based approached are needed in order to get a good approximation of the model.

PCE is a very effective approach for performing UQ, but for approximating functions with discontinuities, the model has its limitations. When performing UQ on such a discontinuous function, simulation-based sampling approaches can be a better alternative. More detailed information about polynomial chaos expansion will be given in chapter 2.

2.2.3. Sensitivity analysis

Performing a sensitivity analysis is, as briefly discussed before, useful for describing how the uncertainty in the output is affected by the uncertainty in the input. Besides, it is also useful for finding unimportant parameters and for reducing the dimension of the problem by removing the input parameters with almost no influence on the output uncertainty.

There are various methods for performing sensitivity analysis. For instance, one can do a qualitative or quantitive analysis. If one wants to do a qualitative analysis, where only the correlation between input and output is graphically represented, one-parameter-at-a-time approaches like scatter plots can be applied. Another distinction between methods for performing sensitivity analysis are a local or global analysis. A local analysis looks at the influence of one parameter, whereas a global analysis looks at the contribution of all the parameters, together with interaction effects. Interaction effects are the effects of a combination of two, or more, parameters.

This research focusses on quantitative, global sensitivity analysis (GSA) since we are interested in the contribution of each single input parameter. For a quantitative, global sensitivity analysis, there are two main methods that have been applied to multiphase flow models, the Morris method and Sobol's method. Sobol's method also takes into account interaction effects and will be used for performing a sensitivity analysis in this work.

Sobol's method

Sobol's method is a global sensitivity method and takes into account the entire parameter space, i.e. it investigates the connection between input and output of a model and ranks the contribution of each input parameter on the output uncertainty. One of the main advantages of Sobol's method is that it allows to distinguish between the total and the interaction effect of a specific input parameter on the output uncertainty. It is a variance based method [5].

The variance measures how far each number in a set is located from the mean. The variance of the output quantity of interest y is given by:

$$V(y) = V(f(X)) = \sigma^2 = \int \left(f(X) - \mu\right)^2 \rho_X(X) dX, \tag{2.10}$$

where $V(X)$ is the variance, σ is the standard deviation, μ is the mean and X is a random variable.

A variance based method decomposes the variance of the output of the model into fractions which can be attributed to inputs or sets of inputs. These (partial) variances are computed from the decomposition of the function of random variables. Furthermore, the variances are normalized with the total variance to represent the Sobol indices. The Sobol indices are sensitivity indices that describe the effect of a variable X_i on the output. Sobol indices can be of first order or higher order. A first order index describes the contribution of one single parameter, whereas a second order index describes the contribution of interaction effects between two parameters, and so on. The indices take values between 0 and 1: if the value is relatively high it implies that the contribution of the input variable on the uncertainty to the output is high.

Traditionally, Sobol's indices are computed using simulation-based approaches like Monte Carlo. The Sobol indices can also be computed with the PCE approach. In chapter 3.3, a more in-depth analysis of Sobol's method will be given.

2.2.4. UQLab

The previously mentioned UQ methods are available in UQLab. This is a framework for uncertainty quantification, developed by ETH Zürich. It is open-source for academic purposes and easy to use. When downloading the required UQLabCore, one can carry out uncertainty propagation through Monte Carlo sampling, sensitivity analysis, polynomial chaos expansion, and more [12]. UQLab will be used in this research.

2.3. Methodology

Similar to the literature ([6], [2], [18]), a general framework is created in this thesis, presented in fig. 2.10. It follows 4 steps, which, in theory, can be applied on every black box model. The first step is to identify and quantify the sources of uncertainty in the input, following the steps presented by Cremaschi [2] in section 2.2. These sources of uncertainty will be fed to a model blackbox. The output distribution for the quantity of interest will be calculated using a flow prediction model, either SFC or PIPESIM for this research. Step 4 consists if performing a sensitivity analysis. The sensitivity analysis is done using Sobol's method and can be used to reduce the dimension of the problem by excluding unimportant parameters.
The whole framework is executed by using UQLab.

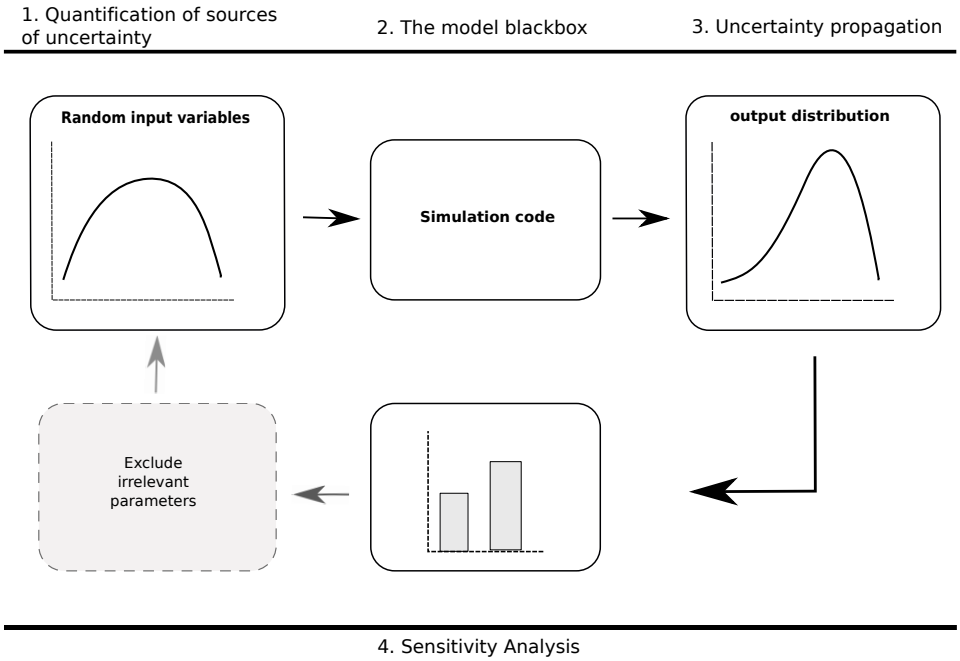

Figure 2.10: A graphical explanation of the model description.

3

UQ methods for the propagation

The goal of this section is to provide an introduction to the various methods, before applying UQ and SA to the Shell software tools with a large number of input parameters. This is substantiated with a simple example of performing uncertainty quantification and sensitivity analysis on a classic fluid mechanics relation, namely the Churchill relation.

3.1. Uncertainty Quantification

We are interested in studying the effect of uncertainties on the output quantity of interest. Here, both the Monte Carlo sampling and polynomial chaos expansion are used on the Churchill relation. The Churchill relation is a relation for determining the friction factor in fully developed pipe flow, which only depends on the scaled wall roughness $\frac{\epsilon}{D}$ and the Reynolds number Re.
The Churchill relation is given by:

$$f(Re,\epsilon) = 2\left[\left(\frac{8}{Re}\right)^{12} + \frac{1}{(A+B)^{\frac{3}{2}}}\right]^{\frac{1}{12}}, \tag{3.1}$$

$$A = \left(-2.457\ln\left[\left(\frac{7}{Re}\right)^{0.9} + 0.27\frac{\epsilon}{D}\right]\right)^{16}, \tag{3.2}$$

$$B = \left(\frac{37530}{Re}\right)^{16}, \tag{3.3}$$

where f is the Fanning friction factor, Re the Reynolds number, D is the pipe diameter and ϵ is the wall roughness. The Reynolds number is defined as:

$$Re = \frac{\rho U D}{\mu}, \tag{3.4}$$

where μ is the dynamic viscosity, U is the velocity, and ρ is the density.

This correlation holds for all types of flow, but for laminar flows (Re<2000) the equation can be simplified to:

$$f(Re) = \frac{16}{Re}. \tag{3.5}$$

The Fanning friction factor depends on three input variables, the Reynolds number, the wall roughness and the pipe diameter. For this example, we are interested in studying the effect of uncertainties in the Reynolds number and in the wall roughness on the friction factor. The pipe diameter is set to 0.3 m.

Both analytical results and simulation results obtained with UQLab are presented. Examples of how to implement UQ using the UQLab toolbox, applied on the Churchill relation, can be found in appendix A.

3.1.1. Simulation-based approaches

Simulation-based approaches describe a probabilistic input by a distribution rather than by a point value. The two input parameters, the Reynolds number *Re* and the wall roughness ϵ, are assumed to have a normal distribution. The Reynolds number has a mean μ of 4000, with a standard deviation σ of 10% of the mean. The wall roughness, ϵ, has a mean of $3{\cdot}10^{-4}$ m, with an associated deviation of 10% of the mean,

$$Re \sim \mathcal{N}(4000, 400), \quad \epsilon \sim \mathcal{N}(3 \cdot 10^{-4}, 3 \cdot 10^{-5}).$$

In order to ensure that the random variables attain strictly positive values, the normal distributions are truncated at $\mu \pm 3\sigma$.
The distribution of the friction factor is calculated with Monte Carlo sampling using 2000 samples.The resulting distribution of the friction factor is presented in fig. 3.1.

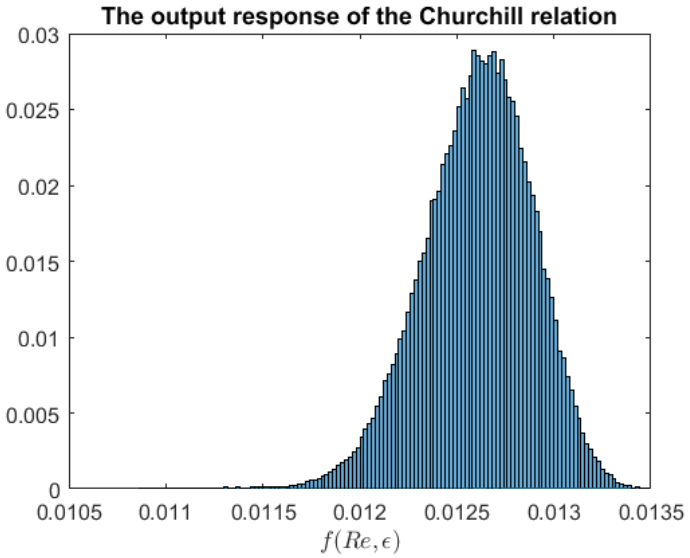

Figure 3.1: The response histogram of the Fanning friction factor, calculated using Monte Carlo sampling with 2000 samples in UQLab.

3.1.2. Functional expansion-based approaches

The output model can be approximated with different polynomial types. These polynomials depend on the type of distribution of the input variable X. The polynomial is built from a set of univariate orthogonal polynomial basis functions, ϕ_k. The orthogonality relation is given by [13]:

$$\int \phi_j(X)\phi_k(X)\rho_X dX = \delta_{jk}, \tag{3.6}$$

where j and k correspond to the polynomial degree, ρ is the PDF of the input variable. For the commonly used distribution types, these polynomials are given by:

Table 3.1: Common distributions and their orthogonal polynomials basis functions.

$\rho(\mathbf{X})$	$\phi(\mathbf{X})$
Uniform	Legendre polynomial
Normal	Hermite polynomial

The model is approximated by a polynomial, constructed from polynomial basis functions. The approximated function is given by:

$$y = f(\mathbf{X}) \approx \sum_{a \in \mathbb{R}^M} \hat{y}_a \phi_a(\mathbf{X}), \tag{3.7}$$

where the coefficients $\hat{y}_a$ can be built for instance using quadrature rules:

$$\hat{y}_a \approx \sum_{k=1}^{N} f(x_k)\phi_a(x_k)w_k. \tag{3.8}$$

The weights w_k and nodes x_k are determined by the marginal PDFs of the independent input parameters, and they correspond to the roots of the corresponding polynomial basis functions, like for instance the ones given in table 3.1 [13].

Let us provide an example using the Churchill relation. For the sake of simplicity, we consider the Churchill relation for a laminar flow. Following eq (3.5), the Churchill relation simplifies to $f = \frac{16}{Re}$. Now assume a uniform distribution for *Re*, ranging between 1000 and 2000; *Re* ~ *U(1000,2000)*.

Re has a uniform distribution, the corresponding orthogonal polynomial basis functions are Legendre polynomials. These polynomials are conventionally constructed on the interval [-1, 1]. Each polynomial may be expressed using Rodrigues' formula:

$$\phi_n = \frac{1}{2^n n!}\frac{d^n}{dx^n}\left[\left(x^2-1\right)^n\right], \tag{3.9}$$

where n represents the degree of the polynomial.
The weights and nodes are also computed for the basis interval of [-1,1] and adjusted for a change of interval.

Table 3.2: The modified Legendre nodes and weights for a different interval.

-	[-1, 1]	[a,b]
nodes	$\phi_n(x_i)$=0	$\tilde{x_i}$=$\frac{b-a}{2}\cdot x_i + \frac{b+a}{2}$
weights	$w_i = \frac{2}{(1-x_i^2)[\phi_n'(x_i)]^2}$	$\tilde{w_i} = w_i \cdot \frac{b-a}{2}$

The polynomial for a different interval can be constructed from the shifted nodes, presented in table 3.2. Take for example the first order polynomial $\phi_1 = x$. Rewriting the equation, the polynomial becomes:

$$\phi_1(\tilde{x}) = (-\frac{b+a}{2} + \tilde{x_i})\frac{2}{b-a} = -3 + 0.002\tilde{x}. \tag{3.10}$$

For the interval [1000, 2000], the first three Legendre polynomials are given in table 3.3.

Table 3.3: The first Legendre polynomials for interval [-1, 1] and [1000, 2000].

$[-1,1]$	$[1000,2000]$
$\phi_0 = 1$	$\phi_0 = 1$
$\phi_1 = x$	$\phi_1 = 0.002x$-3
$\phi_2 = \frac{1}{2}$ (3x^2-1)	$\phi_2 = 0.000006x^2$ - 0.018x + 13

Following eq. (3.8) the Churchill relation can be approximated using polynomials and coefficients.
For example, consider an expansion with 2 samples.
First, we calculate the nodes, which are the roots of the 2nd order Legendre polynomial, and the weights:

$$x_0 = 1211.3 \quad x_1 = 1788.7,$$

$$w_0 = 0.5 \quad w_1 = 0.5.$$

Then the coefficients y_i are calculated with Gauss Legendre quadrature rules:

$$\hat{y_0} = w_0 f(x_0)\phi_0(x_0) + w_1 f(x_1)\phi_0(x_1), \tag{3.11}$$

$$\hat{y_1} = w_0 f(x_0)\phi_1(x_0) + w_1 f(x_1)\phi_1(x_1). \tag{3.12}$$

The coefficients and polynomials are used to approximate the output function, using eq. (3.7) .

This can also be done for more samples to get a more accurate prediction of the output. Fig. 3.2a and 3.2b show how the output is approximated using polynomials. The nodes can be seen on the x-axis, which correspond to the calculated roots of the polynomial. One can see that with only 4 samples, the output approximation is already quite accurate. This is because the function under consideration is very smooth in the interval considered.

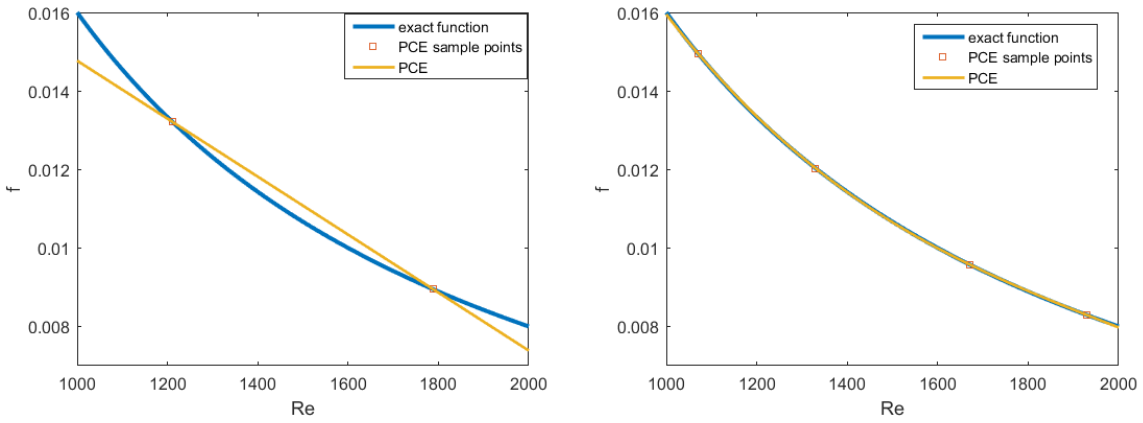

(a) 2 samples

(b) 4 samples

Figure 3.2: The approximation of $f = \frac{16}{Re}$ using polynomial chaos expansion.

The approximation of a polynomial using quadrature rules in higher dimensions, needs a number of integration points in each dimension, leading to $N = (p+1)^M$ integration points, where N represents the number of integration points, p is the maximal polynomial degree and M is the number of input variables, also referred to as the dimension.

If a problem reaches a high-dimensional state, i.e. the total number of input variables is high, the number of integration points will become large, resulting in high computational costs. This is called the curse of dimensionality. In order to alleviate this problem, methods using sparse grids can be applied.

3.1.3. Functional expansion-based approaches on sparse grids

A problem is considered to be high-dimensional when $M > 4$. A sparse grid is a smart way to minimize the number of integration points, but still keep a good accuracy in higher dimensions. A sparse grid can be applied on the quadrature method, using Smolyak' sparse quadrature. But there are also other methods that can be used to calculate the polynomial coefficients, where a sparse grid can be applied. An example of a sparse grid is shown in fig. 3.3.

Sparse quadrature

Smolyak was one of the first to propose sparse grid methods. Weights and nodes are constructed from a combination of lower order standard quadrature terms. The idea is that these weights and nodes yield the same accuracy, but fewer points are needed to reach this accuracy [15]. In UQLab, Smolyak's sparse quadrature can also be applied and is an efficient approach for high-dimensional problems ($M > 4$). However, if a non-nested quadrature rule is chosen like Smolyak sparse quadrature, it will need even more integration points than full grid quadrature for low dimensional problems.

The example of a sparse grid, shown in fig. 3.3, is an example of a nested grid. Nesting of nodes is a very efficient approach for constructing high dimensional grids. For every new iteration with increasing nodes, the old nodes are reused and therefore it takes less computational time to compute the new iteration. Unfortunately, nested quadrature rules are not implemented in UQLab.

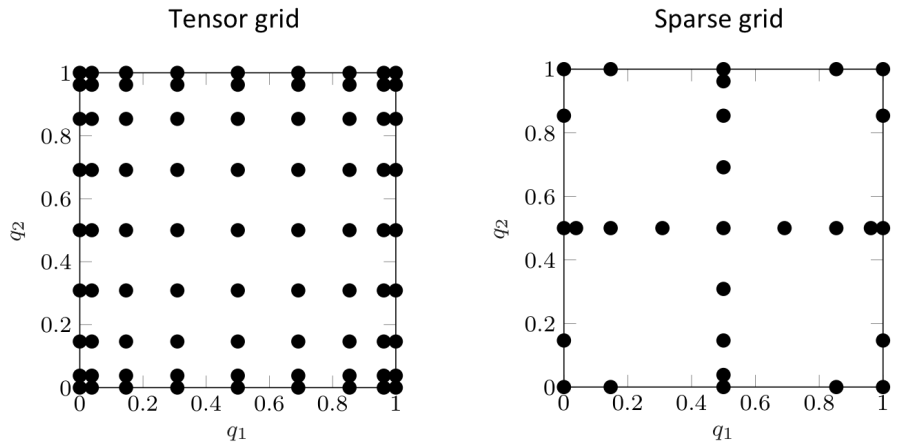

Figure 3.3: An example of a sparse grid.

Least squares minimization

Another method for calculating the polynomial coefficients, is by using least squares minimization. Least squares minimization determines the coefficients of the polynomial by relying on the sample points where the original model is evaluated, which is also referred to as the experimental design [23]. Recalling the polynomial chaos expansion presented in eq. (3.7), the exact expansion of the model under consideration can be written as a function of the polynomial chaos expansion and a residual ϵ:

$$Y = f(\mathbf{X}) = \sum_{a \in \mathbb{R}^M} \hat{y}_a \phi_a(\mathbf{X}) + \epsilon. \tag{3.13}$$

The coefficients are computed by minimizing, as the name already suggests, the least squared residuals [23].

$$\hat{y} = \arg\min \frac{1}{N} \sum_{i=1}^{N} \left(f(\boldsymbol{X_i}) - \sum_{a \in \mathbb{R}^M} \hat{y}_a \phi_a(\boldsymbol{X_i}) \right)^2. \tag{3.14}$$

This method is furthermore referred to as Ordinary Least Squares (OLS). A benefit of this approach is that the number of model evaluations, i.e. samples, can be set to a desired amount, based on the experimental design. For quadrature, the number of model evaluations is determined based on the polynomial degree by $N = (p+1)^M$. This results in restrictions in the model evaluations, given that the number of samples will always be an exponential function. OLS on the other hand can be evaluated at any choice of experimental design. Since least-squares is based on the sample points, the sampling technique has an influence on the accuracy and efficiency of the method. In UQLab, the default mode of OLS is Monte Carlo sampling. If one wants to apply a sparse grid on this approach, one can apply the Least Angle Regression method (LARS).

Least angle regression

Often only low order interactions between input variables tend to be important. The least-angle regression method, being referred to as LARS, considers which variables and which coefficients to take into account [13]. LARS is a modification of OLS, and adds an extra penalty term, $\lambda||\mathbf{y}||_1$, which forces the minimization to favor low rank solutions [23]:

$$\hat{y} = \arg\min \frac{1}{N} \sum_{i=1}^{N} \left(f(\boldsymbol{X_i}) - \sum_{a \in \mathbb{R}^M} \hat{y}_a \phi_a(\boldsymbol{X_i}) \right)^2 + \lambda||\mathbf{y}||_1. \tag{3.15}$$

LARS only selects the number of regressors that have the largest impact and from here provides a sparse polynomial chaos expansion. The detection of the significant coefficients is called adaptive PCE. For more information on the implementation of LARS, the reader is referred to the UQLab manual [13].

3.2. Comparison of methods

Computational costs tend to rise with increasing complexity of the model. Therefore, it is important to find an appropriate approach for performing UQ. One method is to perform an error estimation in order to find the minimum number of samples required to converge to a desirable order of magnitude for the error.

Error estimation

The error estimation is based on the difference between a reference value, for instance for the mean, of the parameter of interest, μ_{ref}, and the expectation, μ_y for various samples of the output function $y(\mathbf{X})$. For each UQ technique the function is presented by $y = f(Re, \epsilon)$.

$$\epsilon = |\frac{1}{\mu_{ref}}(\mu_y - \mu_{ref})|. \tag{3.16}$$

Again, consider the example of the Churchill relation. For f, the reference value of both mean and the standard deviation is an unknown variable. Therefore we have to approximate this. For this research, we made use of a reference solution that was determined based on a sufficiently high order PCE model. Differences in error behavior could be caused by the accuracy of the reference solution. For the Churchill relation, the polynomial degree 30 is used for obtaining the reference values.
The error estimation of the mean and the standard deviation of the friction factor, using different sampling techniques, can be seen in fig. 3.4 and fig. 3.5. Both the Monte Carlo sampling results and the results obtained using OLS and LARS are averaged over 3 runs. This is because these 3 methods use random samples for each run, and therefore results can be different for each run. An average over 3 runs will result in better reproducible results.

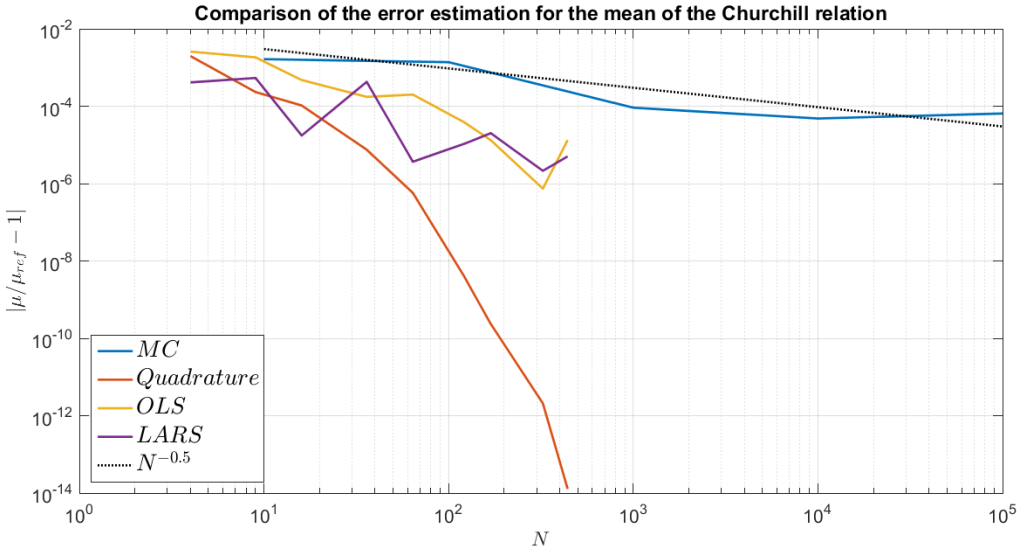

Figure 3.4: The error estimation of the mean of the friction factor for different samples using different methods, obtained with UQLab.

Following eq. (2.9), we can deduce the convergence ratio for Monte Carlo sampling when using a logarithmic scale.

$$\epsilon \sim \frac{C}{\sqrt{N}} = C \cdot N^{-0.5},$$

$$\log(\epsilon) = \log(C) + \log(N^{-0.5}),$$

$$\log(\epsilon) = \log(C) - 0.5\log(N),$$

which presents the general equation format for a linear slope, in the form of $y = ax + b$. In other words, the error in the approximation of the parameter using Monte Carlo sampling converges linear with a slope of 0.5 for a logarithmic scale. A convergence rate of 0.5 can indeed be observed in both fig. 3.4 and fig. 3.5.

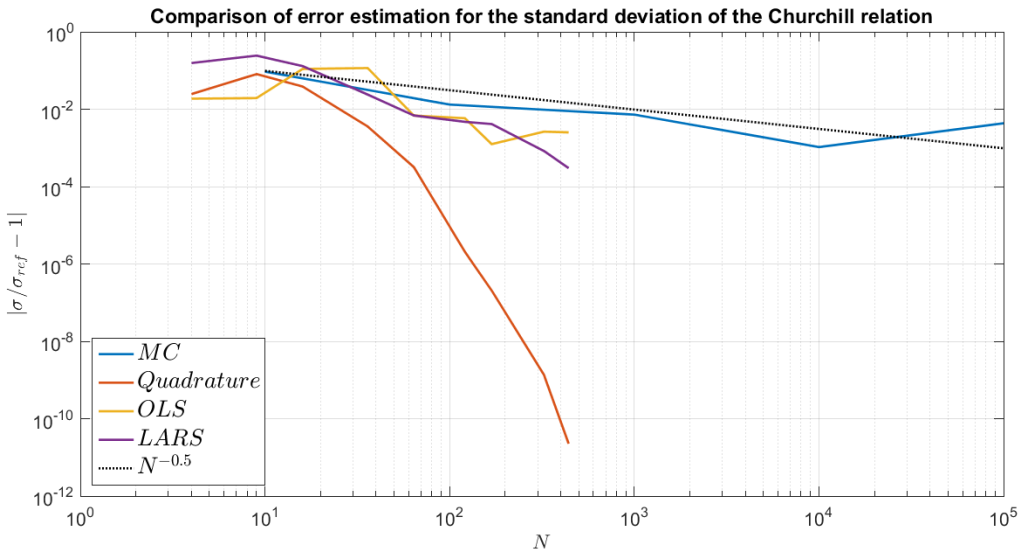

Figure 3.5: The error estimation of the standard deviation of the friction factor for different samples using different methods, obtained with UQLab.

For PCE, the expectation is that the error estimation will have a spectral convergence rate. For quadrature based PCE, the convergence rate is spectral. OLS and LARS do not have a spectral convergence rate. Let us graphically evaluate the PCE model for the Churchill relation, together with the distribution of the nodes of the polynomial, for the 441 samples. From here, more clarity is provided on the behavior of the different PCE models for the Churchill relation.

From fig. 3.6b and fig. 3.6c it can be deduced that the distribution of the nodes is dependent on the choice of distribution for the input parameters for both LARS and OLS. Both input parameters are presented with a (truncated) normal distribution, and therefore, as can be seen in the figure, there is a low occurrence of nodes close to the boundaries of the domain. The function under consideration will have a low probability in the boundary region of the domain and therefore few nodes could in theory, approximate this function. However, approximating the model with a polynomial requires a sufficiently number of nodes on the boundary in order to obtain stable results. If only a few nodes are present on the boundary, the polynomial could approximate the function incorrectly and wiggles could form. Fig. 3.6a shows a more dense distribution of the nodes along the boundary.

The difference between the true model and the PCE model per node has been evaluated to highlight the error in the PCE model. Fig. 3.7b and fig. 3.7c clearly show an increasing error close to the boundary of the domain, whereas fig. 3.7a more or less has a constant residual error between the models, except for one peak close to the boundary. Still, this error is of the order $O(10^{-8})$, which is 10000 times as accurate compared to the error of the order $O(10^{-4})$ for LARS and OLS.

For two (truncated) normal distributions, quadrature is shown to be the preferred method. Furthermore, PCE using quadrature rules is computationally cheap. Note that the CPU time is dominated by model runs and not by pre- and post-processing with UQLab. The number of samples that are needed to reach a high order of accuracy will be the reason a model is computational cheap or expensive. Based on fig. 3.4 and fig. 3.5, PCE is considered computationally cheap.

Based on the results, the assumption is made to only consider PCE using quadrature rules for the calculation for low dimensional problems ($M < 4$). For high dimensional problems, either LARS or sparse quadrature could be considered, but the most efficient approach will be obtained after applying sparse methods on a high dimensional problem.

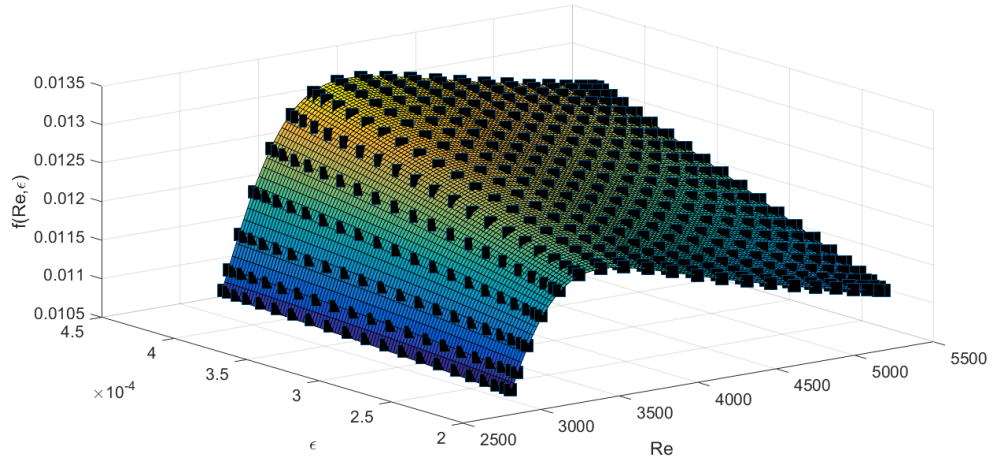

(a) Quadrature rules

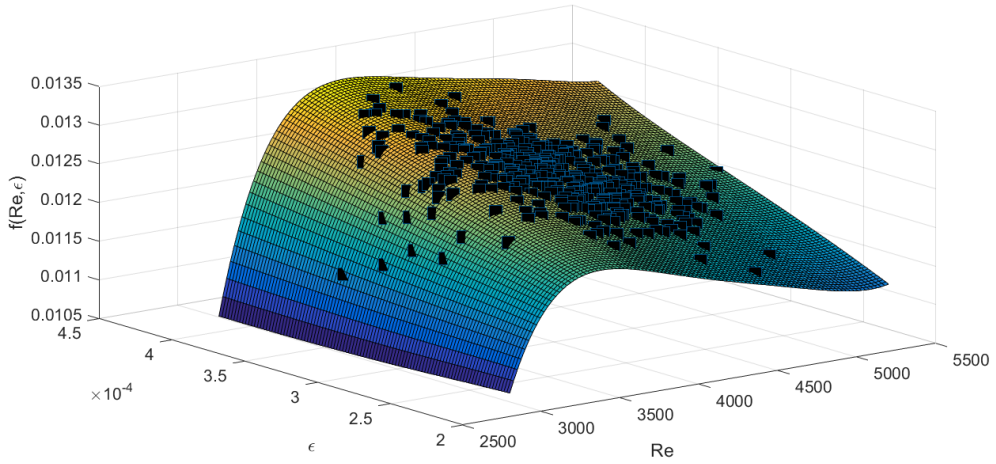

(b) OLS

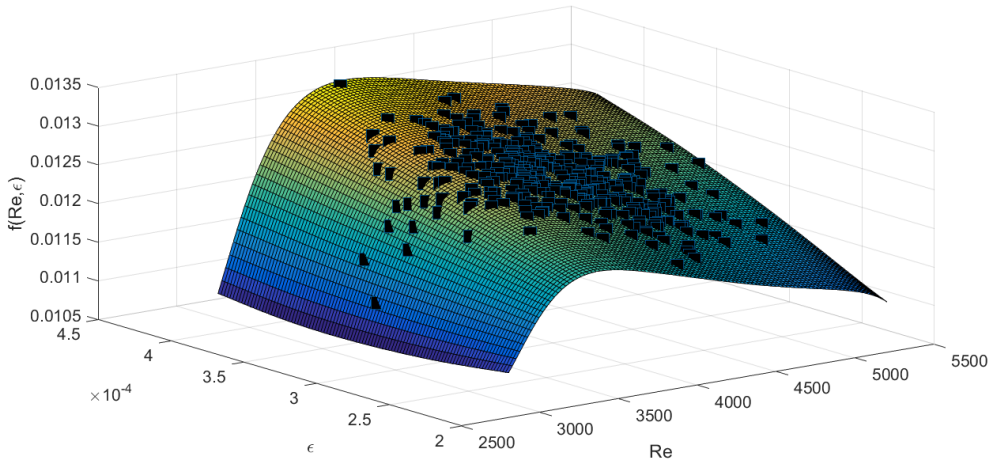

(c) LARS

Figure 3.6: The evaluation of the PCE models at 411 nodes for the Churchill relation.

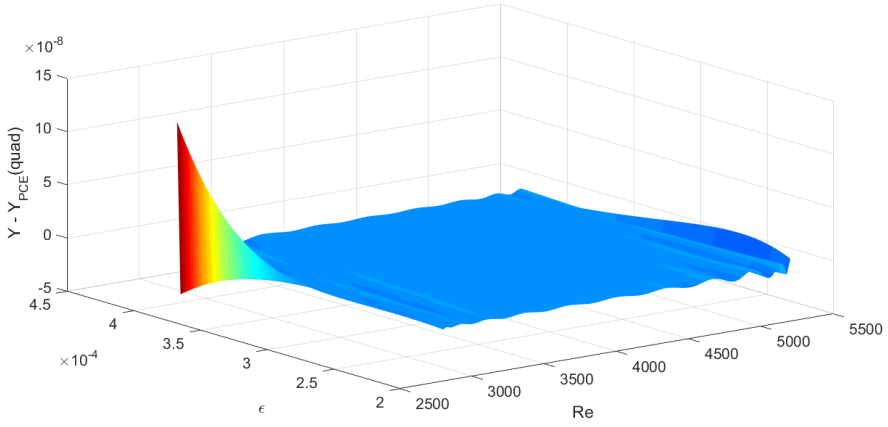

(a) Quadrature rules

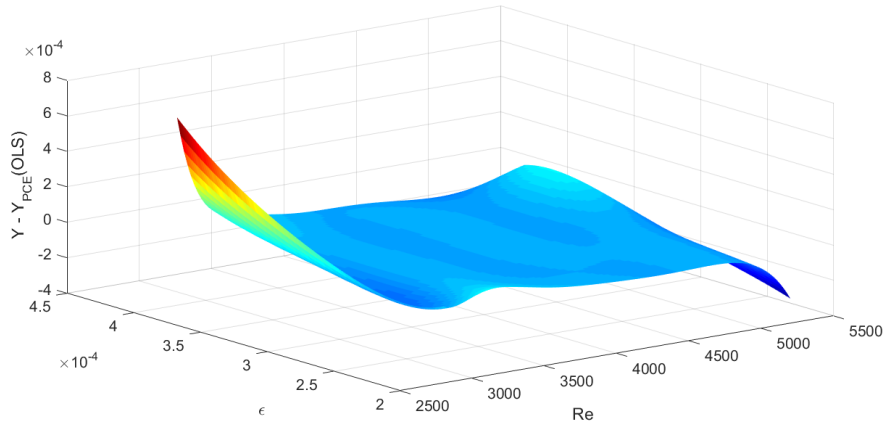

(b) OLS

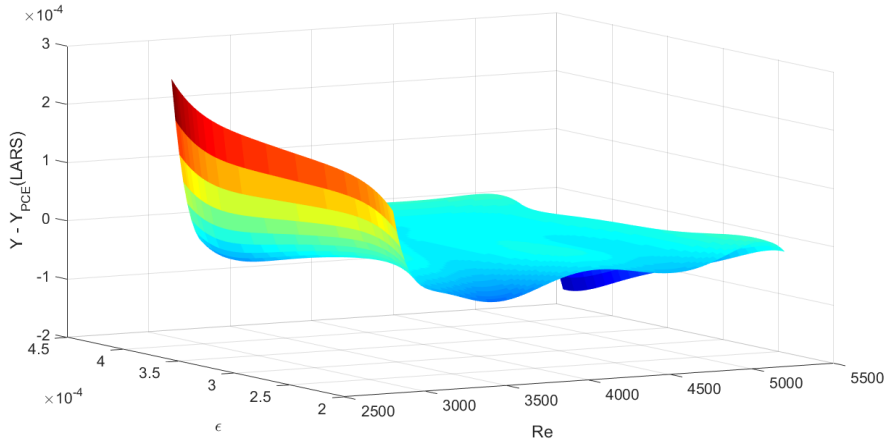

(c) LARS

Figure 3.7: The error between the PCE model and the true model at 411 nodes for the Churchill relation.

3.3. Sensitivity analysis

The Sobol method was briefly introduced in section 2.2.3. As mentioned, Sobol's method is a variance based method and makes use of the decomposition of the variance of the output of the model into partial variances. These partial variances are computed from the decomposition of the function of random variables, representing the output quantity of interest:

$$y = f(\mathbf{X}) = f_0 + \sum_{i=1}^{p} f_i(x_i) + \sum_{1 \le i \le j \le p} f_{ij}(x_i, x_j). \tag{3.17}$$

f_0 represents the mean response of the function y, f_i represents the independent contributions of all the parameters and f_{ij} represents the interaction effects between two parameters. Higher order terms represent unincorporated high-order residual effects, which ensure that the expansion will provide an exact representation. These terms are often ignored, since the effect of these terms is often negligible [15].

The zeroth-, first-, and second order terms are defined by [15]:

$$f_0 = \int_{\mathbb{R}^M} f(x)\rho_x(x)dx, \tag{3.18}$$

$$f_i(x_i) = \int_{\mathbb{R}^{M\sim i}} f(x)\rho_{\sim i}(x_{\sim i})dx_{\sim i} - f_0, \tag{3.19}$$

$$f_{ij}(x_i, x_j) = \int_{\mathbb{R}^{M\sim i,j}} f(x)\rho_{\sim i,j}(x_{\sim i,j})dx_{\sim i,j} - f_0, \tag{3.20}$$

where $\mathbb{R}^M$ presents the whole parameter space, $\mathbb{R}^{M\sim i}$ presents the parameter space without parameter X_i, etc.
The variance is decomposed as:

$$V(y) = \sum_i V_i + \sum_i \sum_{j>i} V_{ij}, \tag{3.21}$$

where V_i is the first order variance and V_{ij} is the second order variance.

From the decomposition of the function, the (partial) variances can be computed as follows:

$$V = V(y) = \int_{\mathbb{R}^M} f^2(x)dx - f_0^2, \tag{3.22}$$

$$V_i = \int_{\mathbb{R}^{M\sim i}} f_i^2(x_i)dx_i, \tag{3.23}$$

$$V_{ij} = \int\int_{\mathbb{R}^{M\sim i,j}} f_{ij}^2 dx_i dx_j, \tag{3.24}$$

when these (partial) variances are normalized with the total variance, they represent the Sobol indices:

$$S_i = \frac{V_i}{V(y)}, \quad S_{ij} = \frac{V_{ij}}{V(y)}, \tag{3.25}$$

and:

$$\sum_i S_i + \sum_i \sum_{j>i} S_{ij} + ... = 1, \tag{3.26}$$

where S_i is the first order sensitivity index and describes the effect of the variable X_i on the output.
S_{ij} is the second order sensitivity index, which quantifies the second-order interaction between input variable X_i and X_j.

S_{Ti} is the total sensitivity index of variable X_i, given by:

$$S_{Ti} = S_i + \sum_j S_{ij} + \sum_j \sum_k S_{ijk}..., \tag{3.27}$$

where S_{ijk} represents higher order interaction effect between 3 input parameters, X_i, X_j and X_k.

The total sensitivity index represents the sum of Sobol indices where the input variable X_i is involved [14]. Remember the interpretation of the Sobol indices: if the value of S_i is relatively high, it implies that the contribution of the variance of the input variable X_i on the variance of the output is high. If a Sobol index is low, the contribution of the variance of the input parameter is low and might be negligible.

A sensitivity analysis for the complete Churchill relation, depending on both Re and ϵ with the normal distributions as described before, is performed using UQLab. In UQLab, one needs to specify the sensitivity analysis method, here Sobol's method, and the degree of interactions. Since the friction factor is only depending on two variables, this degree of interaction is set to two.

Sobol's indices are often computed using Monte Carlo sampling. Sobol's indices can also be computed using PCE. Looking at eq. (3.7), the function of interest is expanded into polynomials and coefficients. Due to the orthogonality of the polynomials, the total and partial variance of the function can directly be computed from the coefficients [14]:

$$V_t = \sum_{\substack{a \in \mathbb{R}^M \\ a \neq 0}} \hat{y}_a^2, \tag{3.28}$$

$$V_i = \sum_{\substack{a \in \mathbb{R}^a \\ a \neq 0}} \hat{y}_a^2. \tag{3.29}$$

Sobol's method is a variance based method. The error estimation for the standard deviation of the Churchill relation, presented in fig. 3.5, shows that for 10^4 Monte Carlo samples, the same order of accuracy can be obtained with only 25 PCE samples.

Fig. 3.8 shows the Sobol indices computed using both PCE and Monte Carlo for the same order of accuracy in the variance. For more detail, the value of the indices is also presented in table 3.4. From the index values, one can conclude that the variance of the the wall roughness, ϵ, has more influence on the variance of the output than the Reynolds number Re for this choice of input representation. The difference in contribution is ~ 0.1, or 10%.

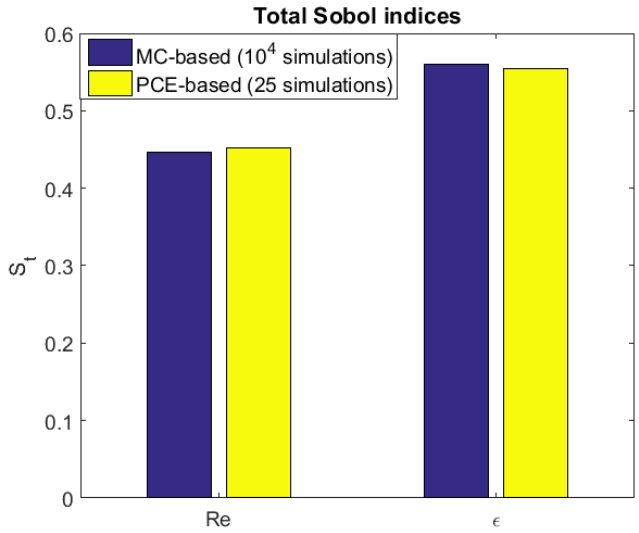

Figure 3.8: A comparison of the total Sobol indices for PCE and Monte Carlo sampling.

Table 3.4: Sobol's indices using both PCE and Monte Carlo sampling.

	Monte Carlo $[S_{Re}\ S_e]$	**PCE** $[S_{Re}\ S_e]$
Sample size	10^4	25
S_1	[0.4405 0.5529]	[0.4449 0.5486]
S_{12}	0.0066	0.0065
S_t	[0.4471 0.5595]	[0.4514 0.5551]

Recall the equations (3.26) and (3.27). When checking the computed indices with these equations, it turns out the equations hold and UQLab computes the Sobol indices accurately.

4

Uncertainty propagation on 0-D steady state models

Shell Flow Correlations is a 0D steady state model that calculates output quantities of interest, like liquid holdup and pressure drop and constructs a flow pattern map. Both the output quantities and flow pattern maps have many uncertainties associated with them. In this chapter, these uncertainties are investigated. First, the output quantities of interest for a stratified flow regime will be discussed and compared to literature using Monte Carlo sampling. We also investigate more efficient approaches, such as PCE. Furthermore, an example of UQ on flow pattern maps will be provided, to highlight uncertainties in flow pattern transition predictions.

4.1. Uncertainties in a stratified flow regime: SFC compared to literature

A general framework is created with UQLab, that calls a dynamic library consisting of the calculation domain of SFC [24] and can be found in appendix B. The framework is validated using literature.
Picchi and Poesio [5], which will be referred to as Picchi in this chapter, performed uncertainty quantification and sensitivity analysis on the liquid holdup and pressure drop in a stratified flow regime using Monte Carlo sampling. The results are compared with the results obtained with the SFC. We investigate more efficient techniques than MC, such as PCE, discussed in sections 2.2.2 and 3.1.1.

4.1.1. Uncertainty Quantification

We will follow the 3 steps presented in section 2.2, following Cremaschi [2], to perform uncertainty propagation on the SFC.

Identify the type of uncertainty

The focus will be on the input parameters of the SFC. The input parameters are presented with a distribution that represents the uncertainty. The model relations, used by SFC to generate output, are not taken into account. SFC is a blackbox model and we will not interfere with the calculations.
SFC works with the input parameters, as given in table 4.1.

Select the appropriate mathematical representations

Picchi based the representation of the input uncertainty on experimental data, obtained from previous experiments in his laboratory. All input parameters are presented with a probability density function of a certain distribution type, as shown in table 4.2. The midrange of a uniform distribution is presented with the mean μ in table 4.2. Two cases are investigated: a horizontal stratified flow with an inclination of 0° and a downward inclined stratified flow, with an inclination of -1°.

Physical constraints require that all inputs should strictly be positive quantities, and therefore, the normal distributions are truncated at a 99.7% confidence level, as is presented in the table by $\mu \pm 3\sigma$.

Table 4.1: Input parameters of the SFC.

Input parameter description	**Unit**
Superficial gas velocity	m/s
Superficial liquid velocity	m/s
Water cut	fraction
Density of gas	kg/m^3
Density of oil	kg/m^3
Density of water	kg/m^3
Viscosity of gas	Ns/m^2
Viscosity of oil	Ns/m^2
Viscosity of water	Ns/m^2
Surface tension - O/G	N/m
Surface tension - W/G	N/m
Surface tension - O/W	N/m
Pipe hydraulic diameter	m
Pipe inclination angle	degrees
Wall roughness	m

Table 4.2: Input uncertainty representation, as presented by Picchi [5].

Input parameter	**Distribution type**	μ	σ	**range**
D, pipe diameter	uniform	0.022	-	$\mu \pm 0.001$
β, inclination angle	uniform	0, -1	-	$\mu \pm 0.1$
U_{sg}, superficial gas velocity	normal	1	0.033	$\mu \pm 3\sigma$
U_{sl}, superficial liquid velocity	normal	0.1	0.0184	$\mu \pm 3\sigma$
ρ_g, gas density	normal	1.2	0.1	$\mu \pm 3\sigma$
ρ_l, liquid density	normal	1000	0.5	$\mu \pm 3\sigma$
μ_g, gas viscosity	normal	$1 \cdot 10^{-5}$	$2 \cdot 10^{-6}$	$\mu \pm 3\sigma$
μ_l, liquid viscosity	normal	0.001	$6.25 \cdot 10^{-5}$	$\mu \pm 3\sigma$
σ_{LG}, liquid-water surface tension	normal	0.072	0.0025	$\mu \pm 3\sigma$

Choose an appropriate propagation method

Finally, we should choose an appropriate propagation method to quantify the uncertainty in the output. Picchi chooses Monte Carlo as a sampling technique, reasoning that the model under consideration has low computational costs, and a simple universal approach like Monte Carlo is therefore a suitable propagation method. We follow this approach and perform Monte Carlo sampling with 10^5 samples.

Monte Carlo

Picchi performed UQ only with Monte Carlo. As shown in table 4.2, there are two cases that need to be tested and compared with SFC, a horizontal stratified flow and a downward inclined stratified flow. Picchi lists the mean and deviation of the output obtained for the two cases. All results are presented in table 4.3. Picchi graphically presents the results of the downward inclined stratified flow, presented in fig. 4.1.

Table 4.3: The obtained output, for both horizontal stratified flow and downward inclined stratified flow for Picchi and the SFC.

Flow pattern	**Output q.o.i.**	**Picchi**		**SFC**	
		μ	σ	μ	σ
Horizontal stratified	Pressure drop	-139.72 Pa	58.88 Pa	-148.59 Pa	61.227 Pa
	Liquid holdup	0.626	0.066	0.6532	0.0671
Downward inclined stratified	Pressure drop	-16.24 Pa	2.0914 Pa	-17.046 Pa	3.1608 Pa
	Liquid holdup	0.24	0.0336	0.259	0.0334

SFC presents the pressure drop per pipeline length. The pipeline from the study of Picchi has a length of 9 m, and in order to obtain comparable results, the results obtained by the SFC are multiplied with 9 and presented in table 4.3. Recalling the fact that the software used by Picchi is unknown, a slight difference in results can be expected, since the closure relations and model assumptions are likely to be different from SFC.

The distributions of the output quantities of interest are graphically presented for a downward inclined stratified flow, as shown in fig. 4.1 and fig. 4.2. These figures highlight how the output quantities of interest are influenced by applying input uncertainty to the model.

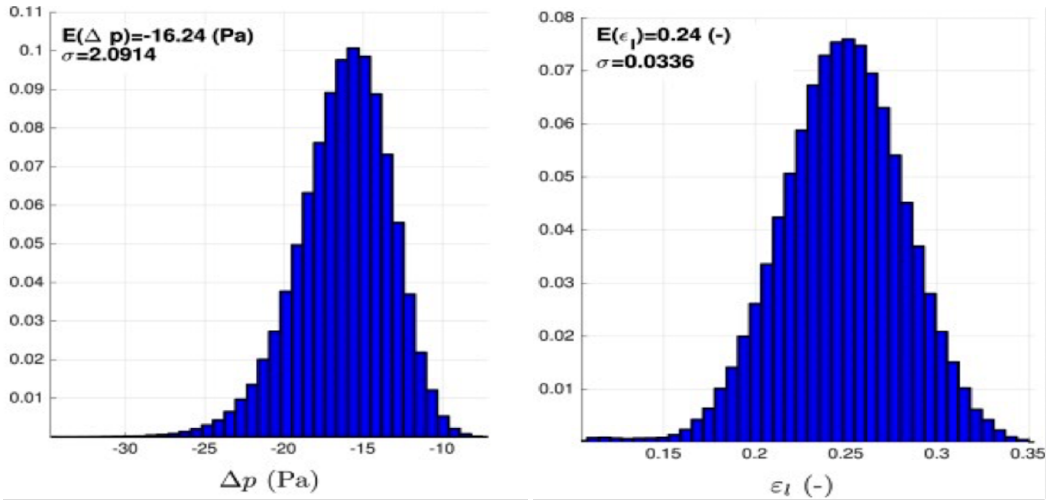

Figure 4.1: The output quantities of interest for a downward inclined stratified flow, taken from Picchi [5].

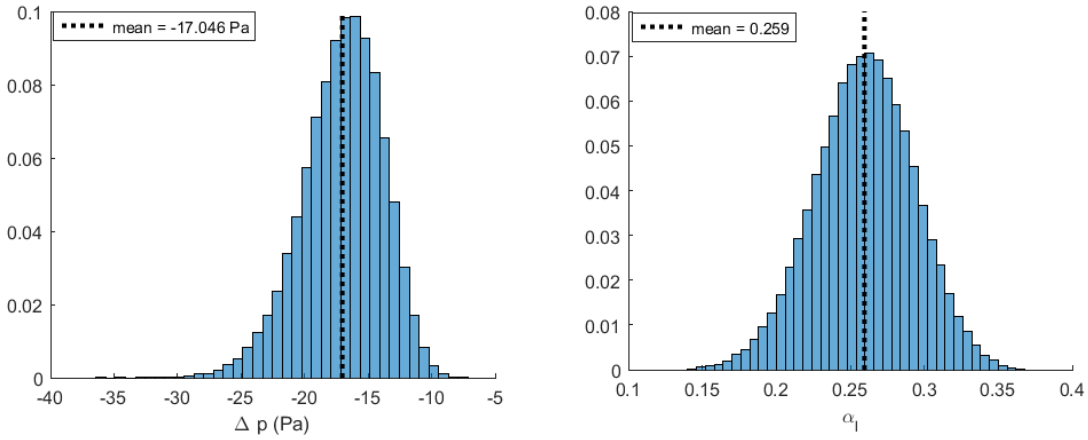

Figure 4.2: The output quantities of interest for a downward inclined stratified flow, obtained from SFC.

4.1.2. Sensitivity analysis

A sensitivity analysis on 0D model is applied. From the sensitivity analysis, more insight in relevant parameters with respect to uncertainty can be obtained. With this knowledge, the input uncertainty of these relevant parameters can be narrowed, and hereby reduced.

Picchi performed both local, global, quantitative and qualitative sensitivity analysis. For both cases of table 4.3, we chose to highlight the results of the global sensitivity analysis, given that this method highlights the contribution of all input parameters in comparison to each other. Picchi performed a global sensitivity analysis using Sobol's indices, which we introduced in sections 2.2.3 and 3.3. The results are graphically presented and commented on where further explanation is required.

Horizontal stratified flow

The results of Sobol's method for a horizontal stratified flow are presented in fig. 4.3a and fig. 4.3b, where the results obtained by Picchi and the results obtained by SFC are plotted in the same figure.

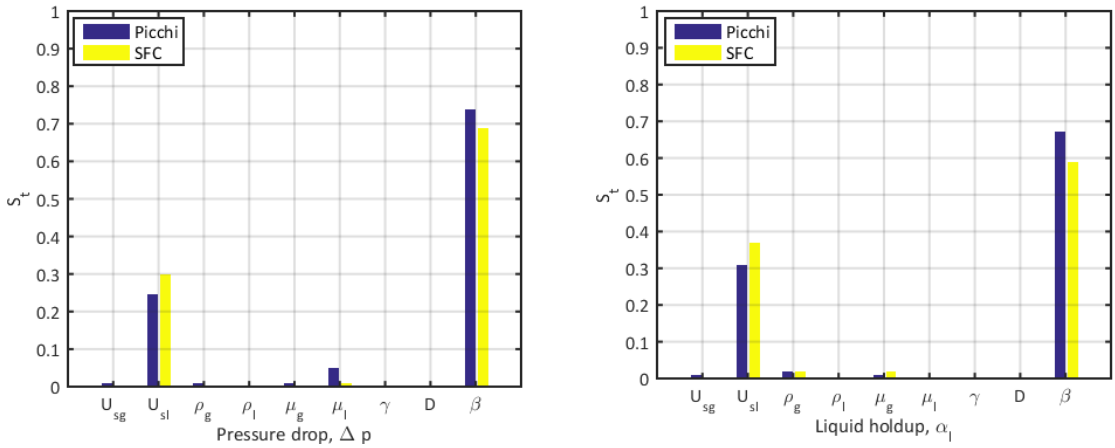

(a) Pressure drop

(b) Liquid holdup

Figure 4.3: The Sobol indices for a horizontal stratified flow, taken from Picchi [5] and SFC.

The results are similar for both models, and small differences can be addressed to different software, which uses different model relations.
The inclination angle is the most critical parameter with respect to uncertainty for both output quantities of interest, followed by the superficial liquid velocity. This is due to the choice of inputs. The inclination angle ranges from -0.1° to 0.1°. From fig. 4.4 we see that a small increase in the inclination angle from 0 to 0.1, influences the stability of the flow and a transition from stratified flow to slug flow appears. Slugs have a large contribution to liquid holdup and pressure drop and these quantities will be different for a stratified flow. A different choice for the uncertainty range can result in a different range of sensitive parameters.

Downward inclined stratified flow

The results of Sobol's method for a downward inclined stratified flow are presented in fig. 4.5a and fig. 4.5b, where the results obtained by Picchi and the results obtained by SFC are again plotted in the same figure. Again, the results obtained by Picchi and SFC are similar. One interesting observation is that the uncertainty associated in the liquid holdup is almost completely due to the uncertainty in the superficial liquid velocity, with a Sobol index close to 1 for the superficial liquid velocity.

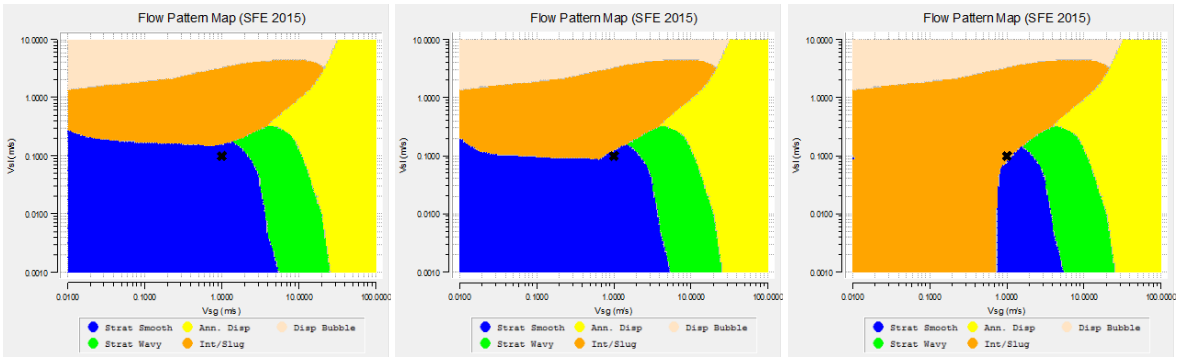

(a) -0.1 ° inclination (b) 0 ° inclination (c) 0.1 ° inclination

Figure 4.4: The different angles.

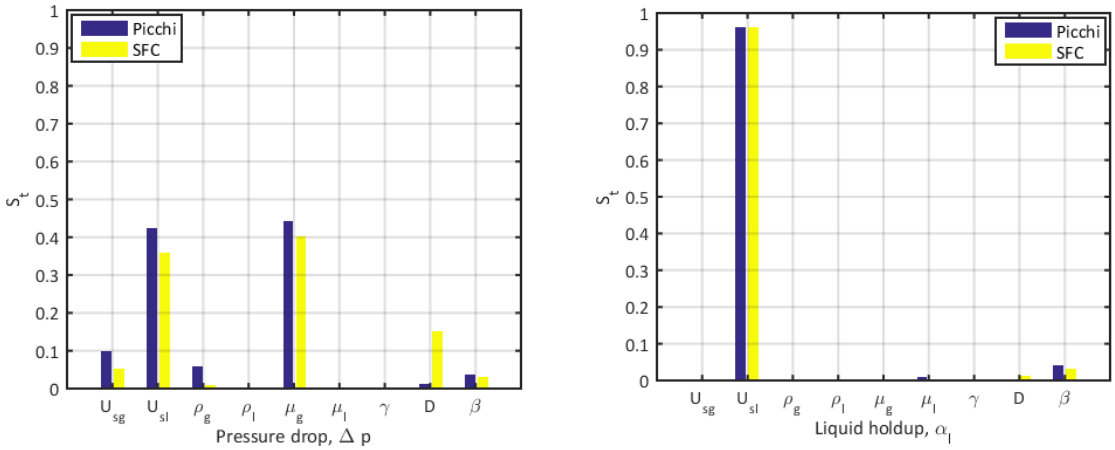

(a) Pressure drop (b) Liquid holdup

Figure 4.5: The Sobol indices for a downward inclined stratified flow, taken from Picchi [5] and SFC.

Let us further investigate the influence of the superficial liquid velocity on the liquid holdup. Thereto the uncertainty associated with the superficial liquid velocity is reduced by a factor 2, i.e, the superficial liquid velocity is now presented by: $U_{sl} \sim \mathcal{N}(0.1, 0.0092)$.
The new output distribution for the liquid holdup and the sensitivity indices are presented in fig. 4.6a and fig. 4.6b. The new output distribution has a mean of 0.26, which is similar as previously obtained, but the standard deviation is decreased, from 0.0334 to 0.0177, also with a factor two. The sensitivity index of the superficial liquid velocity decreased, although the inclination angle sensitivity index has increased.

In this example it was shown how by reducing the input uncertainty, the output uncertainty is reduced, but also how the corresponding sensitivity indices are influenced by this modification. The choice of the input distributions will determine the uncertainty in the output, and choosing a representative uncertainty range for the input is therefore a challenging and crucial task.

The wall roughness is an important input parameter for the determination of the pressure drop and liquid holdup, but is not considered by Picchi. We perform UQ on both tests cases, where the wall roughness is also considered to have an associated uncertainty, together with the input parameter representations presented in table 4.2. The uncertainty in the wall roughness is presented with an uniform distribution, ranging from 0.01 to 0.03 mm. These are typical values for an average rough pipeline, as described in [4]. From the sensitivity analysis we obtain that the wall roughness does not have an effect on liquid holdup and pressure drop for this choice of input parameters. Therefore, we follow the approach of Picchi and do not take into account uncertainties associated with the wall roughness for the test cases.

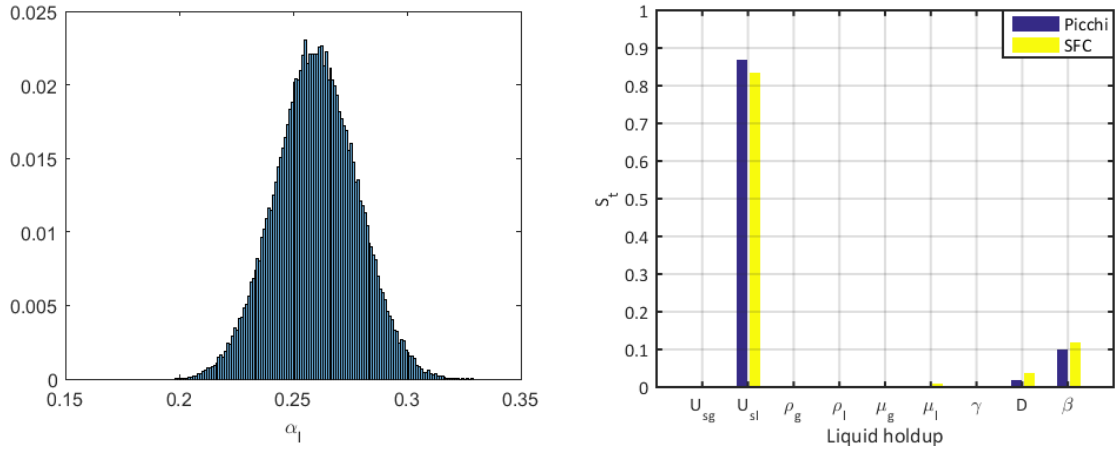

(a) Probability distribution

(b) Sobol indices

Figure 4.6: Liquid hold-up probability distribution (a) and Sobol sensitivity indices (b) for a downward inclined stratified flow. The uncertainty associated to the superficial liquid velocity is reduced by a factor of two.

4.2. Efficiency improvements with polynomial chaos expansion

Polynomial chaos expansion will need less samples to reach a high order of accuracy in predictions. Picchi does not make use of the polynomial chaos expansion approach when performing UQ on a stratified flow regime, but only considers 10^5 Monte Carlo samples. We will perform uncertainty quantification on the SFC problem using PCE, and compare the results with the results obtained with Monte Carlo sampling. Based on the results of the sensitivity analysis, obtained using Monte Carlo, we choose to eliminate input parameters with negligible effect from the list of input parameters under consideration, to avoid unnecessary higher-dimensional problems. We make the assumption that every input parameter with a contribution lower than $< 5\%$, i.e. a Sobol index < 0.05, is negligible.

4.2.1. Horizontal stratified flow

For a horizontal stratified flow, we limit ourselves to two input parameters, the inclination angle β and the superficial liquid velocity U_{sl}, presented in table 4.4.

Table 4.4: Input uncertainty representation of sensitive input parameters for a horizontal stratified flow.

Input parameter	**Distribution type**	μ	σ	**range**
β, inclination angle	uniform	0	-	E(β) $\pm$ 0.1
U_{sl}, superficial liquid velocity	normal	0.1	0.0184	E(U_{sl}) $\pm 3\sigma$

Since the problem is 2-dimensional, we do not apply a sparse grid method, but perform PCE using quadrature rules in a similar way as described in section 3.1.1. For comparison with the Monte Carlo sampling method, the error convergence ratio is compared. No exact reference solution for the pressure drop and liquid holdup is known. A reference solution is computed with a high order polynomial, i.e. a 20th degree polynomial. This serves as a reference value for the mean and standard deviation of both the pressure drop and liquid holdup.

Fig. 4.7 shows the error estimation compared to the number of samples N. For both the liquid holdup and the pressure drop, the error convergence of the mean is more accurate when using PCE than Monte Carlo. Note that the error estimation of Monte Carlo is averaged over 3 runs, to get reproducible and more accurate results.

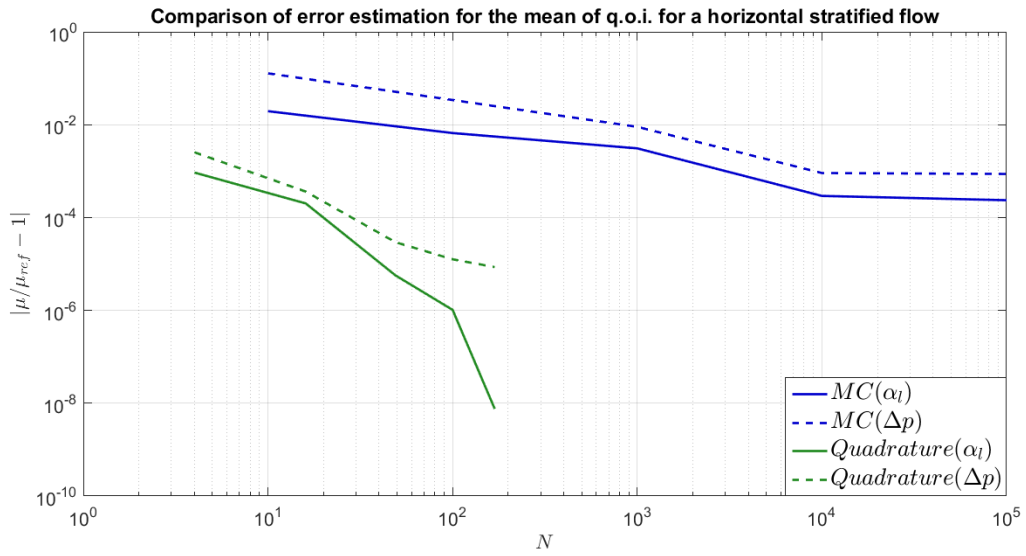

Figure 4.7: The error estimation of the mean of the quantities of interest for a horizontal stratified flow.

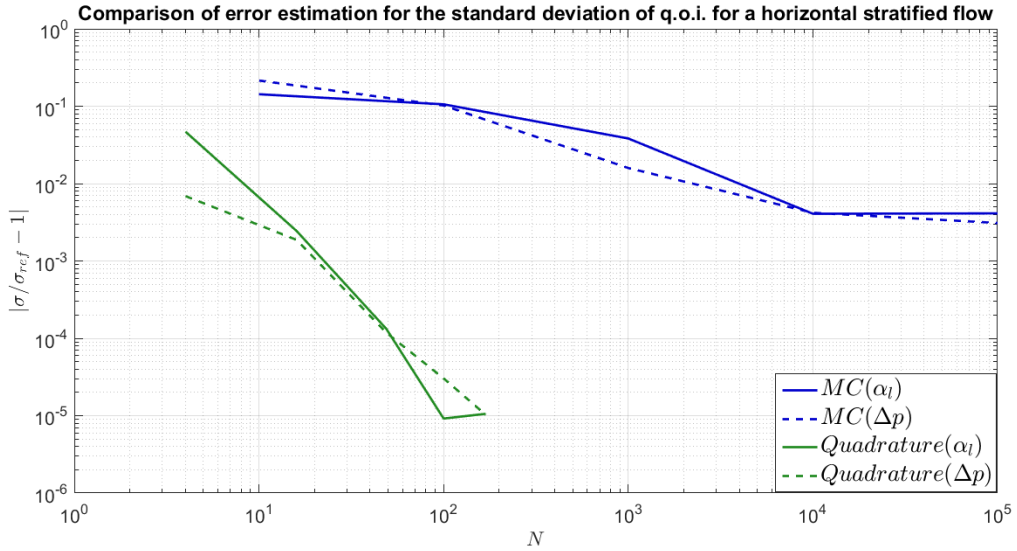

Figure 4.8: The error estimation of the standard deviation of the quantities of interest for a horizontal stratified flow.

The error convergence of the standard deviation, obtained using Monte Carlo and PCE, is presented in fig. 4.8. Let us consider the error approximation of the standard deviation at 10^4 samples using Monte Carlo sampling. From the figure, we can deduce that with approximately 15 PCE samples, the same accuracy in the standard deviation of the liquid holdup and pressure drop can be obtained. Therefore, PCE is a more efficient approach, since fewer samples are needed in order to reach a high order of accuracy, and therefore is computational cheap.

We perform SA on a horizontal stratified flow, to validate if only 15 PCE samples result in the same Sobol indices as the computation with 10^4 Monte Carlo samples. The results are presented in fig 4.9.

Since the number of samples using quadrature rules is determined by $N = (p+1)^M$, it is not possible to evaluate the model at exactly 15 samples. Instead, the quadratic functions that is most close to the determined samples is taken, the third degree polynomial, resulting in $(3+1)^2$ samples. Indeed, the results from Picchi are comparable to the results obtained using only the sensitive parameters and PCE.

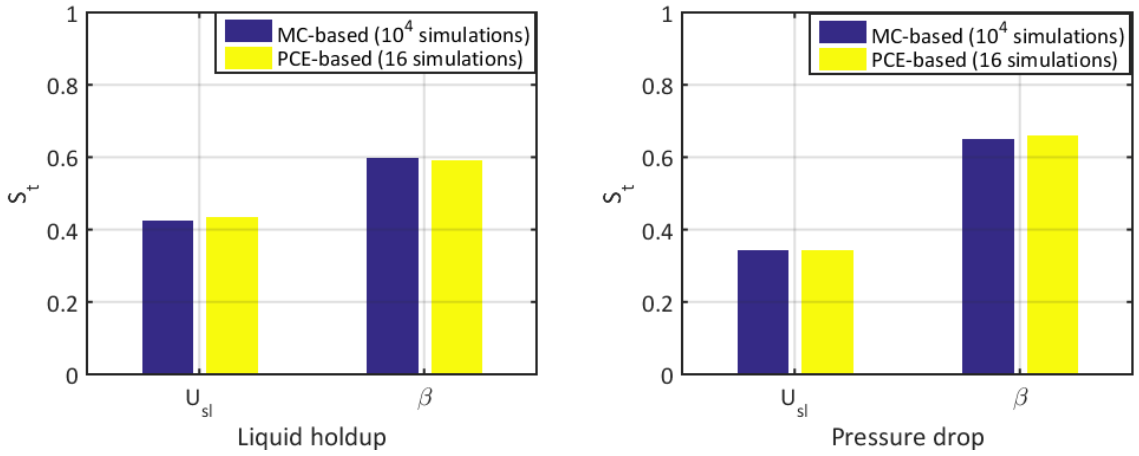

(a) Liquid holdup

(b) Pressure drop

Figure 4.9: The Sobol indices computed using the minimum amount of PCE samples, as follows by the error estimation, for a horizontal stratified flow.

4.2.2. Downward inclined stratified flow

Let us consider the testcase of the pressure drop for a downward inclined stratified flow. From the sensitivity analysis, presented in fig. 4.5a, we narrow the input parameters down to 4 parameters, that have the most significant contribution to the pressure drop. The sensitive input parameters are presented in table 4.5.

Table 4.5: Input uncertainty representation for sensitive input parameters for a downward inclined stratified flow.

Input parameter	**Distribution type**	μ	σ	**range**
D, pipe diameter	uniform	0.022	-	E(D) $\pm$ 0.001
U_{sg}, superficial gas velocity	normal	1	0.033	E(U_{sg}) $\pm 3\sigma$
U_{sl}, superficial liquid velocity	normal	0.1	0.0184	E(U_{sl}) $\pm 3\sigma$
μ_g, gas viscosity	normal	$1 \cdot 10^{-5}$	$2 \cdot 10^{-6}$	E(μ_g) $\pm 3\sigma$

The problem is 4-dimensional, therefore we do not apply a sparse grid method, but perform PCE using quadrature rules. For comparison with the Monte Carlo sampling method, the error convergence ratio is compared. A reference solution is computed with a high order polynomial, the 10th degree polynomial. The results are presented in fig. 4.10 and in fig. 4.11.

Fig. 4.10 and fig. 4.11 show that PCE needs fewer samples to reach a high order of accuracy. These error convergence plots for both the horizontal - and downward inclined stratified show the influence of choice of sampling approach on the accuracy of the predictions. Monte Carlo sampling results will need more samples to reach a high order of accuracy, the comparison of the PCE sampling will need less samples.

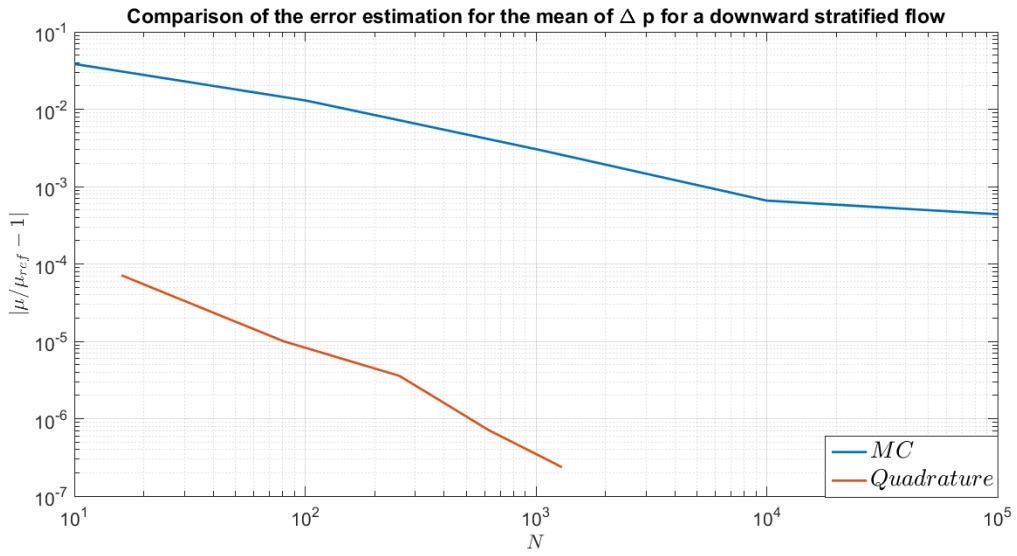

Figure 4.10: The error estimation of the mean of the pressure drop for a downward inclined stratified flow.

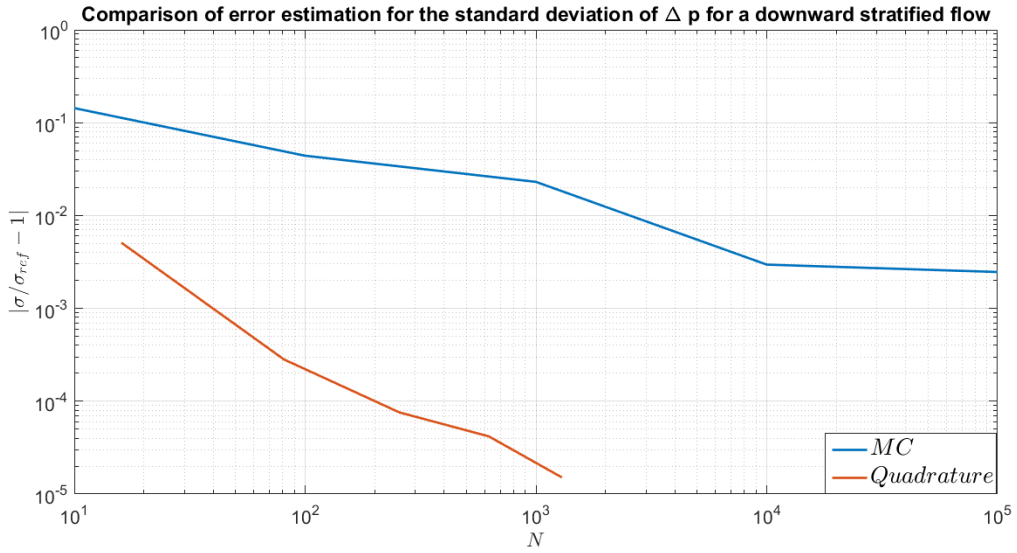

Figure 4.11: The error estimation of the standard deviation of the pressure drop for a downward inclined stratified flow.

We compare the PCE convergence ratio for the different stratified cases to both each other and to the Churchill relation test case. The SFC model is a more complex, non-linear, model than the Churchill relation, and the associated non-linearities can delay the spectral convergence. Furthermore, the dimension of the problem is higher for the case of downward inclined stratified flow, so more samples are needed before spectral convergence will be observed.

For the comparison of the different methods, we made use of error convergence plots and a reference solution. Additional differences in error behavior can be caused by the accuracy of the reference solution. This is further discussed in chapter 6.2.

For the SFC, a reference solution using a high polynomial degree will result in a good indication for engineering purposes, since an accuracy in the mean and standard deviation of quantities of interest of $O(10^{-4})$ in assumptions is accurate enough for design applications.

4.3. Flow Pattern Map uncertainty of the SFC

So far, we have investigated the influence of uncertainty on flow characteristics of a stratified flow. SFC is also commonly used for calculating flow pattern maps. For every flow pattern, the input is characterized by a certain combination of input parameters. Based on the input parameters, SFC calculates the fow pattern stability, which is used to describe the transition from one flow pattern to another. As discussed in section 2.1.1, flow pattern boundaries are strongly dependent on fluid property characteristics of the phases. Imperfect knowledge of the input parameters can result in a different flow pattern than desired, which can have consequences for the pipeline capacity. Therefore, a level of confidence of the flow regime transition is desired. In this section, an example of how to apply UQ to flow pattern maps is given, in order to obtain a quantitative degree of confidence on the model predictions.

4.3.1. Determination of a flow pattern

Taitel & Dukler [28] compared experimental data and theory for the construction of a flow pattern map, as shown in fig. 4.12. The results differ, which could be due to uncertainties in both experimental and model data. The experimental results can have uncertainty in the flow pattern map construction due to limitations in the measurement equipment, whereas the model can have uncertainties in model assumptions and input parameters.

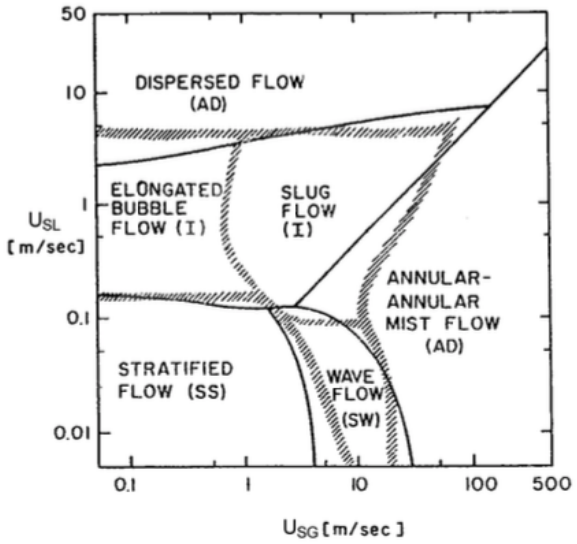

Figure 4.12: Comparison of theory (///) and experimental data (-) of a flow pattern map for air-water, 25° horizontal pipeline with D = 2.5 cm. Taken from Taitel & Dukler [28]. The theory is obtained from Mandhane [30].

The Technical Guidelines for SFC [25], present the following basic process for determining the flow pattern in SFC. First, a certain flow field is assumed, and from here its stability is verified under given conditions for the superficial gas velocities, the liquid holdup, et cetera. If the flow pattern is unstable, a new flow pattern is assumed and the stability verification is repeated for the conditions. This process is repeated until a steady flow pattern is reached.

The flow patterns are tested in order of increasing complexity. One starts with a homogeneous flow, following a stratified flow pattern, and from here continues to annular flow, bubble flow and finally intermittent/slug flow. The flow pattern decision tree is also graphically represented in fig. 4.13.

The transition from stratified flow to slug flow has a large modeling uncertainty, as is highlighted by Dhoorjaty [20]. The stability of a stratified flow is verified using the Kelvin-Helmholtz instability. In the next section, this stability criterion is further discussed.

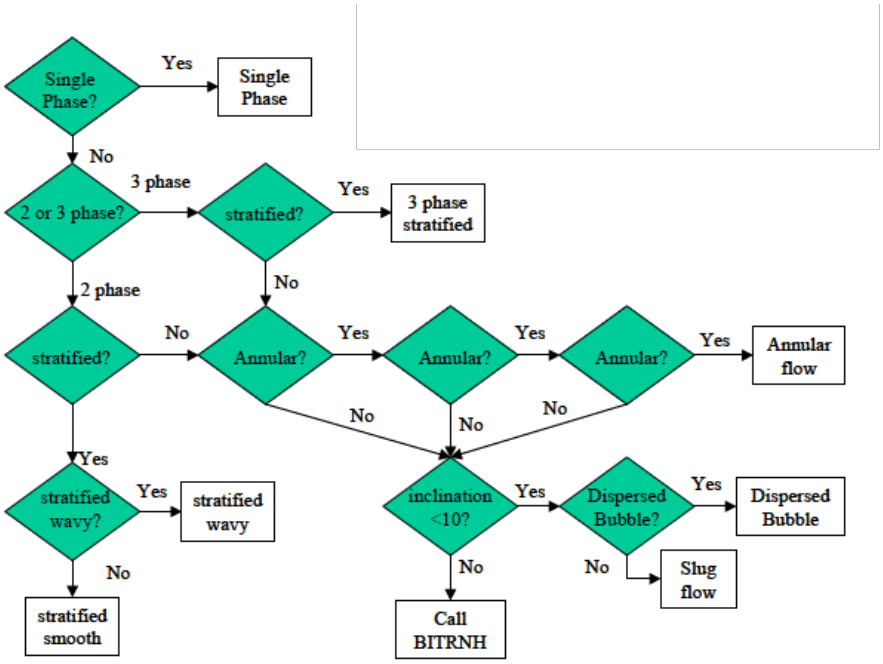

Figure 4.13: The flow pattern decision tree, taken from the Technical Guide for Shell Flow Correlations [25].

4.3.2. The Kelvin Helmholtz instability

The stability criterion for a uniform, incompressible stratified flow, consisting of separate phases with different densities and velocities, is known as the Kelvin Helmholtz instability. If the velocity difference across the interface exceeds a critical value, instabilities will occur [26]. If these instabilities grow, a transition from a stratified flow to a slug flow will occur.

The critical velocity difference for the Kelvin Helmholtz instability is given by [27]:

$$\frac{2(U_g - U_l)^2}{gD\cos\beta} > \frac{\alpha_g}{\alpha'_l}\left(1 + \frac{\rho_g}{\rho_l}\frac{\alpha_l}{\alpha_g}\right)\frac{\Delta\rho}{\rho_g}, \tag{4.1}$$

where U_g and U_l are the gas and liquid velocities, $\Delta\rho$ is the density difference, given by $(\rho_l - \rho_g)$ and α'_l is the derivative of the liquid holdup with respect to the relative film height, $\frac{h_L}{D}$, given by [25]:

$$\alpha'_l = \frac{2}{\pi}\sqrt{1 - \left(1 - 2\cdot\frac{h_L}{D}\right)^2}. \tag{4.2}$$

The original Kelvin Helmholtz criterion predicts critical gas velocities that are too high. Therefore, the criterion was modified with an extra empirical constant by Taitel & Dukler [28]. This constant represents the finite-amplitude waves, reasoning that these finite-amplitude waves have a bigger effect on the stability than the disturbances. The term can be multiplied to the righthand side of eq. (4.1) and is presented by:

$$C_2 = 1 - \frac{h_L}{D}. \tag{4.3}$$

The uncertainty associated with the Kelvin Helmholtz instability is investigated using the SFC. Note that the SFC makes use of the Viscous Kelvin Helmholtz instability (VKH). The difference between the (Inviscid) Kelvin Helmholtz instability (IKH) and the VKH is that the VKH also makes use of the contribution of shear forces between the fluid layers, whereas the IKH assumes that the fluids are inviscid and shear stresses can be neglected.

Barnea & Taitel [29] show that the IKH stability criterion lies above the VKH stability criterion in the flow pattern map, as shown in fig.4.14. For sufficiently high viscosities, the IKH and VKH curves almost coincide.

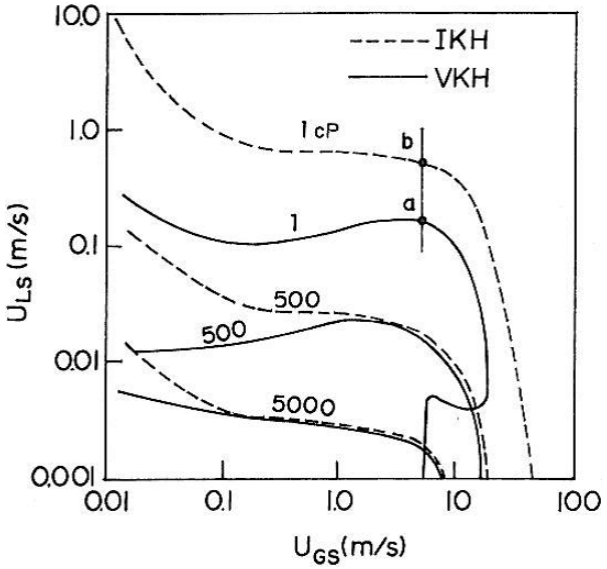

Figure 4.14: The effect of viscosity on the VKH and IKH neutral stability criteria. Air-liquid, atmospheric pressure, horizontal pipe, $D = 5$ cm. Taken from Barnea & Taitel [29].

For sake of simplicity, we first consider the Inviscid Kelvin Helmholtz instability for the uncertainty propagation. To apply the criterion given in eq. (4.1), a value is needed for the liquid holdup. The values of the input parameters that will influence the stability of the flow, based on the IKH stability criterion, are fed to SFC. From there, a liquid holdup is obtained, that can be used to verify the IKH stability criterion. The stability criterion in SFC will be different from the IKH stability criterion, as highlighted in fig. 4.14. In order to assure that the quantities of interest are calculated for the correct flow regime, the flow regime is forced at stratified (wavy) flow in SFC.

4.3.3. Results of UQ on IKH

We want to investigate how the stability of the flow is affected by applying uncertainties on the input. The stability of the flow using the IKH stability criterion needs to satisfy:

$$\sqrt{\frac{\alpha_g\left(1+\frac{\rho_g}{\rho_l}\frac{\alpha_l}{\alpha_g}\right)\Delta\rho g D\cos\beta\cdot C_2}{2\alpha_l'\rho_g(U_g-U_l)^2}}<1. \tag{4.4}$$

Otherwise, instabilities will form and the stratified (wavy) flow will evolve in a slug flow regime.
We want to investigate how the uncertainty is propagated around the stability criterion, to obtain a quantifiable degree of confidence in the predictions, i.e., what is the probability of slug flow, and what will be the probability of a stratified flow.
Again, we will follow the steps presented by Cremaschi [2] to identify the types of uncertainty, representations and propagation method.

Select the type of uncertainty

The focus will be on the input of the SFC, but not all input is taken into account. Following Liao et al. [31], who investigate the numerical stability of the two-fluid model, we can neglect the surface tension for the two-fluid model. This is because surface tension will only act on a small scale and the waves, which determine whether the perturbations will become unstable and flow transition will occur, are usually much longer scale. The liquid and gas viscosities are not taken into account, given we are investigating the IKH. The parameters that have an associated uncertainty with them, are presented in table 4.6.

Table 4.6: Input parameters of the SFC that are taken into account for the IKH.

Input parameter description	**Unit**
Superficial gas velocity	m/s
Superficial liquid velocity	m/s
Density of gas	kg/m^3
Density of liquid	kg/m^3
Pipe hydraulic diameter	m
Pipe inclination angle	degrees
Wall roughness	m

Select the appropriate mathematical representations

The testcase considered is an inviscid air/water stratified flow in a round pipe. The flow properties with an associated uncertainty, i.e. density and velocity, are presented by a normal distribution. This is because a normal distribution is commonly used to present a measurement error, and these flow properties are very difficult to measure precisely. The other flow properties are presented by the typical values for water and air at room temperature.

Typical superficial velocities where the stability criterion is around its neutral stability point, are U_{sg} = 3.5 m/s and U_{sl} = 1.2 m/s.

The pipeline properties, like the pipe diameter, wall roughness and the inclination angle, are represented by a uniform distribution. In reality, these uncertainties cannot be measured during operation, and are therefore considered to have unknown moments. The Guidelines for Hydraulic Design and Operation of Multiphase Flow Pipeline Systems [4] give the following indications for wall roughness for steel pipelines:

- Smooth pipeline: 0.01 mm.
- Average pipeline: 0.01-0.03 mm.
- Rough pipeline: 0.05-0.1 mm.

For this research, the indication for an average steel pipeline is used and the wall roughness is approximated with a uniform distribution between 0.01 and 0.03 mm. Liao et al. [31] performed a computational instability analysis for an inviscid air/water stratified horizontal flow, with a pipe diameter of 0.078 m. These values will also be used in the stability analysis of the IKH.
For first indications, all input variables are assumed to have an uncertainty of 10% of the mean associated with them, except for the wall roughness, where an interval is given based on literature. All these properties and their distribution are presented in table 4.7.

Table 4.7: input uncertainty representation for a transition flow regime.

Input parameter	**Distribution type**	μ	σ	**range**
D, pipe diameter	uniform	0.078	-	E(D) $\pm$ 0.0078
β, inclination angle	uniform	0	-	E(β) $\pm$ 0.1
ϵ, wall roughness	uniform	$2 \cdot 10^{-5}$	-	E(ϵ) $\pm$ $1 \cdot 10^{-5}$
U$_{sg}$, superficial gas velocity	normal	3.5	0.35	E(U_{sg}) $\pm 3\sigma$
U$_{sl}$, superficial liquid velocity	normal	1.2	0.12	E(U_{sl}) $\pm 3\sigma$
ρ_g, gas density	normal	1.2	0.1	E(ρ_g) $\pm 3\sigma$
ρ_l, liquid density	normal	1000	1	E(ρ_l) $\pm 3\sigma$

Choose an appropriate propagation method

For this demonstration, we perform UQ using 10^5 Monte Carlo samples. This is because it is a straightforward and easy approach and it will present us with some insights into the stability of the flow.
The random vector, consisting of random samples from the input variables, is used as input for the SFC, from where a liquid holdup and relative film height distribution are obtained. These distributions are used for calculating the IKH. The gas and liquid velocities are calculated using the liquid holdup, following eq. (2.7).

Fig. 4.15 presents the distribution of the liquid holdup and the IKH stability criterion. The stability criterion is around 1, highlighting that the stability criterion is affected by the application of UQ, and does not always remain stable.

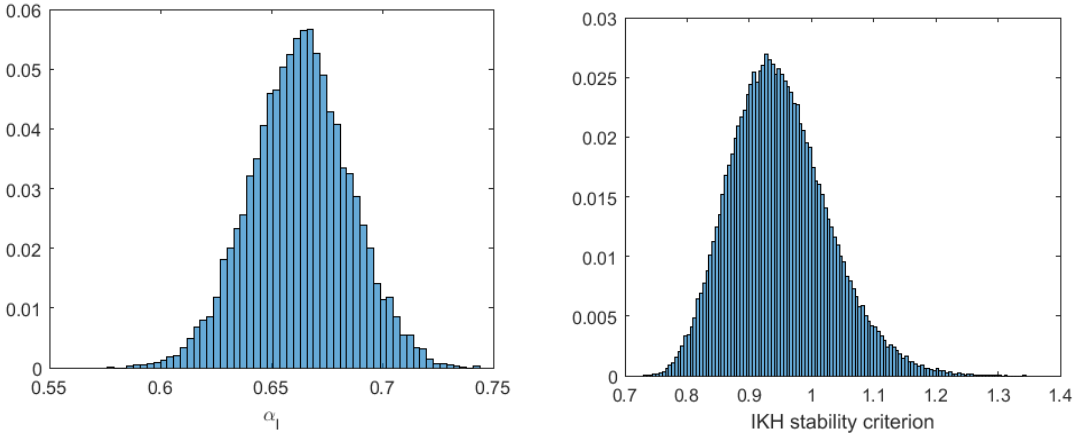

(a) Liquid holdup (b) Stability criterion IKH

Figure 4.15: The distribution of the liquid holdup and IKH stability criterion for the transition regime from stratified to slug flow.

As explained in fig. 2.4, the confidence in multiphase flow predictions can be increased by applying UQ to predictions. From UQ, an output distribution function, the PDF, can be obtained, presented in fig. 4.15. A PDF describes the relative likelihood a model takes on a certain value, but can also provide insight into the likelihood the model takes on a range of values. This is presented in fig. 4.16, where the blue shaded area presents the area of interest, the probability of a stable flow.

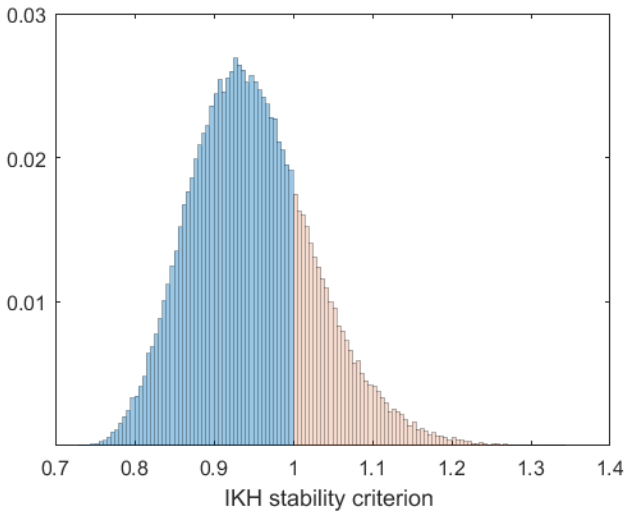

Figure 4.16: The PDF of the IKH stability criterion, where the probability for a stratified flow is highlighted blue.

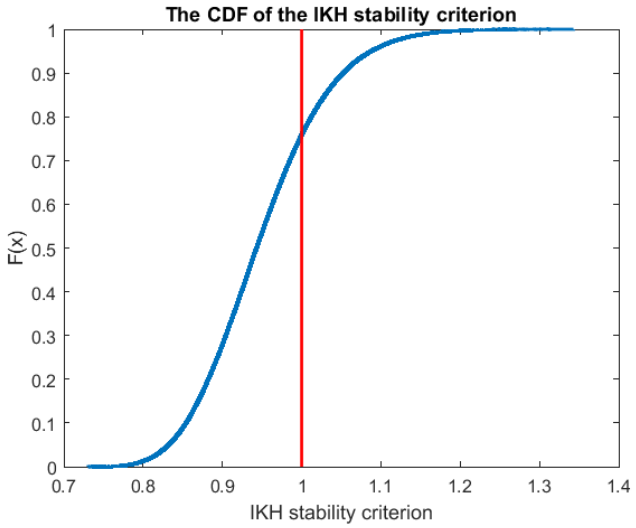

Figure 4.17: The cumulative density function of the IKH, with the red line highlighting the neutral stability point.

A likelihood that a value is within a range, i.e., a confidence range, can be better presented using the cumulative distribution function (CDF). A CDF is the integral of the PDF and presents the probability that the quantity of interest will take a value less than or equal to a certain value in the distribution range. The CDF will vary from 0 to 1, representing the probability. Using a CDF, we can evaluate the probability that the IKH is less or equal to 1, presented in fig. 4.17.

When calculating a flow regime using the input presented in table 4.7, there is a 78% probability of a stable, stratified flow, according to the IKH stability criterion.

4.3.4. Results of UQ on VKH

In order to determine a flow pattern, the SFC makes use of the Viscous Kelvin Helmholtz instability. This equation is an extension on eq. (4.1), where the effect of shear stresses is added. This results in a more complicated equation.
The effect of uncertainty on the VKH stability criterion is not as easy to obtain as for the IKH stability criterion. Still, a prediction on the probability of the stability of the flow is possible. We assume a point close to the transition boundary of stratified flow to slug flow in SFC, as shown in fig. 4.18. The marked point on the flow map is calculated using the mean of the input parameters of interest.

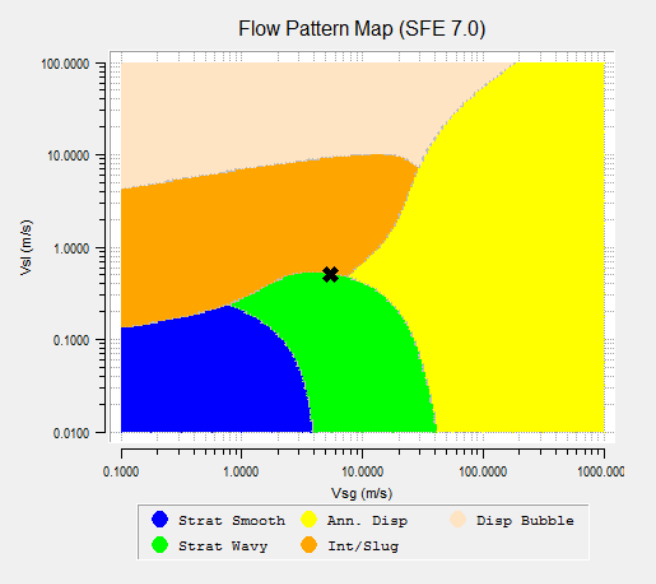

Figure 4.18: The point on the flow map close to the transition from stratified to slug flow, calculated with SFC, using the mean of the input parameters of interest.

The input uncertainties are similar to table 4.7, but viscosity is also added. Values of typical gas - and water viscosities are used and presented with a (truncated) Gaussian distribution. The superficial gas and liquid velocities differ. Typical superficial velocities where the VKH stability criterion is around its neutral stability point, are U_{sg} = 5.5 m/s and U_{sl} = 0.5 m/s. Again, a 10% uncertainty will be added to both the viscosities and velocities.

An output distribution can be obtained for the output quantities of interest, using Monte Carlo with 10^5 samples as an appropriate sampling approach. Since the stability criterion of the VKH is more complicated, we consider the SFC as a blackbox model and take into account output quantities of interest obtained by the SFC. The output distribution of the liquid holdup and pressure drop are presented in fig. 4.19.

Both the liquid holdup and the pressure drop have a distribution with two peaks, of which one represents the stratified flow regime and the other represents the slug regime. For the pressure drop, the right peak identifies the distribution for the stratified flow regime, whereas the left peak in the distribution represents the slug regime. For the liquid holdup, the right peak also represents the liquid holdup for the stratified flow regime, whereas the left peak represents the slug flow regime.

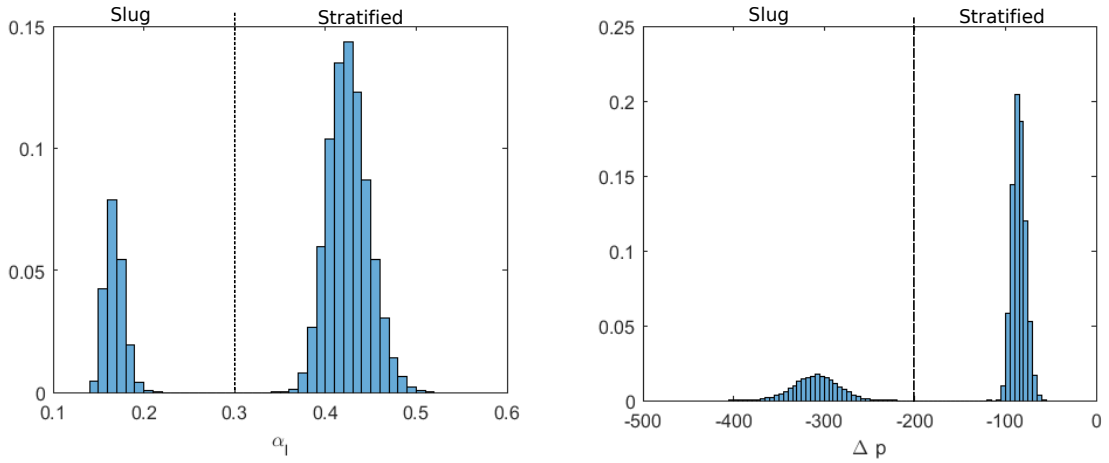

(a) The liquid holdup

(b) The pressure drop

Figure 4.19: The output quantities of interest for a transition regime.

As explained in fig. 2.6, these results match the expectation of the behavior of the pressure and liquid holdup in a pipeline. A higher production, i.e. a higher velocity and a slug flow regime, results in a higher pressure drop and lower liquid hold up, whereas a lower production results in the opposite.

We obtain a CDF for both the liquid holdup and pressure drop. Since every peak in the distribution represents a flow regime, the CDF can provide insight to the probability of a stratified flow, and hereby to the stability of the flow. Both CDFs are compared to check if the results add up. The CDFs are presented in fig. 4.20.

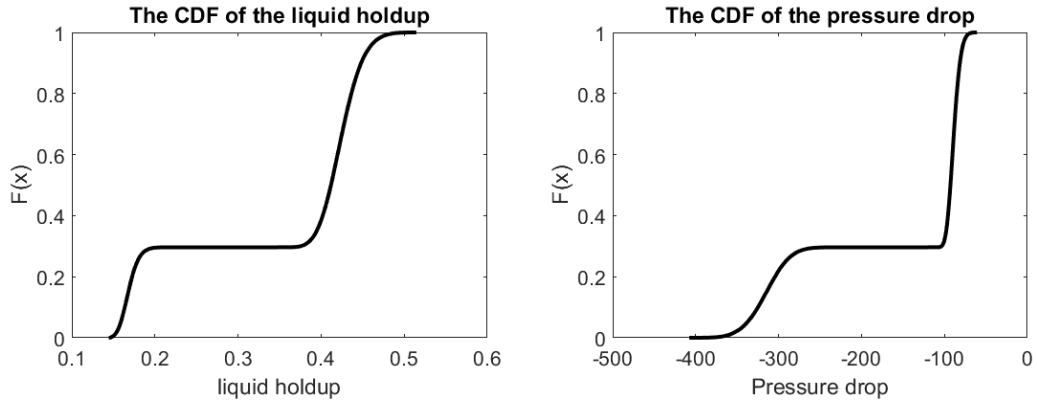

(a) The CDF for the liquid holdup

(b) The CDF for the pressure drop

Figure 4.20: The CDF for the quantities of interest, obtained for a transition from stratified to slug flow.

From both CDFs it follows that using the uncertainty representation of 10%, a 70.3% probability of a stratified flow, and thus stable flow, can be guaranteed. The confidence interval of 70% only accounts for a single point along the VKH stability region. In order to obtain an accurate confidence interval along the transition regime of a multiphase flow, more sample points need to be taken. This interval, as presented in fig. 4.21, serves as an example of how to apply UQ to SFC, in order to obtain more confidence in model predictions. The transition lines are presented in terms of probability. A probability of 1 means a 100% probability the flow is stable. Pereyra [19] recommended a transition band instead of a sharp transition line, to highlight the uncertainty. A transition band with probability is presented, which not only highlights uncertainty, but also provides insight into how the uncertainty is propagated.

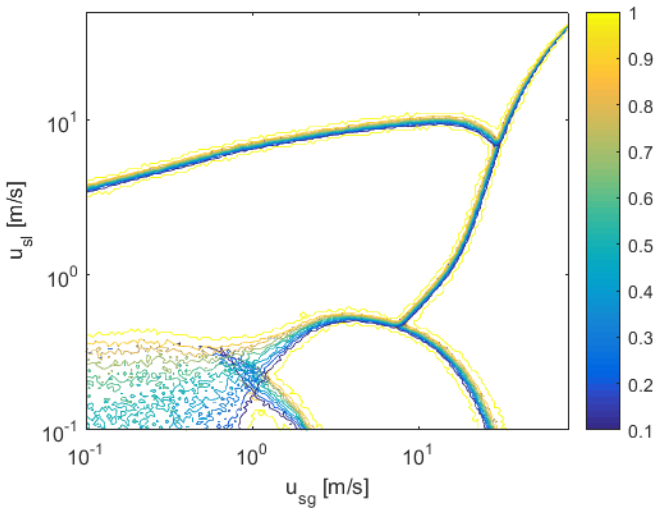

Figure 4.21: A schematic confidence interval around the VKH stability criterion.

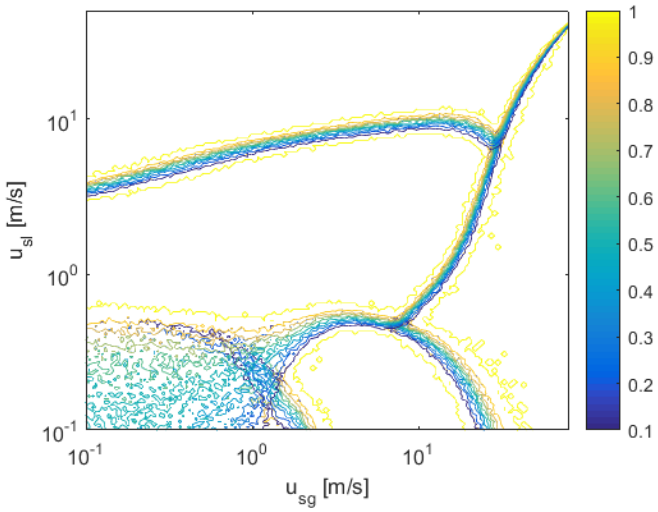

Figure 4.22: A schematic confidence interval around the VKH stability criterion, with an increased uncertainty of factor 2.

Let us increase the uncertainty of the input parameters, i.e. the standard deviation, with a factor 2, to see how the stability regions of the flow pattern map are influenced by the larger uncertainty range. The results are presented in fig. 4.22. We obtain a large uncertainty in the stratified flow region in both cases, as can be seen in fig. 4.21 and fig. 4.22. The flow regime in the left bottom presents the stratified flow regime, as can also be seen in fig. 4.18.

From [25], we obtain that for a stratified flow, even a small difference of the inclination angle plays a crucial role for the determination of the stability of the flow. This was also highlighted in fig. 4.4. We have applied a uniform distribution with an uncertainty range of [-0.1, 0.1] for the inclination angle in fig 4.21 and increased the uncertainty with a factor 2 in fig. 4.22.
We construct a new probabilistic flow pattern map with the increased uncertainty of a factor 2 for the input parameters. This time we do not consider the inclination angle to have an associated uncertainty, but present the inclination angle with a deterministic value of 0. The flow pattern map is presented in fig. 4.23.

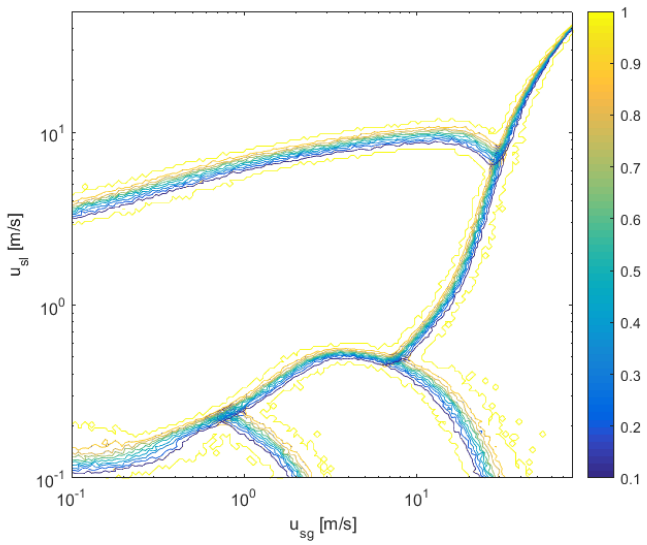

Figure 4.23: A schematic confidence interval around the VKH stability criterion, with an increased uncertainty of factor 2 and a set value for the inclination angle.

As can be seen from fig. 4.23, the uncertainty in the flow pattern map has decreased. We can conclude that the inclination angle is a crucial input parameter for the determination of a stratified flow. Uncertainties in the form of small fluctuations in the downward inclination of the pipe angle can result in large uncertainties in the prediction of the flow pattern. Presenting a flow pattern map in a probabilistic setting can provide more insight in the uncertainty propagation along the transition.

5

Uncertainty propagation on 1-D steady state models

This research is focussed on characterizing uncertainties in steady state flow assurance models. So far, we have investigated uncertainty on 0-D models. In this chapter, we extend the research from a 0-D model to a 1-D model. A commonly used 1-D model in the industry is PIPESIM. That tool can either be used for the design of a pipeline, or during operations. In this chapter, the added value of UQ applied to PIPESIM is further explained. We substantiate this by performing UQ on a PIPESIM model that represents a real gas field in operation.

5.1. The use of PIPESIM in the industry

For both the operation and the design of a pipeline, UQ can provide more insight. The use of PIPESIM for both will be introduced briefly.

5.1.1. The design of a multiphase flow pipeline

When oil or gas needs to be transported, a pipeline network needs to be designed. The design of a multiphase flow pipeline is based on simulation tools. Pipeline systems have specific design criteria per project, like hydraulic capacity and slug catcher volume, depending on various requirements. The requirements are set first, e.g. capacity, minimum temperature, maximum pressure. PIPESIM is used to assess whether certain designs fulfill the requirements.

For the design, a large number of choices needs to be made in order to obtain the right pipeline properties and operating conditions. The Guidelines for the Hydraulic Design and Operation of Multiphase Flow Pipeline Systems [4] provide a long list of options, but only a few important parameters will be highlighted here.

The first design criteria are based on the fluid composition; whether it is an oil or gas field, how many fluid phases are present and what is the composition of the field. One of the input quantities of interest that needs to be measured is the condensate-to-gas-ratio (CGR), (in the case of a gas field) or a gas-to-oil-ratio (GOR), (in the case of an oil field). The CGR, or GOR, describes the ratio of the liquid volumetric rate to the gas volumetric rate and tends to vary over the lifetime of a field. Together with the water cut, these quantities are most important for describing the fluid composition.

Pipeline properties are important design criteria as well. First of all, the pipeline diameter is decisive for the hydraulic capacity. The wall thickness is determined based on the maximum required operational pressure.

The thermal properties of the system also play a role in the design of a multiphase pipeline. The inlet temperature of the fluid can vary and will have an effect on the liquid management in the pipe.

The reservoir pressure is also an important parameter, because it determines to a large extent the inlet pressure for the pipeline. The pipeline design needs to be suitable for the required production capacity. For the design, a hydraulic curve is obtained to assess the influence of the inlet pressure on the production, as explained in fig. 2.6. Since an unstable production is not desired a pipe diameter is determined based on the hydraulic curve.

Currently, in order to assure that the design criteria are met, extra margins are added to output quantities of interest, as calculated by using PIPESIM. An additional 5% to 10% margin is added to the maximum production of the multiphase flow pipeline design, which will result in an increase of the pipe diameter. The 5% additional margin compensates for inaccuracies in the pressure drop prediction, where the 10% additional margin on the maximum production takes account for an unexpected increase in production. Also, an additional margin of 25% is added to the slugcatcher volume [4].

Using UQ, more confidence in assumptions and predictions can be obtained and these margins can be determined more precisely. In the previous chapter, we already demonstrated how confidence can be applied to predictions, by performing UQ on the flow pattern map and obtaining intervals. This can also be done for pipeline design predictions. This can result in, for example, a smaller margin on the pipe diameter and lower material costs.

5.1.2. The operation of a multiphase flow pipeline

Fig. 1.1 already indicated the difference between field data and model predictions. Often during production, steady-state predictions do not match field data. By applying UQ and SA, more insight in the difference between the field data and model data can be obtained. This information can be used to improve the steady state models.

Input parameters of interest relevant for the operation of a multiphase flow pipeline differ from the input parameters of interest for the design of a multiphase flow pipeline. For example, the pipe diameter cannot be changed anymore when the pipeline is operational, and therefore will not be interesting when applying UQ on PIPESIM.
The wall roughness is an interesting input parameter, since over the lifetime of a pipeline, the wall roughness will increase and it cannot easily be measured during operation. Therefore, an estimate needs to be made with respect to the wall roughness over the lifetime of the pipeline.
Also, the fluid composition can change over time and this is important for operational settings. Finally, the outlet pressure is a parameter that needs to be considered as well. Operational conditions are based on a set outlet pressure and an unknown inlet pressure of the pipeline.

For demonstration, let us consider an example of a multiphase flow pipeline in operation, which is the Goldeneye field. Performing UQ will provide a general, systematic approach for highlighting uncertainty. The application of UQ obtains a confidence interval on the quantity of interest. Furthermore, a sensitivity analysis can provide insight into which input parameters have an influence on output uncertainty, and with this information, the PIPESIM model used for the Goldeneye field can be improved.

The improvement of the model based on operation conditions will also be beneficial for the design of a pipeline. The model can be better calibrated with field data and predictions will be more accurate. Together with the application of UQ, this will result in better informed decision making.

5.2. Case study for the Goldeneye field

Goldeneye is the name of a gas-condensate field, located 100 km offshore in the North-Sea. The location of the field is presented in fig. 5.1. The field has been in production for 6 years, from 2004 until 2010.

5.2.1. Case description and PIPESIM model

During the production of the Goldeneye field, field production data were obtained for the last year of production. These field data provide more insight in the accuracy of flow assurance models.
A benchmarking study [32] was performed for the steady state conditions of the Goldeneye field. From the field data, 4 different intervals were selected for which the production data were steady. For the 4 intervals, the pressure drop was calibrated while varying the wall roughness. The main finding is that a wall roughness of 0.2 mm results in a pressure prediction accuracy of 2% when comparing PIPESIM with the late field data for 3 of the 4 cases. This highlights the importance of characterizing the uncertainty in the input parameters of interest. With the application of UQ, a time consuming, manual benchmarking study could be replaced by applying uncertainty quantification, which takes into account multiple input parameters.

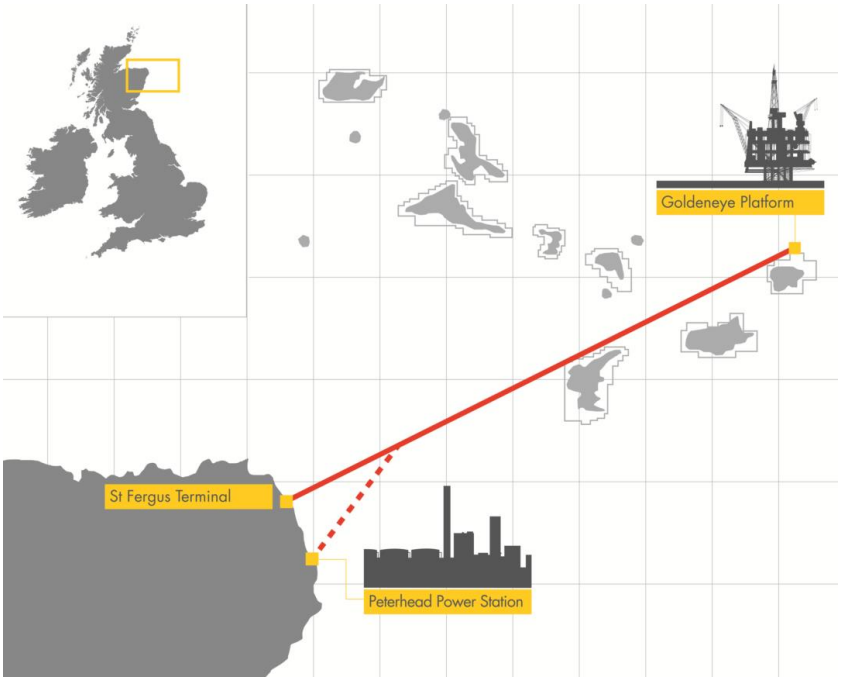

Figure 5.1: The location of the Goldeneye field.

The detailed information of one period of steady state production in August 2010 is taken as a testcase for the application of UQ. A selection of the field data is presented in table 5.1.

Table 5.1: Selection of the field data, used for the selected steady state interval.

Quantity	**Measured data**
Date	August 2010
Production (offshore data)	151 [MMSCFD]
Export pressure	75.0 [bar]
Outlet pressure	55 [bar]
Mass flow outrate	47.63 [kg/s]
Export temperature	56.8 [$^{\circ}C$]
Outlet temperature	8.8 [$^{\circ}C$]
Ambient temperature	11.5 [$^{\circ}C$]

We will perform UQ on the Goldeneye field, taking into account the important key parameters for operations of a multiphase flow pipeline. The Goldeneye model, created in PIPESIM for the benchmarking study, is presented in fig. 5.2a. This PIPESIM model has been validated using field data. The model consists of 2 risers and multiple branches. Every branch differs in the pipe diameter and the wall thickness.

The initial PIPESIM model is simplified to a single branch model. The simplified model is presented in fig. 5.2b. A mean value for the diameter and for the wall thickness is determined, based on the branches of the original model. The elevation profile and pipeline length are the same as for the initial model. The single branch model is verified with the original model, as can be seen in fig. 5.3. The system pressure, calculated with PIPESIM, is plotted versus the pipeline length for both models. These results are in line with the inlet pressure of 75 bar and system outlet pressure of 55 bar, presented in table 5.1. From fig. 5.3 the pressure along the pipeline distance can be seen. The two risers at the beginning of the pipeline results in a pressure increase at the beginning of the model. Furthermore, the pressure decreases along the pipeline. Differences in pipeline inclination result in small peaks and drops along the profile.

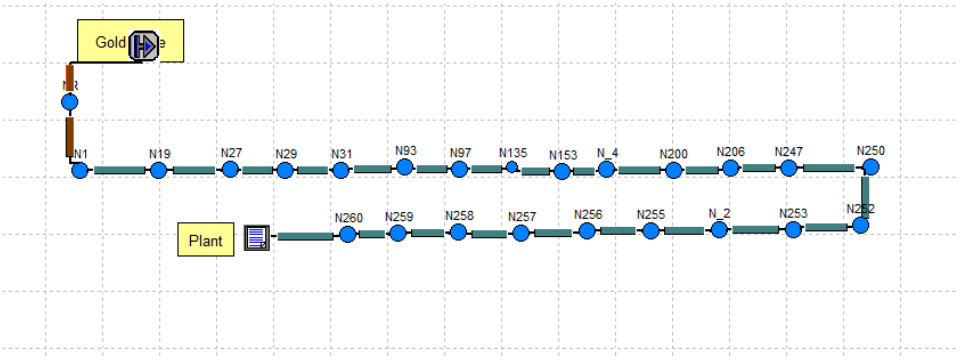

(a) The initial PIPESIM model of the Goldeneye field [32].



(b) The simplified PIPESIM model of the Goldeneye field.

Figure 5.2: The two PIPESIM models.

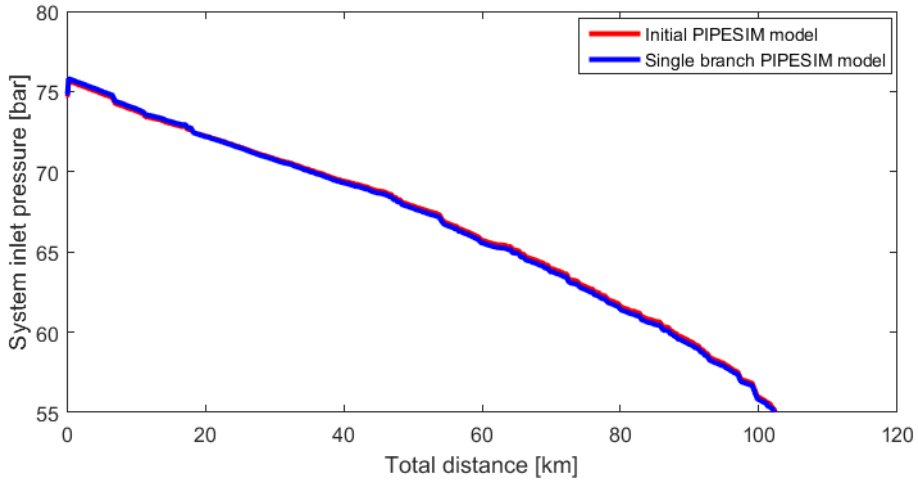

Figure 5.3: The comparison of the two models.

An interface, similar to the framework presented in fig. 2.10, is created with UQLab. UQLab calls PIPESIM using an external server, OpenLink [33]. The interface is presented in appendix B.

5.2.2. Uncertainties in the Goldeneye field

Let us follow the steps of Cremaschi to perform uncertainty propagation on a PIPESIM model.

Identify the type of uncertainty

PIPESIM works with a large number of input parameters and one simulation takes approximatety 126 seconds using the UQLab interface. In order to avoid high computational costs, the example of UQ on the Goldeneye field is kept as simple as possible. Therefore, only 3 input parameters, with expected influence on quantities of interest like pressure drop and liquid holdup, are considered. These input parameters are presented in table 5.2.

Table 5.2: Input parameters of interest for PIPESIM.

Input parameter description	Unit
Outlet pressure	bar
Ambient temperature	°C
Wall roughness	m

Unfortunately, applying uncertainty to the fluid composition was not possible in the interface between PIPESIM and UQLab. This is further discussed in chapter 6.2.

Select appropriate mathematical representations

The uncertainty of the input is based on either literature or field data. The choice of mathematical representation for every input parameter will be discussed briefly.

Ambient temperature

From the Guidelines for the Hydraulic Design and Operation of Multiphase Flow Pipeline Systems [4], data for the seasonal effects on the seabed temperature at the Central North Sea are obtained: a mean, 90% - and 99% exceedance level are presented. The exceedance level is the level of confidence, i.e., 90% exceedance means that only 10% of the measurement data exceeds this value. This information is presented in fig. 5.4.

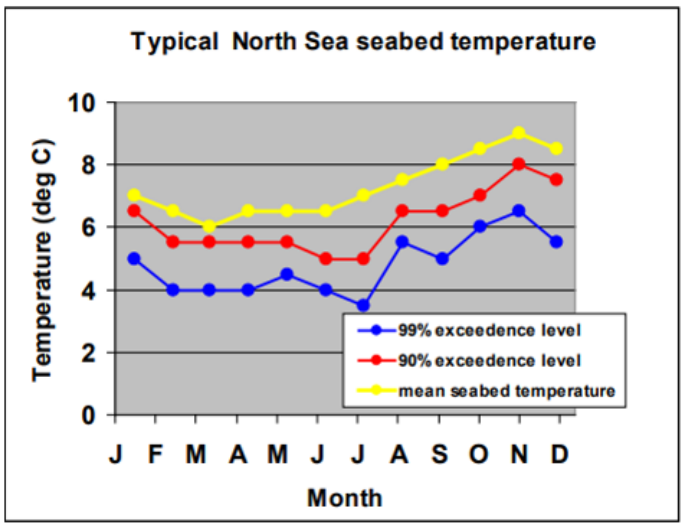

Figure 5.4: Metocean data for the seasonal effects on the seabed temperature at 90 m water depth in the Central North Sea, taken from the Guidelines for the Hydraulic Design and Operation of Multiphase Flow Pipeline Systems [4].

From fig. 5.4, a distribution for the ambient temperature of the Goldeneye field that matches the percentiles needs to be found. The data presented in fig. 5.4 give a mean temperature of 7.8 °C, a 90% exceedance level for a ambient temperature of 6.5 °C and a 99% exceedance level for a temperature of 5.8 °C. Applying a normal distribution results in a proper fit, which matches the criteria from fig. 5.4.
After empirical investigation, the distribution is set at $T_{amb} \sim \mathcal{N}(7.8, 0.95)$. A CDF is obtained to check the probability at 99% and 90%, presented in fig. 5.5. For clarity, (1-CDF) is plotted to obtain a 99% percentile at the lower boundary of the ambient temperature. For the choice of distribution parameters, a 99% percentile is obtained at 5.65 °C and a 90% percentile is obtained at 6.6°C.

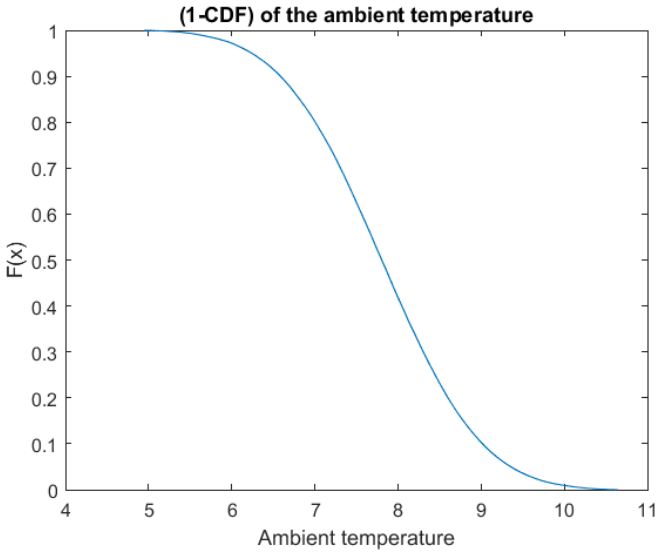

Figure 5.5: CDF reconstruction, based on fig. 5.5. A 99% percentile is obtained for 5.65 °C, a 90% percentile at 6.6 °C.

However, Goldeneye is not located at the Central North Sea area, and different mean temperatures are measured. The mean ambient temperature for the seabed surrounding the Goldeneye field is measured at 11.5 °C for August 2010. The standard deviation is multiplied with a factor that presents the the difference in mean temperature of the Goldeneye and the Central North Sea.

Wall roughness
At the time of the installation of the pipeline, the pipeline had a wall roughness of 0.01 mm. During operations, the wall will corrode and the wall roughness will increase. A typical value for a rough pipeline is around 0.1 mm, as discussed in sec. 4.3.2, although the wall roughness can increase even more. With this information, a distribution to present the wall roughness is created, taking 0.01 mm as the minimum, 0.1 mm as a mean, and no upper limit.
A distribution that can represent this type of uncertainty is the Gumbel distribution. The Gumbel distribution is based on extreme value theory. The maximum Gumbel distribution is commonly used to describe the maximum value of a random variable. For instance, the Gumbel distribution is used in hydrology to analyze annual maximum values of daily rainfall. The Gumbel distribution for the wall roughness is presented in fig. 5.6. The Gumbel distribution uses the following notation: $X \sim \mathcal{G}(\mu, \beta)$, where β is related to the standard deviation by: $\sigma_X = \frac{\pi\beta}{\sqrt{6}}$.

System outlet pressure
The representation of uncertainty in the system outlet pressure is determined based on field data. The mean of the outlet pressure is set at 55 bar, but small fluctuations in the outlet pressure will occur, as can be seen in fig. 5.7. From these data, the standard deviation is determined. Large peaks are removed from the dataset, because those are not representative for inaccuracies in the pressure drop prediction. Based on the dataset without peaks, the standard deviation is set at 0.48 bar.

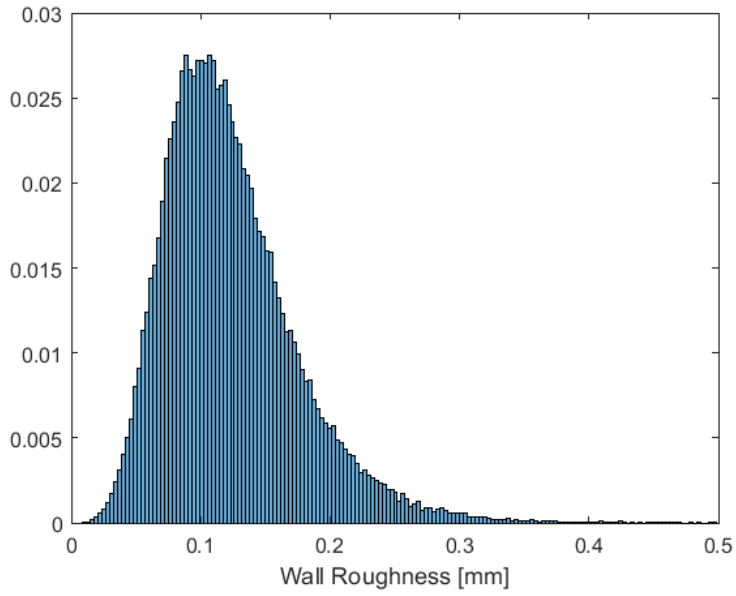

Figure 5.6: The PDF of Gumbel distribution for the wall roughness.

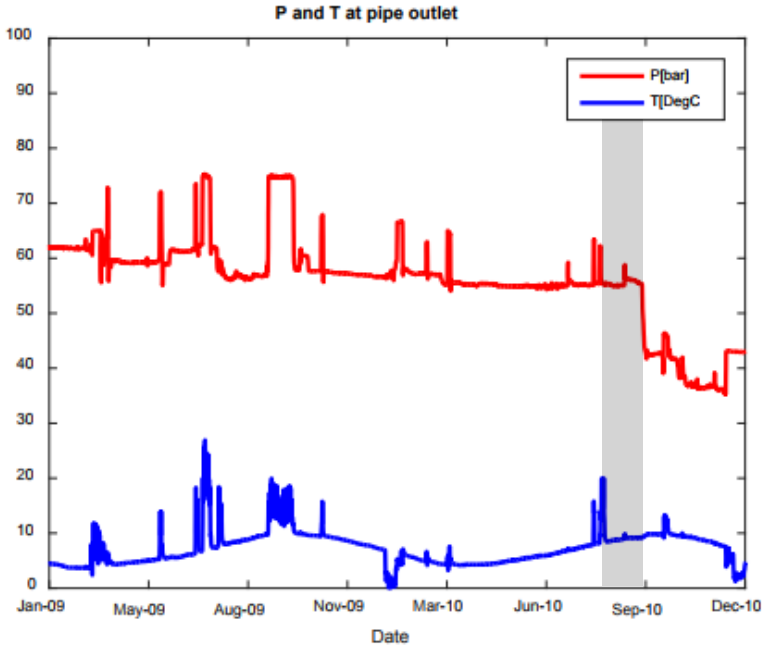

Figure 5.7: The measured pressure and temperature at the outlet of the pipeline, obtained from Lommerse [32].

To summarize, the input parameters and uncertainty representation are presented in table 5.3.

Table 5.3: Input representation for parameters of interest for PIPESIM.

Input parameter	**Distribution type**	μ	σ	**Range**
Outlet pressure	Normal	55	0.48	$\mu \pm 3\sigma$
Ambient temperature	Normal	11.5	1.106	$\mu \pm 3\sigma$
Wall roughness	Gumbel	0.1	0.04	$[0.01, 0.5]$

Choose an appropriate propagation method

The UQLab framework applied on PIPESIM is computationally relatively expensive: one sample takes approximately 126 seconds. The choice is made not to use Monte Carlo, but to directly use the functional expansion-based approach, since PCE can speed up computations using less nodes, as discussed in section 4.2.

Polynomial Chaos Expansion

Two different simulations are obtained. First, the input parameters of interest are presented with an input distribution. Based on the input representation, PCE samples are obtained. For each PCE sample, i.e. for each combination of outlet pressure, ambient temperature and wall roughness, a hydraulic curve is constructed by varying the inlet gas flow rate.

Given the complexity and computational costs of the model, only 64 PCE samples are considered, of which each PCE sample is again evaluated 10 times to construct the hydraulic curve. This results in 640 simulations. First, input files are created using the input variables in UQLab. These input files are run externally on a different, faster, machine, in order to decrease computational time. This is schematically presented in fig. 5.8.
Quadrature rules are used, since the problem is considered to be low dimensional, since $M < 4$.

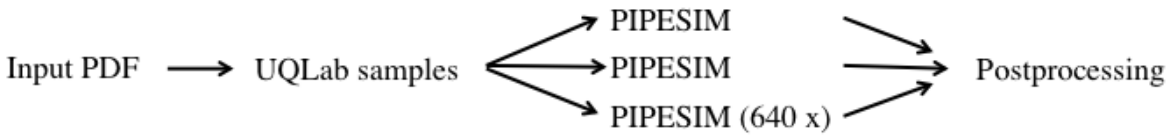

Figure 5.8: A schematic overview of the processing of the PCE samples.

The hydraulic curve is presented in fig. 5.9. The mean of the sample set is presented with a black line. The standard deviation of the uncertainty in the inlet pressure is presented with a gray shaded area. This figure shows how the uncertainty is propagated, i.e., by applying input uncertainty and feeding this to PIPESIM, the output uncertainty is highlighted.

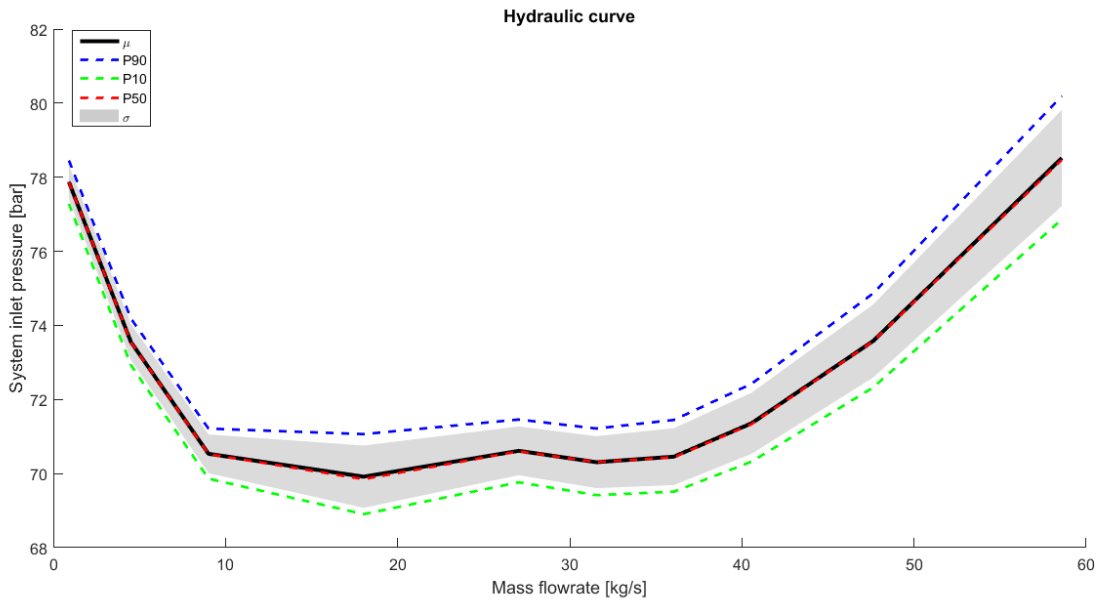

Figure 5.9: The hydraulic curve of the Goldeneye field. The black line presents the mean of the system inlet pressure. The grey shaded area presents the standard deviation of the inlet pressure. The red (P50), blue (P90) and green (P10) lines presents the percentile intervals.

Based on the output uncertainty range, more insight can be obtained in how the uncertainty is propagated. Intervals, with a degree of confidence in the predictions can be presented. Historically, a low/mid/high case is obtained to assess the effect on uncertainties when designing a pipeline. These cases do not provide insight into the probability quantities of interest will be lower of higher than the low/mid/high case. With the application of UQ, a P90/P50/P10 degree of confidence in predictions can be obtained. This highlights the probability that the quantity of interest will be within the uncertainty region. For example, a P90 level of confidence means a 90% probability that the simulation result will be within the uncertainty range. Compared to a simple low/mid/high case computation, our analysis provides more insight in how uncertainty is propagated and will contribute to a more realistic evaluation of the effect of uncertainties when designing a pipeline. The P90/50/10 intervals are presented in fig 5.9.

Let us consider the influence of uncertainty for the input quantities of interest at a given flow rate. The initial PIPESIM model is evaluated at a mass flow rate of 47.6 kg/s; therefore we choose to investigate the uncertainty in output quantities of interest at the same mass flow rate. Fig. 5.10 presents the PDF for quantities of interest, the liquid holdup and the pressure drop.

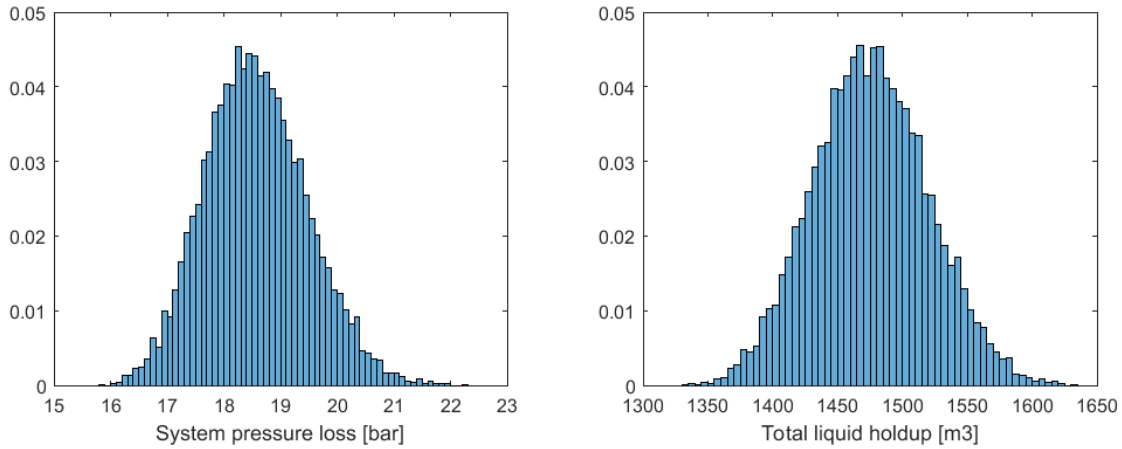

(a) Pressure drop (b) Liquid holdup

Figure 5.10: The pdf of the quantities of interest at a mass rate of 49.6 kg/s.

The inlet pressure is determined based on a set outlet pressure in PIPESIM. The uncertainty distribution of the inlet pressure is presented in fig 5.11. This propagation of the uncertainty in the inlet pressure for a flow rate of 47.6 kg/s is also visible in fig. 5.9.

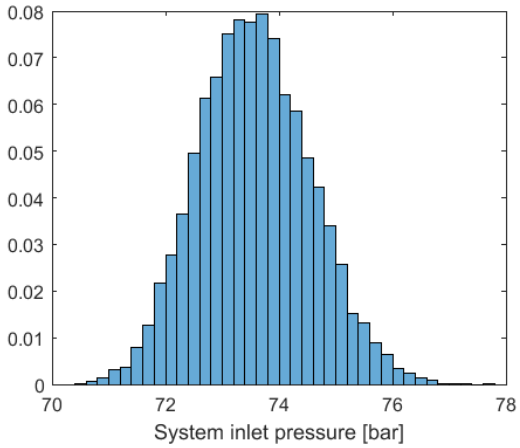

Figure 5.11: The PDF of the inlet pressure of the Goldeneye field.

The deterministic PIPESIM model computed a total liquid holdup of 1496 m^3. When applying uncertainty on input parameters, the liquid holdup will have an associated uncertainty and ranges from 1320 to 1650 m^3. When representing the liquid holdup distribution with a CDF, a probability of 65% is obtained that the liquid holdup will be lower than 1496 m^3. If we consider the fact that the design and operations of a pipeline rely on steady state models, we can conclude that the predictions of the deterministic model are conservative. There is a 65% probability the liquid holdup will be lower, i.e. a 65% probability less liquid will accumulate in the pipeline, and therefore the extra margins on the hydraulic capacity and slugcatcher volume might perhaps be lowered.

5.2.3. Sensitivity analysis

We perform a global sensitivity analysis using the PCE sampling approach, as discussed in section 3.3, with 64 samples for a flow rate of 49.6 kg/s. The results are presented in fig. 5.12.
The uncertainty in the pressure drop is almost completely due to the wall roughness. The uncertainty in the liquid holdup is due to the uncertainty in all three input parameters, where the ambient temperature is the most critical input parameter with respect to uncertainty.

The benchmarking study performed by Lommerse [32] only took into account the uncertainty in the wall roughness with respect to the pressure drop. We now observe that the wall roughness is indeed the most important (in fact the only) factor influencing the pressure drop given the uncertainty ranges defined in table 5.3. However, when also considering the liquid holdup, we see that both the wall roughness and the ambient temperature have an effect.

When calibrating parameters to match field data, as is done in [32], it is important to know these sensitivities. In this case, calibrating the wall roughness to match the measured pressure loss is the correct approach; however, this will differ from case to case. Furthermore, for matching the liquid holdup, more parameters should be considered.

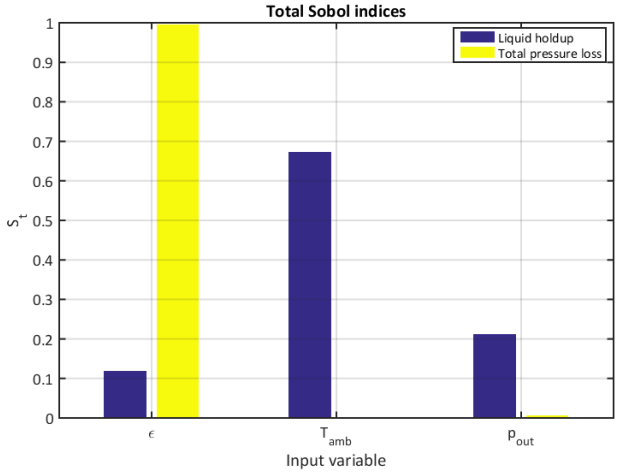

Figure 5.12: The Sobol indices of the Goldeneye field for the output quantities of interest.

The improvement of the Goldeneye PIPESIM model serves as an example of what UQ can contribute to the assessment and improvement of models. By applying UQ and SA on PIPESIM models, more insight can be obtained in the influence of uncertainty in input parameters on output quantities of interest.

6

Conclusions and recommendations

In this chapter, conclusions and recommendations for further work are presented.

6.1. Conclusions

This research has given an insight in how Uncertainty Quantification (UQ) can improve the confidence in model predictions, used for pipeline design and operations.

The goal of this research was: *Investigation of the effect of uncertainties in the input parameters on the output quantities of interest for steady state multiphase flow models for pipelines.*

A general and systematic approach was presented, where input uncertainty was identified and represented with a PDF and propagated through two steady state multiphase flow models with Monte Carlo sampling and Polynomial Chaos Expansion (PCE). The main findings for each of the two models will be given below.

6.1.1. 0-D model

First, UQ was applied on a 0-D steady state model, the Shell Flow Correlations, and the results are validated using literature as a reference: the Monte Carlo approach from Picchi & Poesio [5]. We showed that our results are consistent with [5]: the uncertainty in the liquid holdup and pressure drop for a horizontal stratified flow is only due to the contribution of the uncertainty in two parameters, the superficial liquid velocity and the inclination angle. The uncertainty in the pressure drop for a downward stratified flow is due to the contribution of 4 parameters, being the two superficial velocities, the gas viscosity, and the pipe diameter respectively, whereas the uncertainty in the liquid holdup is almost completely due to the uncertainty in the superficial liquid velocity.
Second, we showed that PCE outperforms Monte Carlo sampling, used by [5]. We have showed that compared to Monte Carlo sampling, PCE will need approximately 1000 times less samples, to reach a desired order of accuracy for the pressure drop and the liquid holdup of a horizontal stratified flow. The computation time for a single sample evaluation is almost fully determined by the computer time for the model simulation, which is the same in the two models. Therefore, PCE is our proposed approach.
Finally, UQ is applied to the construction of a flow pattern map with a quantifiable degree of uncertainty, that is an extension of the existing deterministic flow pattern map (in which the uncertainty associated with input parameters is not present). This allows the quantification of the probability that a flow regime (e.g. slug, stratified) occurs under given conditions.

These are significant improvements compared to existing work that handles uncertainties in multiphase flow models.

6.1.2. 1-D model

UQ is also applied on a steady state 1-D model, PIPESIM. Field data were obtained from a condensate-gas field, the Goldeneye field, and compared with a PIPESIM model. Based on the experiences with the 0-D model, we employed PCE as a sampling method for UQ on PIPESIM. A benchmarking study on the Goldeneye field is used to investigate the effect of 3 input uncertainties with respect to 2 output quantities of interest. Our study shows that besides the wall roughness, which was used in the original benchmarking study, also the ambient temperature and the outlet pressure of the pipeline are important parameters influencing the liquid holdup and pressure drop. This demonstration of the application of UQ on the Goldeneye field served as an example of what UQ could contribute to the assessment and improvement of models.
Previous predictions, obtained using a deterministic setting, calculated a total luid holdup of 1496 m^3. We can now predict that the total liquid holdup of a pipeline, when taking into account uncertainties, will have a 65% probability to be lower than this value.

To summarize, a general, systematic approach is designed for applying UQ on two multiphase models for pipelines. This will help increase the confidence in predictions, because more insight in the probability of predictions using uncertainties is obtained. We can conclude that PCE is a more efficient approach for applying UQ than Monte Carlo sampling, which has not been applied yet on flow assurance models. The findings of applying UQ on these models give more insight in the propagation of uncertainties in predictions of steady-state multiphase flow models.

6.2. Recommendations

This research has given a number of first insights in the effect of uncertainties on steady state multiphase flow models. It is a demonstration of what UQ can contribute to better informed decision making, using probabilities in predictions that take into account uncertainties. There are several steps that can be taken to further improve and understand model predictions. Both short-term and long-term recommendations are proposed for further research:

Short-term recommendations for further research:

- **Determination of the input distribution**
  The choice of input distribution is decisive for the resulting uncertainty in the output. Field data, literature or expert knowledge should be available for a good indication of the input distribution that represents uncertainty. Currently, when there were no data available to describe the input distribution, an assumption of 10% of the mean was made for the uncertainty range.

- **OpenLink software possibilities**
  OpenLink is the interface that makes it possible to call PIPESIM using external software, like Matlab and UQLab. However, not all the dynamic libraries of OpenLink that have a functionality associated with them, worked properly in Matlab. The FluidCompositional dynamic library, which should be used to change the fluid composition, was not available in Matlab. Therefore, it was decided that the fluid composition was not treated as an input parameter with associated uncertainty. However, in reality the fluid composition is an important input parameter for pipeline design and operation that deserves further investigation.

- **The application of a sparse grid**
  In this research, PCE was only applied on lower dimensional problems. However, pipeline design and operations generally depends on a large number of input parameters, and sparse grid PCE is a promising method that should be taken into account. Furthermore, this research made use of the methods that were available in UQLab. UQLab does not make use of nesting. A nesting of grids is a very efficient approach for higher dimensional problems, and should be investigated in further research, where more input parameters are taken into account.

Long-term recommendations for further research:

- **Propagation of model assumptions**
  This research focusses on the effect of uncertainty in input parameters on output quantities of interest. There are two main uncertainties in model predictions, namely model assumptions and imperfect knowledge of input parameters. A recommendation for further research is to investigate the effect of uncertainty in model assumptions on the quantities of interest on the model uncertainties.

- **Calibration**
  The findings of uncertainty propagation and sensitivity analysis for both input parameters and model assumptions can be used for calibration of both the model assumptions and the input parameters. This will help to increase the confidence in model predictions.

- **Dependent variables and dimensionless numbers**
  The input parameters are assumed to be independent, but in reality, parameters can be dependent. Furthermore, dimensionless numbers can be used for the pipeline assessment and can contribute to the reduction of the dimension of the problem. The relation between input parameters and dimensionless numbers, and the effect of dependent parameters could be investigated further, for more efficient and realistic predictions.

- **Extension to dynamic modelling**
  This research focussed on steady state models. However, dynamic models are used for model predictions on short periods of time to provide more inside in transient operations, like for instance pigging and ramp-up operations. To study the effect of uncertainties on dynamic operations, it is recommended to apply UQ on dynamic models.

A

The application of the UQLab toolbox

The UQLab toolbox makes it very easy to apply UQ. An example of how to implement the methods used in this research is provided. One needs to define the input parameters and sampling strategy in a structured way, and from here UQLab calculates the output quantity of interest. Recall the framework for applying UQ. Every step that needs to be performed is highlighted here, taking the Churchill relation as a reference .

A.1. Quantification of sources of uncertainty

First, UQLab needs to be called. Furthermore, the input needs to be defined. For the input, specify the distribution type, its typical parameters (for the Churchill example μ and σ). If truncated, specify the bounds.

```
 %start uqlab
uqlab

%Probabilistic input model
Input.Marginals(1).Name = 'Re';
Input.Marginals(1).Type = 'Gaussian';
Input.Marginals(1).Parameters = [4000 400];
Input.Marginals(1).Bounds = [2800 5200];

Input.Marginals(2).Name = 'e';
Input.Marginals(2).Type = 'Gaussian';
Input.Marginals(2).Parameters = [3e-4 3e-5];
Input.Marginals(2).Bounds = [2e-4 4e-4];

myInput = uq_createInput(Input) ;
uq_print(myInput);
```

A.2. The model blackbox

The computational model, where the calculation of the output quantity of interest is specified, needs to be added to UQLab.

```
% Define the model and add it to UQLab
Model.mFile = 'uq_Churchill'
myModel = uq_createModel(Model);
```

A.3. Uncertainty propagation

Random variables are obtained from the input and sampling strategy of choice. This is used to evaluate the model. For the example of the Churchill relation, let us take Monte Carlo sampling.

```
% Define a sampling strategy
X = uq_getSample(2000, 'MC') ;
Y = uq_evalModel(myModel,X) ;
```

PCE can also be applied using the UQLab toolbox. One needs to specify the input for the PCE model, the PCE method, polynomial degree (or in the case of OLS and LARS the sampling size) and from here UQLab creates a PCE model.

```
metamodelPCE.Input = myInput;
metamodelPCE.Type = 'Metamodel';
metamodelPCE.MetaType = 'PCE';
metamodelPCE.Method = 'Quadrature' ; %'LARS', 'OLS'
metamodelPCE.Quadrature.Type = 'Full';

metamodelPCE.Degree = 20;
myPCE = uq_createModel(metamodelPCE);
```

A.4. Sensitivity analysis

The sensitivity analysis using Sobol's indices is also straightforward. Specify the method for the sensitivity analysis, sample size and maximum order for the indices. Thereafter, UQLab creates a sensitivity analysis.

```
SobolModel.Type = 'Sensitivity';
SobolModel.Method = 'Sobol';
% Specify the maximum order of the Sobol'  indices calculation
SobolModel.Sobol.Order = 2;

SobolModel.Sobol.SampleSize = 2000;
% Create and add the sensitivity analysis to UQLab
SobolAnalysis = uq_createAnalysis(SobolModel);
SobolResults = SobolAnalysis.Results;
```

B

The interface of the steady-state models

An interface is created between UQLab and the steady state models. For each multiphase flow model, the interface is presented.

B.1. SFC

```
%% load SFC
setenv('MW_MINGW64_LOC','C:\Apps\TDM-GCC') % compiler for C++
if not(libisloaded('SFC'))
    loadlibrary('SFC_FRONT64.dll','sfc_front.h','alias','SFC');
end

% libisloaded('SFC_FRONT64')
libfunctions('SFC');
input_arr(1) = 0; % FLOW PATTERN (FREE=0),
input_arr(2) = X(:,1); % SUPERF. GAS VELOCITY, [m/s],
input_arr(3) = X(:,2); % SUPERF. LIQUID VEL, [m/s],
input_arr(4) = 0;  % WATERCUT (WC), [fraction],
input_arr(5) = X(:,3); % DENSITY GAS, [kg/m3],
input_arr(6) = X(:,4); % DENSITY OIL, [kg/m3],
input_arr(7) = 1000; % DENSITY WATER, [kg/m3],
input_arr(8) = X(:,5); % VISCOSITY GAS, [Ns/m2],
input_arr(9) = X(:,6); % VISCOSITY OIL, [Ns/m2],
input_arr(10) = 0.001; % VISCOSITY WATER, [Ns/m2],
input_arr(11) = X(:,7); % SURFACE TENSION O/G, [N/m],
input_arr(12) = 0; % SURFACE TENSION W/O, [N/m],
input_arr(13) = X(:,8); % PIPE DIAMETER, [m],
input_arr(14) = X(:,9); % PIPE INCLINATION,
input_arr(15) = X(:,10); % WALL ROUGHNESS,[m],
input_arr(16) = 0.0e0; % ENTRAINMENT, [fraction of liquid],
input_arr(17) = 0.67e0; % PHASE INVERSION,
input_arr(18) = 1.0e0; % LINEAR EMULSION FACTOR, [-]
input_arr(19) = 1.0e0; % QUADRATIC EMULSION FACTOR, [-]
input_arr(20) = 1.0e0; % SMOOTHING FACTOR, [-]
input_arr(21) = 0.0e0; % POWER LAW / HERSCHEL-BULKLEY EXP (N)
input_arr(22) = 0.0e0; % POWER LAW CONSISTENCY
input_arr(23) = 0.0e0; % YIELD STRESS
input_arr(24) = 0;   %FOAM CONCENTRATION

% input for dll
indx = [4,2,1,1,6,0,0,1,2,0,2,0,0,0,0,0,0,1,0,0]; % SFC 2-phase option

% convert to right structure
% for C++; (input_arr, index, arr) = (doublePtr, Int16Ptr, doublePtr)
arr = libpointer('doublePtr', zeros(1,200));
indx = int16(indx);
calllib('SFC','sfc_front',input_arr,indx,arr); % call dll and compute output arr (arr)
```

```
%% output
output(:,1) = arr.Value(1); % Liquid holdup [-]
output(:,2) = arr.Value(2)+arr.Value(3); %Pressure drop (gravitational + frictional)
```

B.2. PIPESIM

```
%% activate dll
addpath('\\AMSDC1-NA-V508\julia.klinkert$\Cached\My Documents\MATLAB\Julia\PipeSim\UQLab_test\')
case_name = 'Ge_PIPESIM_115_1Branch.bps'
c = actxserver('NET32COM.ISingleBranchModel')
c.OpenModel(case_name)

j =0;
  for i = 1:100
      test = c.GetNameList(i);
      if (iscell(test)) % & test))
          j = j+1;
          names(j).list = test;
      end
 end

%write uncertainties to pipe branch
c.SetPropertyVal(char(names(3).list), 'PIPE ROUGHNESS', X(:,1), 'mm')
c.SetPropertyVal(char(names(3).list), 'TEMPERATURE NODE', X(:,2), 'C');

d.BoundaryConds.CalculatedVariable = 1;
d.BoundaryConds.FluidType = 1;
d.BoundaryConds.OutletPressure_SI = X(:,3); %Pa; default: 42.5561 bar
d.PermuteStepMode = 2;

test_case = sprintf('test%d%d%d.bps',[X(:,1) X(:,2) X(:,3)]);
allFiles = dir('\\AMSDC1-NA-V508\julia.klinkert$\Cached\My Documents\MATLAB\Julia\PipeSim\UQLab_test');
allNames = {allFiles.name}
check = ismember(test_case,allNames);

% Check if model exists and run the model
 if (check == 0)
        c.SaveModel(test_case);
        c.RunSingleBranchModel2(true,'-b',false);
 end

 %% Getting results
cs = sprintf('test%d.plt',(X(:,1)+k));
results = actxserver('WELLCURVE.ReadData');
results.OpenFile(cs);

x = results.GetNumberofVariables;
Variables = results.GetAllData();

for j = 1:x
      Output(j).Names = cellstr(results.GetVariableName(j));
      Output(j).Variables = Variables{j,1}{1,1}{1};
 end

output(:,1)= Output(6).Variables; %Total liquid holdup (m3)
output(:,2)= Output(2).Variables; %System pressure loss (bar)
```

Bibliography

[1] C.E. Brennen, *Fundamentals of Multiphase Flows*, Cambridge University press, 2005

[2] S. Cremaschi, G. Kouba, H. Subramani, *Characterization of confidence in multiphase flow predictions*, Energy&Fuels, 2012, 26, 4034-4045

[3] B. Keinath, *Decision analysis in multiphase flow: uncertainty, risk and application*, BHR Group 2017

[4] R.A.W.M. Henkes, *Guidelines for the Hydraulic Design and Operation of Multiphase Flow Pipeline Systems*, Shell Report GS.09.51858, 2015

[5] D. Picchi, P. Poesio, *Uncertainty quantification and global sensitivity analysis of mechanistic one-dimensional models and flow pattern transition boundaries predictions for two-phase pipe flows*, International Journal of Multiphase flow 2017, 90, 64-78

[6] H. Holm, P. Saha, V. Suleymanov, T. Vanvik, N. Hoyer, *Shtokman flow assurance challenges - A systematic approach to analyze uncertainties - Part 2*, BHR Group 2011

[7] G.B. Wallis, *One-dimensional two-phase flow*, McGraw Hill Higher Education, 1969

[8] B. Sanderse, *Governing equations of single- and multi-phase flow in one-dimensional pipeline*, Shell Report SR.13.13992, 2013

[9] G. Iaccarino, *Quantification of uncertainty in flow simulations using probabilistic methods*, VKI Lecture Series, Stanford University, Sept. 8-12, 2008

[10] R. Dwight, *CFD 4: Lecture Notes*, Delft University of Technology, April - May 2017

[11] S. Lee, W. Chen, *A comparative study on uncertainty propagation methods for black-box-type problems* Structural and Multidisciplinary Optimization 2009, 37(3), 239-253

[12] C. Lataniotis, S. Marelli, B.Sudret, *UQLab user manual - The input module*, Report UQLab-V0.9.102, Chair of Risk, Safety & Uncertainty Quantification, ETH Zurich, 2017

[13] S. Marelli, B.Sudret, *UQLab user manual: Polynomial Chaos Expansions*, Report UQLab-V0.9.104, Chair of Risk, Safety & Uncertainty Quantification, ETH Zurich, 2017

[14] S. Marelli, C. Lamas, B.Sudret and K. Konakli, *UQLab user manual - Sensitivity Analysis*, Report UQLab-V1.0-106, Chair of Risk, Safety & Uncertainty Quantification, ETH Zurich, 2017

[15] R. C. Smith, *Uncertainty Quantification, Theory, Implementation, and Applications*, Society for Industrial and Applied Mathematics, 2014

[16] K. Klavetter, D. Posluszny, J. Warr, S. Cremaschi, C. Sarica, H. J. Subramani, *Uncertainty analysis of multiphase flow models: a comparison of three propagation approaches*, BHR Group 2012

[17] D. Posluszny, K. Klavetter, S. Cremaschi, C. Sarica, H. J. Subramani, *Uncertainty analysis of multiphase flow modelling: A case study for vertical flows*, BHR Group 2010

[18] N. Hoyer, M. Kirkedelen, M. B., Biberg, D., Johnson, G. W., Valle, A., Johansson, P. S., Nossen, J, *A structured approach for the evaluation of uncertainties in flow assurance systems*, BHR Group 2012

[19] E. Pereyra, C. Torres, R. Mohan, L. Gomez, G. Kouba, O. Shoham, *A methodology and database to quantify the confidence level of methods for gas-liquid two-phase flow pattern prediction*, Chemical Engineering and Design 2012, 90, 507-513

[20] P. Dhoorjaty, D. Erickson, R. Kotwa, M. Mai, P. Parthasaranty *Assessment and sensitivity analysis of multiphase flow pipeline models against experimental and field data*, BHR Group 2017

[21] H. Abdulmouti, *Bubbly Two-Phase Flow: Part I- Characteristics, Structures, Behaviors and Flow Patterns* American Journal of Fluid Dynamics 2014, 4(4): 194-240

[22] J.M.C. van 't Westende, *Droplets in annular-dispersed gas-liquid pipe-flows* Ph.D. thesis, Delft University of Technology, 2008

[23] N. Fajraoui, S. Marelli, B.Sudret, *On optimal experimental design for sparse polynomial chaos expansions* RSUQ report, 2017-001

[24] P.I. Rosen Esquivel, S. Olijerhoek, *Software Interface Description of the Shell Flow Correlations*, Shell Report SR.15.12531, 2015

[25] R.H.A. IJzermans, R. Lacy, *Technical description Shell Flow Correlations*, Shell Report GS.09.51663, 2009

[26] D.E. Veling, J.J. Kreeft, *Numerical Simulations of the Kelvin Helmholtz instability*, Shell Report SR.15.11375, 2015

[27] Prof. dr. R.V.A. Oliemans, *Applied Multiphase flows*, Lecture Notes, Delft University of Technology, 1998

[28] Y. Taitel, A. Dukler, *A model for predicting flow regime transitions in horizontal and near horizontal gas-liquid flows*, AIChE Journal 1976, 22, 47-55.

[29] D. Barnea, Y. Taitel, *Kelvin-Helmholtz stability criteria for stratified flow: viscous versus non-viscous (inviscid) approaches*, International Journal of Multiphase Flow 1993, 19, 639-649

[30] J.M. Mandhane, G.A. Gregory, K. Aziz, *A flow pattern map for gas-liquid flow in horizontal pipes*, International Journal of Multiphase Flow 1974, 1, 537-551

[31] J. Liao, R. Mei, J.F. Klausner, *A study on the numerical stability of the two-fluid model near ill-posedness*, International Journal of Multiphase Flow 2008, 34, 1067-1087

[32] L. Lommerse, *Goldeneye - Benchmarking of Steady State Models Against Low Flow Field Data*, Shell Report SR.17.10676, 2017

[33] Schlumberger, *PIPESIM 2012.2.1. Open Link Reference Manual*, 2015